DEVELOPMENT OF AN ELECTROCHEMICAL CHOLESTEROL BIOSENSOR BASED ON POLY (PROPYLENE IMINE) DENDRIMER- QUANTUM DOTS NANOCOMPOSITE

By

KEFILWE VANESSA MOKWEBO

Mini-dissertation in fulfilment of the requirement for the degree

MASTER OF SCIENCE

in

NANOSCIENCE

in the

FACULTY OF SCIENCE

of the

UNIVERSITY OF JOHANNESBURG

Supervisors : PROF O.A AROTIBA

: PROF S.O OLUWAFEMI

JANUARY, 2018

DECLARATION

I hereby declare that this dissertation, which I herewith submit for the research qualification

MASTER IN NANOSCIENCE

To the University of Johannesburg, Department of Applied Chemistry, is, apart from the recognised assistance of my supervisors, my own work and has not previously been submitted by me to another institution to obtain a research diploma or degree.

_____ on this ____ day of _____

(Candidate)

_____ on this ____ day of _____

(Supervisor)

_____ on this ____ day of _____

(Co-supervisor)

_____ on this ____ day of _____

(Co-supervisor)

DEDICATION

I dedicate this mini-dissertation to the following:

1. My heavenly Father (God) who has always been by my side throughout my life and education.
2. My deceased mother Ntombi Bertha Mokwebo, my aunt Mavis Gadifele Moeng who took me in and raised me to be a responsible young woman I am today, my brother Mphoentle Mokwebo and cousins.
3. My electrochemistry and nanomaterial research group, my nanoscience friends Pretty Maleka, Tinxwalo Ngwenya, Thapelo Moima, Bonolo Mosikatsi, Neo Monaheng, Kabo Matshetshe, Idris Azeez, Talifhani Mushiana and Mthobisi Zulu for their continuous support and guidance.

ACKNOWLEDGEMENTS

First and foremost I would like to acknowledge God as He has always been behind everything I do and my successes. Thank you Lord Jesus Christ for being a father to the fatherless, for giving me strength, love, wisdom and guidance through the Holy spirit to carry out and complete this work.

I will also like to extend my gratitude to the following people and organisations for their contributions and assistance towards the completion of this work:

- My supervisors, Prof O.A Arotiba and Prof S.O Oluwafemi for their guidance, support and understanding throughout the work. You were not only my research supervisors, but you were also my advisors, spiritual father and also a shoulder to cry on when it was tough. I really appreciate everything you have done for me and taught me. I will always be grateful. I would also like to thank Dr Mabuba for acting as my supervisor when my supervisors were not around.
- I extend my appreciation to Mr Idris Azeez, who assisted me a lot in electrochemistry Lab. There are a lot of things I didn't know in electrochemistry, but you took time under your busy schedule to teach me and I appreciate it a lot.
- I also like to thank Ms Vuyelwa Ncapayi for her assistance in the synthesis part of my work and Mr Eric, Mr Thapelo Moima and Dr Barani for their assistance in microscopic and spectroscopic characterization of my materials.
- Thank you to Mr Fakayode for proof-reading my thesis and also to my electrochemistry and nanomaterial group for listening to my presentations. I am a better presenter because of the presentations we always had in the group.
- Thank you to my family for raising me up and supporting me in everything.
- Thank you to the Department of Science and Technology and National Nanoscience Postgraduate Teaching and Training Programme (NNPTTP) for financial support.

PUBLICATIONS AND PRESENTATIONS

Conference presentation:

- Vanessa Mokwebo (2017), “Development of an Electrochemical Cholesterol Biosensor on a Quantum Dot/Dendrimer Nanocomposite platform.” Poster presented at International Workshop on Biosensors, October 12-14th 2017, Rabat, Morocco. **Poster presentation.**

Manuscript:

- K.V Mokwebo, S.O Oluwafemi, O.A Arotiba. A cholesterol electrochemical biosensor on CdTe/CdSe/ZnSe quantum dots-poly (propylene imine) dendrimer nanocomposite immobilization layer. Biosensors and Bioelectronics. Submitted.

ABSTRACT

One of the parameters that cause cardiovascular diseases (CVDs) is high level of cholesterol in the blood. Therefore, monitoring of cholesterol level is of great importance, especially to elderly people and people with high risk of such diseases. This work explores the applicability of poly (propylene imine) dendrimer (PPI) and CdTe/CdSe/ZnSe quantum dots (QDs) in developing a suitable platform for the development of an enzyme-based electrochemical cholesterol biosensor with enhanced analytical performance. The as-synthesized mercaptopropionic acid (MPA) capped CdTe/CdSe/ZnSe QDs was synthesized in an aqueous phase and characterized using photoluminescence (PL) spectroscopy, ultraviolet-visible (UV-vis) spectroscopy, transmission electron microscopy (TEM), powdered X-ray diffraction (XRD), fourier transform infrared (FTIR), scanning electron microscopy (SEM) and energy dispersive X-ray (EDX) spectroscopy. The absorption and emission maxima red-shifted as the reaction time and shell growth increased. The increase in PL intensities shows proper passivation of the QDs surface with PL quantum yield (PLQY) of 33.8 %, 69.2 % and 57 %, for CdTe, CdTe/CdSe and CdTe/CdSe/ZnSe QDs respectively. The XRD patterns of all the as-synthesized QDs consist of three diffraction peaks corresponding to (111), (220) and (311) cubic zinc blended structures. The estimated particle size of CdTe/CdSe/ZnSe QDs from XRD and TEM are 4.32 and 4.08 nm, respectively while the EDX confirmed the presence of corresponding elements. For biosensor design, PPI dendrimer was electrochemically deposited on glassy carbon electrode (GCE) and characterized using cyclic voltammetry (CV) and impedance spectroscopy (EIS) in both phosphate buffer solution (PBS) and ferricyanide solution ($[Fe(CN)_6]^{-3/-4}$) This was followed by drop-drying the QDs on the electrode to form GCE/PPI/QDs. Finally, cholesterol oxidase (ChOx) was drop-dried on the GCE/PPI/QDs electrode to produce GCE/PPI/QDs/ChOx-based electrochemical cholesterol biosensor. Scanning electron microscopy (SEM) was used to characterize screen printed carbon electrode (SPCE) as it was modified with different materials and was able to capture the nano-globular morphology of PPI dendrimer. The GCE/PPI/QDs/ChOx based cholesterol biosensor was able to detect cholesterol in the range 0.1-10 mM with a

detection limit (LOD) of 0.35 μM and sensitivity of 283.3 μA μM^{-1} cm^{-2}. The biosensor was stable for over a month and had greater selectivity towards cholesterol molecule.

Key word: Cholesterol, electrochemical biosensors, quantum dots, poly (propylene imine), dendrimer, enzymes.

TABLE OF CONTENTS

LIST OF FIGURES AND SCHEMES

LIST OF TABLES

LIST OF ABBREVIATIONS

ChOx	Cholesterol oxidase
PPI	Poly (propylene imine)
QDs	Quantum dots
HPLC	High pressure liquid chromatography
PL	Photoluminescence
QY	Quantum yield
PLQY	Photoluminescence quantum yield
FRET	Forster resonance energy transfer
LDL	Low density lipoprotein
HDL	High density lipoprotein
NIR	Near infrared
GOx	Glucose oxidase
HRP	Horseradish peroxide
PBS	Phosphate buffer solution
AA	Ascorbic acid
UA	Uric acid
Glu	Glucose

SWV	Square wave voltammetry
CV	Cyclic voltammetry
EIS	Electrochemical impedance spectroscopy
GCE	Glassy carbon electrode
SPCE	Screen printed carbon electrode
FAD	Flavin-adenine dinuclide
MPA	Mercaptopropionic acid
G3,G2,G4	Generation 3, 2, and 4
NHS/EDC	N-hydroxysuccinimide/(1-ethyl-3-(3-dimethylaminopropyl)carbodiimide hydrochloride
FTIR	Fourier transform infrared
HRTEM	High resolution transmission electron microscopy
XRD	Powdered X-ray diffraction
UV-vis	Ultraviolet-visible spectroscopy
EDX	Energy dispersive X-ray spectroscopy
SEM	Scanning electron microscopy
SAED	Selected area electron diffraction

CHAPTER 1

INTRODUCTION

1.1 BACKGROUND

In the medical field, diagnosis is of great importance in the whole process of disease therapy or treatment because it can promptly predict the onset of a particular disease before its advancement in the body. It can be said that early and correct diagnosis can reduce cost, harm to human and therefore, mortality rate. Diagnosis involves series of physical, biological and chemical methods which are amenable to improvement for a more informed, timely and robust result.[1] Chemically, techniques such as high pressure liquid chromatography (HPLC), mass spectroscopy, calorimetry, spectrophotometry, fluorimetry and polarography are commercially available and have allowed clinicians to detect and study very small biomolecules.[2-6]These techniques may provide valuable information about other characteristics of the biomolecule. For instance, one can know the conformation, molecular weight, chemical structure and how this biomolecule interacts with other molecules.[1] However, these techniques have several disadvantages. These include requirement for sample treatment prior to analysis, high cost of purchase of the instruments, laboratory-based operation, requirement for skilled/trained personnel, less sensitivity, large material requirement and time-consuming operations.[2,3,6,7] For example, when using calorimetric method for detection of cholesterol, a lot of reagents are used while the serum must be separated from the blood to avoid any optical interferences caused by co-contaminant such as haemoglobin in the blood.[5,8] Although these techniques can provide the necessary information, their drawbacks make it difficult for them to be applied in real life situation, outside the lab, where there are hundreds of samples to be analyzed. Therefore, the development of highly sensitive and accurate low-cost devices such as electrochemical biosensors have been introduced. These devices are defined as ‘testing at, point-of-care or near the site of the patient care’.[1]

Since the introduction of biosensors by Cammann, 1977, there has been an improvement over the years in medical, food technology, water pollutant analysis, and agricultural industries. This is due to the ease-of-operation, cost-effectiveness, high sensitivity, portability, and simple fabrication of biosensors.[3,6] A biosensor is a portable analytical device that combines biological receptors with physicochemical transducers to detect or measure the amount of the analyte in the sample. A typical biosensor consists of a bioreceptor (e.g. antibodies, enzymes, viruses or DNA), which is selective toward binding to a target analyte and a transducer (electrode) which converts the analyte-bioreceptor interaction into readable signal, which can be interpreted from the computer or monitor.[1,9] Biosensors have found applications in food processing and storage, environmental monitoring, clinical diagnosis and biodefense due to their excellent characteristics such as high sensitivity, selectivity, stability and fast response time.[9,10]

Biosensor field is growing tremendously and this is due to their wide applications and versatility. Electrochemical biosensors and biosensors in general, have a very successful record in the analytical world. The market size for worldwide biosensors is projected to be valued at $ 27.06 Billion by 2022, growing at compound annual growth rate (CAGR) of 8.84% between 2017 and 2022. Fig. 1.1 shows global biosensor market, by end-users. This market growth is driven by; emergence of new advanced technologies, growing need to manage health issues such as cholesterol and diabetes, increased growth of home care diagnostics, increase in drugs discovery, new disease discovery, environmental monitoring, and agriculture monitoring systems. Advances in technologies such as miniaturization and microfabrication have also enabled deeper penetration of biosensors into a wider range of application in the market. Additionally, the growth in micro-fluidics, nanotechnology, molecular marker, surface characterization, and bio-complementary chemistry are all expected to significantly impact biosensor growth in the future. Nanotechnology is expected to play a very vital role in biosensor development due to the unique optical, mechanical, physical and magnetic characteristics of nanomaterials such as graphene, carbon nanotubes and quantum dots. Ideally, for a biosensor to be useful, it must be precise, specific, highly sensitive, fast, cost-effective, miniaturized and automated and should involve small

sample volumes. Among the different transducing methods, electrochemical method seems like the ones that inherit the above characteristics with miniaturized electrodes and instrument – the potentiostat. Therefore, it is not surprising that most biosensor developed for large range of analytes and for different fields are using electrochemistry as transducing method. Among different bioreceptors used in biosensors, enzymes play a vital role as response-generating arrive sites for the detection of analytes. Therefore, this work exploits the properties of an electrochemical enzyme biosensors to detect cholesterol.[11]

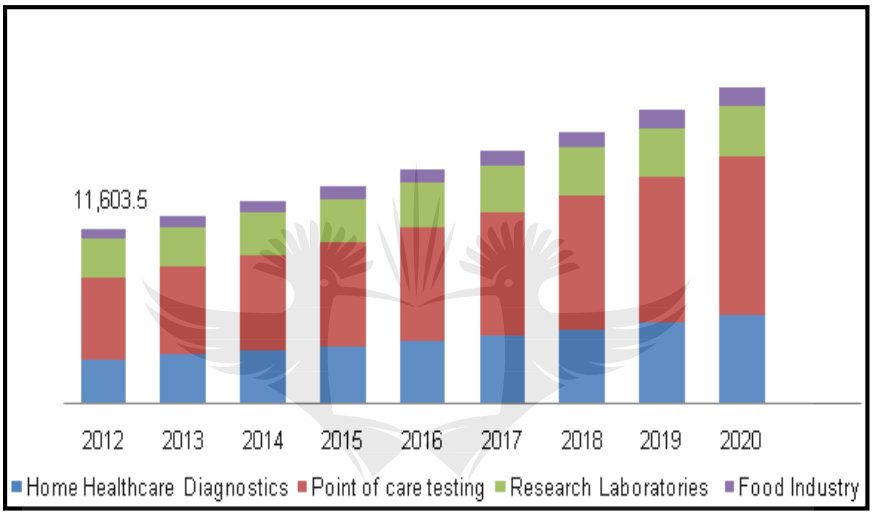

Figure 1. 1: Global Biosensors Market, by End-use (USD Million).[12]

1.2 PROBLEM STATEMENT AND RESEARCH MOTIVATION

Despite the success of electrochemical enzymatic biosensors in the market, there still remain challenges in finding suitable immobilization matrix (working electrode material), enzyme loading capacity of the electrode and immobilization technique that will provide a biocompatible environment for the enzyme.[13-16] Enzymes can only perform their optimum duties (high sensitivity, low detection limit and selectivity) when they are in a “comfortable” environment with good orientation.[17,18] There is a direct relationship between the performance of an electrochemical biosensor, immobilization matrix, and the chemistry used in immobilizing the enzyme on the transducing material. Therefore, it is necessary to look for novel material, immobilization technique and preparation methods that will overcome some of these

challenges. Researchers are investing lot of money and time in integrating biomolecules with nanomaterial-modified electronic components to develop various types of electrochemical biosensors, which will ease and improve the detection/diagnosis processes in the above fields, especially medical field.

The use of nanoparticles such as quantum dots, and dendrimers in enzymatic biosensors can enhance the loading capacity and even provide "better" environment for the enzyme. These nanomaterials can provide large surface area and also improve the stability of the biosensor by limiting the loss of the enzyme activity over time (since the enzyme is encapsulated into the dendrimer).[14,19,20] In addition, the use of dendrimer will also provide a biocompatible environment for the enzyme because it has those physicochemical properties that resembles those of proteins. These nanostructured materials are used to efficiently immobilize the enzyme on the working electrode.

1.3 AIM AND OBJECTIVES

1.3.1 Aim

The aim of this project was to develop an electrochemical biosensor based on an enzyme-immobilized quantum dots/dendrimer nanocomposite platform for the determination of cholesterol.

1.3.2 Objectives of the study

- To synthesize photo-active near infrared (NIR) semiconducting CdTe/CdSe/ZnSe quantum dots (QDs).
- To characterize the as-synthesized QDs and polypropylene imine (PPI) using different analytical techniques.
- To prepare and characterize CdTe/CdSe/ZnSe QDs-PPI dendrimer-Cholesterol oxidase (ChOx) bionanoplatform (electrode).

- To develop an electrochemical cholesterol biosensor based on enzyme-QDs/dendrimer nanocomposite.

1.4 JUSTIFICATION OF THE MATERIALS CHOSEN AS THE BIOSENSOR COMPONENTS

The choice of materials used in modification of the electrode is importance in developing an electrochemical biosensor. In this study, CdTe/CdSe/ZnSe QDs, PPI dendrimer and Cholesterol oxidase (ChOx) were used to develop the bio-nanoplatform proposed. Dendrimer was used as a host that will encapsulate the enzyme and provide better orientation for it. The QDs with their large surface area and electrocatalytic properties were used to increase the surface area and enhance electron transfer between the enzyme active site and electrode surface. The enzyme (ChOx) is used for its selectivity towards cholesterol molecule. Dendrimers have been widely applied in drug delivery, water treatment, solar cells and biosensor fabrication with promising results due to their tree like architecture with multiple peripheral groups and nanoscale cavities.[21-23] Dendrimers have remarkable physicochemical properties, good compatibility with enzyme and are nanoscale macromolecules with host-guest chemistry. They can also behave like artificial enzymes.[21] PPI is commercially available in different generations and safe to use. It's a 3D highly branched globular polymer with different sites for functionalization. It is conducting and electroactive, behaves as a micelle, nanostructured (large surface area) and respond well to pH changes.[21,22] Even though PPI dendrimer have such excellent properties, there are only few reports on its application in developing an enzyme-based biosensor. QDs on the other side have large surface area, excellent stability against environment and chemicals, excellent electrical and chemical properties thereby enhancing charge transfer between the active site of the enzyme and electrode surface. In addition, QDs have higher isoelectric point than enzymes, which allows the enzyme to be easily immobilized on them.[2] For this work, cadmium (Cd) based quantum dots were used and one might think about the toxicity of this metal ion. Firstly, these QDs contain (i) a thick shell of zinc selenide (ZnSe) which reduces the release of Cd into the environment and (ii) PPI, which further reduces the toxicity of the QDs. The toxicity studies reported by Ncapayi on

CdTe/CdSe/ZnSe have shown this material to possess high cell viability against KM-Luc/GFP cell line.[24] This cell line was made by fussing luciferase (Luc) and enhanced-green fluorescent protein (EGFP) genes. It is used in initiating lymph node metastasis.[24] From literature, quantum dots are mostly being employed in photoelectrochemical, fluorescence resonance energy transfer (FRET), fluorescence and electrochemiluminescence biosensors, where their optical properties or both the electrochemical and optical properties are being exploited. For this work only electrochemical properties will be exploited.

1.5 BRIEF OVERVIEW OF THE CHAPTERS

Chapter 1: Introduction

This chapter presents the general introduction, problem statement and research motivation, research aim and objectives, and justification of the material used.

Chapter 2: Literature review

This chapter provides background review on biosensor, enzymes, and nanomaterials employed in cholesterol electrochemical biosensors (e.g. quantum dots), dendrimers, immobilization techniques and cholesterol in general.

Chapter 3: Experimental methodology

This chapter focuses on list of materials used, preparation of solutions, methodology and brief discussion of analytical techniques used to carry out this research project.

Chapter 4: Synthesis and characterization of MPA-capped CdTe/CdSe/ZnSe QDs

This chapter is about synthesis and characterization of MPA-capped CdTe/CdSe/ZnSe quantum dots (QDs).

Chapter 5: Development of PPI/QDs based electrochemical cholesterol biosensor

This chapter consists of preparation of GCE/PPI/QDs/ChOx based cholesterol biosensor, results obtained from application of the designed biosensor, and the discussions thereof.

Chapter 6: Conclusions and recommendations

This chapter provides general conclusion and recommendations based on the results obtained from this research project.

CHAPTER 2

LITERATURE REVIEW

2.1 INTRODUCTION

This chapter elaborates more on what is written in chapter one. The review focuses on electrochemical cholesterol biosensor, types, principle, challenges in enzyme biosensor, enzyme immobilization techniques, and nanomaterials exploited as platforms for designing the biosensor. It further highlights reports on quantum dots (QDs), their synthesis, challenges and their applications in biosensors. It also gives a brief review on dendrimers, as they were also exploited during the study.

2.2 CHOLESTEROL

Cholesterol is a fat-like organic biomolecule found in all cells and it is naturally produced by the liver and the intestines. It plays an important role in the production of vitamin D, steroid hormones, bile acid which assist in lipid digestion and also maintains the cell membrane.[25,26] The other source of cholesterol is the food we eat. Most food such as fatty red meat, eggs, cream and animal fats such as butter contains high level of cholesterol**.** When consumed along with foods that have high level of saturated fat and *trans*- fatty acid, it can lead to increase in the blood cholesterol level.[27-29] Since cholesterol is a fat (that is insoluble in water), it is transported throughout the body or blood by molecules called lipoproteins. The two most important lipoproteins used for transportation are low density lipoprotein (LDL) also known as the “bad” cholesterol and high density lipoprotein (HDL) known as the “good” cholesterol. LDL cholesterol is called a “bad” cholesterol because when it exist at higher concentrations (> 190 $mg.dL^{-1}$), it can build up inside the walls of the arteries, narrowing and blocking them and making it difficult for the oxygenated blood to flow to different parts of the body, thus leading to the risk of cardiovascular diseases.[26] On the other hand, high level of HDL (> 50 $mg.dL^{-1}$) is good because it protects the body against heart diseases by removing the LDL cholesterol from the

blood and prevents it from forming a plaque inside the arteries. Triglycerides (fats from food) also contributes to the total cholesterol level in the body. The recommended total cholesterol level (sum of LDL, HDL and triglycerides) in the body should be below 200 $mg.dL^{-1}$ (5.2 mM), otherwise one is at risk of heart diseases. Fig. 2.1 displays three types of fats that causes cholesterol and their risk values. Even though total cholesterol level is affected by our diet, the body can also produce its own cholesterol. Therefore, people that do not consume excess cholesterol can have hypercholesterolemia and this is due to some genetic metabolic disorder. Hypercholesterolemia caused by genetic disorder is called Familial hypercholesterolemia and it is rare in most cases.[28,30] It mostly occur in the Afrikaans-speaking community of South Africa at a ratio of 1:72, and this is due to concentration of specific gene in a small group of settler in the country over many years.[30,31]

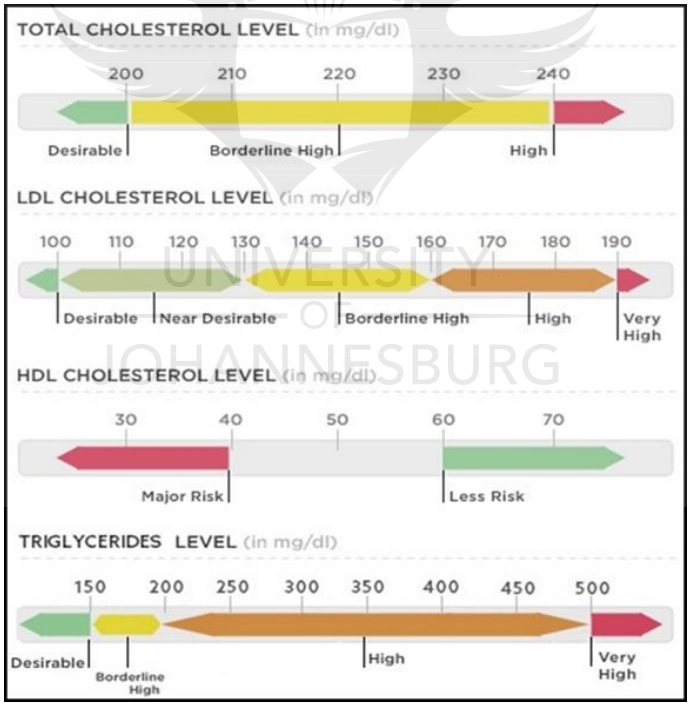

Figure 2. 1: Chart displaying the three types of fats in the body: LDL, HDL and triglycerides. It also displays the good range, along with the risk zone of the fats in the body. It also shows different zones for total cholesterol level (LDL + HDL + triglycerides) in the body.[32]

2.3 CONVENTIONAL ANALYTICAL METHODS FOR CHOLESTEROL DETERMINATION

Diagnosis of diseases, especially early diagnosis, is a very important part of therapy or disease management in the medical field. Early diagnosis of cholesterol levels is very important because it can prevent severe consequences of excess cholesterol in the body. In the analytical world, techniques such as high pressure liquid chromatography (HPLC)[33,34], gas chromatography[35,36], mass spectroscopy[37,38], calorimetry[39,40], spectrophotometry[14,41,42] and fluorimetry[43,44] have been used and have allowed clinicians to detect and study very small biomolecules such as cholesterol molecules. These techniques may provide valuable information about other characteristics of the biomolecule. For instance, one can know the conformation, molecular weight, chemical structure and how this biomolecule interacts with other molecules. However, these techniques requires proper sample treatment prior to analysis due to their sensitivity, they are expensive, requires trained personnel, requires colour indicator reagents, less sensitive and time-consuming.[3,7,45] Although these techniques can provide the necessary information, their drawbacks make it difficult for them to be applied in real life situation, outside the lab, where there are hundreds of samples to be analysed. Therefore, development of highly sensitive and accurate low-cost devices such as electrochemical biosensors have been introduced. These devices are defined as testing at, point-of-care or near the site of the patient care.[1]

2.4 BIOSENSORS

The term “biosensor” was first introduced by Cammann (1977) where he was trying to define the use of enzymes on ion-selective substrate (electrodes).[46,47] The definition of a biosensor was later introduced by IUPAC.[47,48] Biosensors are small (portable) analytical devices that combines biological receptors with physicochemical transducers to directly detect or measure the amount of the analyte in the sample.[47] A typical biosensor consist of a bioreceptor (e.g. antibodies, enzymes, viruses and DNA to name a few) which is selective to the target analyte and a transducer (electrochemical and optical to name a few) which converts the

analyte-bioreceptor interaction into an electrochemical or optical signal.[49,50] Biosensors have found applications in clinical, environmental, industrial and agricultural sectors due to their high sensitivity, selectivity, good stability, low cost and fast response time.[3,51,52] Their small size is also an advantage as they can be carried anywhere.[5,16,53] Electrochemical biosensors are based on electrochemical transduction and they include amperometric, impedimetric and potentiometric methods. Other types include optical biosensors (which uses light and colour as transducing methods), quartz crystal microbalance biosensor (which uses change in mass as transduction signal) etc. Biosensors can also be classified based on the bioreceptor used. In this case we have examples such as enzymatic, DNA, immunosensors and tissue-based biosensors.[47,50]

Biosensors are sometimes classified based on the methods used to acquire the bio-recognition event. In this case we have the label biosensors and label-free biosensors. Label-based transducers are those that uses foreign molecules that are chemically attached to the target molecule to detect molecular presence or activity.[54] Label-based transducers involves the use of expensive labels and labelling procedures. When the label is directly attached to the bioreceptor, it alters its binding properties, and labelling the bioreceptor causes the biosensor to produce a non-specific signal.[1,55] Label-free biosensors are those based on measuring the changes in either current, electronic or surface properties when the target molecule directly bind to the bioreceptor (i.e. enzymes) without the help of a label probe.[54] Even though most people use label-free biosensor, its lack of significant changes when recognizing the bioreceptor-target interaction event is a problem.[1,56] The biosensor reported in this dissertation falls under the enzyme biosensor category. The first enzymatic biosensor was introduced back in 1962 by Clark and Lyons.[16,51,57] Where glucose oxidase was immobilized on amperometric oxygen electrode for the detection of glucose.[57]

2.5 ENZYMES

Enzymes are catalytic proteins which accelerate or catalyse bio-chemical reactions by lowering the activation energy needed to convert substrate into products. Almost

all metabolic processes require enzymes so that the reactions can take place fast enough to sustain life. Enzymes differ from other catalysts by being much more specific when targeting. Generally, enzymes are globular proteins with linear chains of amino acids that folds to produce a three-dimensional (3D) structure. During bio-chemical reaction, the substrates is first recognized by a binding pocket in a similar way to that of antibody-antigen interaction before the redox reaction occurs. This enzymatic redox reaction can be used in amperometric electrochemical biosensors, where the consumption or generation of the electrons can be used to determine the concentration of the substrate through the measured current. The most commonly used enzymes in biosensors are glucose oxidase (GOx), cholesterol oxidase(ChOx) and horseradish peroxidase (HRP).[16]

Enzymes are compatible with several transducing methods and they have the ability to catalyze large number of reactions and detect a group of analytes. Since they are not consumed during chemical reactions, the biosensor can be re-used several times. Compared to other common binding techniques, enzymatic biosensors have lower detection limits. Thus enzyme-based biosensors have recorded more success than other types of electrochemical biosensors. However, enzyme based sensors still have some drawbacks such as stability, enzyme bioactivity and low loading capacity associated with them and they are also very sensitive to their environment.[13-16]

2.5.1 Cholesterol oxidase (ChOx) enzyme

ChOx (3β-hydroxysterol oxidase, EC 1.1.3.6) is an alcohol dehydrogenase/oxidase compound that belongs to the glucose–methanol–choline oxido-reductase family. It's a flavin-adenine-dinucleotide (FAD) containing flavoprotein that catalyses the dehydrogenation of C(3)-OH from cholestane molecules to yield the corresponding carbonyl product (cholestenone) and hydrogen peroxide.[58] During the oxidation of cholesterol, the enzyme cofactor, FAD, is first reduced by accepting a hydride from the substrate. Thereafter transfers the redox equivalents to molecular oxygen in the system yielding hydrogen peroxide. This enzyme also catalyses the isomerization of cholest-5-en-3-one (one of the product of the redox reaction) to cholest-4-en-3-

one.[58] ChOx contain large buried hydrophobic pockets which are protected from the external environment by number of loops with higher mobility than the rest of the protein structure.[59] The hydrophobic pockets of the protein are used to accommodate the steroids (substrate) ring system during catalysis. ChOx active site (binding domain) is positioned over the isoalloxazine ring of FAD-cofactor, consist of eight-stranded β-pleated sheet and six α-helices and also form a crown-like shape site where catalysis and oxidation of cholesterol occurs.[60] Many microoganisms such as streptomyces hygroscopicus and brevibacterium sterolicum have been used as ChOx sources. Fig. 2.2 shows schematic representation of ChOx from Streptomyces.

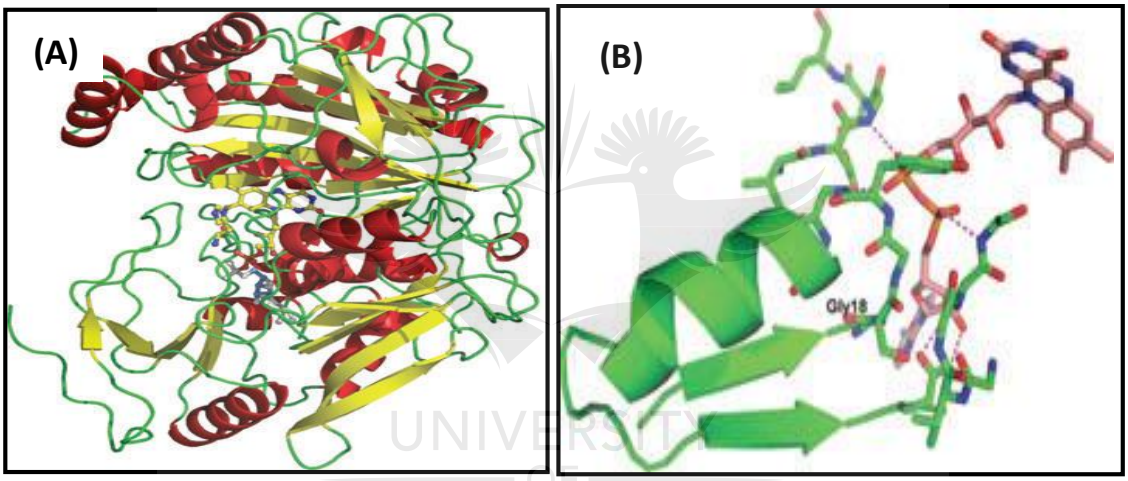

Figure 2. 2: Schematic representation of 3D structure of cholesterol oxidase showing the active-site protected by the loops. (A) Ribbon cartoon, (B) stick atomic representation of Streptomyces from ChOx showing the interaction between the protein and the FAD cofactor.[42]

ChOx catalyzes the oxidation of cholesterol in three chemical steps: The first catalytic step is called reductive half-reaction, where there is hydrogenation of alcohol (OH) group from carbon (C3) of the steroid ring. As a results, two redox electrons (equivalents) are transferred to the FAD-cofactor which then become reduced during the process. In the second step, called oxidative half-reaction, the reduced FAD react with molecular oxygen to regenerate the oxidized enzyme and hydrogen peroxide (H_2O_2) and the substrate is converted into an intermediate cholest-5-en-3-one (e.q 2.1). Finally, the oxidized steroid undergoes isomerization

of the double bond at carbon C5-6 and C4-5 of the steroid ring system, forming the final product cholest-4-en-3-one. The by-product, H_2O_2 is further reduced to produce oxygen, hydrogen ions and electrons as shown in eq. 2.2.

Step 1:

$$S + E\text{-}FAD \rightarrow E\text{-}FAD\text{-}S \rightarrow E\text{-}FADH_2 + P$$

$$E\text{-}FADH_2 + O_2 \rightarrow E\text{-}FAD + H_2O_2 \qquad \text{eq.2. 1}$$

Step 2:

$$H_2O_2 \rightarrow 2H^+ + O_2 + 2e^- \qquad \text{eq.2. 2}$$

Where S is the substrate (cholesterol), E is the enzyme (ChOx), FAD is It's a flavin-adenine-dinucleotide.

2.6 ELECTROCHEMICAL ENZYMATIC BIOSENSORS

Electrochemical enzymatic biosensors are biosensors that combine the high specificity of an enzyme with the sensitivity of electrochemical transducers to determine the concentration of the analyte in the sample. The principle of electrochemical methods is based on the redox reaction that occur between the analyte and the enzyme which produces either ions or electrons. The redox process results in the change in electrical conductivity of the supporting electrolyte. A typical enzymatic biosensor is designed by immobilization of the enzyme on the transducing surface to recognize and bind to its complementary molecule, thus producing an analytical signal through electrochemical transducers. Depending on the measurable property, electrochemical biosensors can be classified into amperometric, potentiometric and conductometric sensors.[16,48,57]

Potentiometric biosensors measures the potential charge accumulated at the working electrode compared to that of the reference electrode in an electrochemical cell. This happens when no current is flowing between these two electrodes.[16,61,62] It provide information about the ionic activity of an electroactive species in a cell. It

uses Nernst equation in eq 2.3 to relate the concentration of the electroactive species to the potential obtained.[16,62]

$$E_{cell} = E_0 - \frac{RT}{nF} \ln Q \qquad \text{eq.2. 3}$$

Where:

E_0 is the constant potential contributed to the cell.

E_{cell} is the observed potential when no current is flowing

R is the universal gas constant (8.314 $J.K^{-1}.mol^{-1}$)

T is the absolute temperature (K)

F is the Faraday constant (96485 C)

n is the number of electrons transferred.

Q is the ratio of ion concentration at the anode to the ion concentration at the cathode.

Ibupoto and co-workers fabricated highly stable, sensitive and selective potentiometric cholesterol biosensor using the nanostructured Co_3O_4 material.[63] The biosensor had a sensitivity of -94.031 $mV.decade^{-1}$, detection limit of 0.035×10^{-7} M and a fast response of 10 s.[63] Another potentiometric biosensor was developed by Nikoleli, where they immobilized polymeric lipid membranes onto a graphene electrodes to assist in enzymatic cholesterol detection.[64] Their proposed biosensor had good reproducibility, selectivity and high sensing capability. And because it was fabricated using biocompatible polymeric membrane, it had potential to be used in real blood samples and other biological applications.[64]

Conductometric or impedance biosensors measure the ability of an electroactive analyte to conduct electrical current between the electrodes and the solution at a

fixed or variable frequency. These kind of biosensors are mostly used in enzymatic biosensors, where the conductivity (ionic strength) of a solution between two electrodes changes as a result of enzymatic reaction.[61] when the target molecule adsorb on the electrode surface, the impedance undergoes detectable signal change. It causes the current to decrease because the adsorbed molecule act as an insulator and increases electron transfer resistance when using a redox couple probe such as ferri/ferrocyanide. The unstable ionic background of clinical samples and the requirement to measure only small conductivity changes in media of high ionic strength, makes it difficult for these type of sensors to be used in clinical analysis.[61,65]. Conductometric sensors are mostly used for environmental monitoring and agriculture. Most of these bioreceptors impede the conductivity of the electrode because they are not that conducting. Singh developed a bi-enzymatic impedance biosensor for total cholesterol estimation using polyprole and platinum nanoparticles as immobilization material.[66] The biosensor had detection limit of 2.5×10^{-4} ML^{-1}, response time of 25 s, sensitivity of 196 ΩmM^{-1} cm^{-2} and a linear range of 2.5×10^{-4} - 6.5×10^{-3} ML^{-1}.

Amperometric enzyme biosensors are electrochemical biosensors that measure current resulting from electrocatalytic biorecognition process between the enzyme (ChOx) and the substrate (cholesterol) at a constant potential. [16,61,67,68] These type of biosensors have higher sensitivity than potentiometric sensors.[16] The measured current is always proportional to the analyte concentration in the solution. Lot of researchers have worked on amperometric cholesterol biosensors. Lata *et al*. exploited the conductivity of gold nanoparticles and carboxylated carbon nanotubes to develop amperometric cholesterol biosensor.[69] The biosensor was based on immobilization of cholesterol esterase (ChE), ChOx and horseradish peroxide (HRP) on the electrode for the hydrolysis, oxidation and elimination of interferences from cholesterol serum, respectively.[69] Nantaphol and co-workers developed a novel paper-based electrochemical cholesterol biosensor using silver nanoparticle-modified boron-doped diamond (AgNPs/BDD) electrode.[70] The filter paper was wax printed to separate the hydrophillic and hydrophobic area of it, AgNPs/BDD electrode was used as the working electrode and the reference and counter electrodes were then screen-printed on the hydrophillic area of the paper. For

amperometic detection of cholesterol, the enzyme ChOx and cholesterol were drop-casted on the hydrophillic area of the filter paper and the production of hydrogen peroxide (H_2O_2) from from the reaction was monitored via the changes in current produced. The novel biosensor had a sensitivity of 49.61μA.$mM^{-1}cm^{-2}$, low detection limit of 0.25 mg.dL^{-1} and a linear range of 0.39 – 270 mg.dL^{-1}.[70]

Indeed, electrochemical enzymatic biosensors have found applications in clinical and environmental analysis. However, there is a need to improve the performance of enzyme biosensors in terms of sensitivity, selectivity and detection limit.[16,61] Therefore, factors such as electrode material, immobilization platform, and immobilization chemistry are considered in improving the biosensor's perfomance.[71]

2.7 ENZYME IMMOBILIZATION CHEMISTRY

Most enzymes are unstable outside their "normal" environment and this hampers their industrial, clinical,environmental and agricultural applications.[72] Thefore, there is a large room for improvement in enzyme technology. For enzymatic biosensors to perform well, certain parameters should be carefully optimized. One of the most important step in developing enzymatic electrochemical bisensor is finding a fixed suitable cost-effective solid support immobilization matrice where the enzyme can be "comfortable" and stable.[72] This will help it to retain its bioactivity for longer, hence its electrochemical properties will be maintained.[72] Immobilization techniques play a critical role in retaining the enzyme bioactivity and also in operational behaviour of enzyme-based electrochemical biosensors. Immobilized enzymes have advantages such as high resistance to both operation and storage environmental conditions (e.g pH. temperature, etc.), allows reusability of the enzyme, allows rapid termination of enzymatic catalytic reaction by removal of the enzyme from the reaction solution and also allows easy separation and recovery of both the enzyme and products, hence product contamination by the enzyme is minimized or completely avoided.[16,72-75] Therefore, one can conclude that enzyme immobilization increases the productivity of biocatalysts and enhances their features, making them more attractive for wide applications.[72]

There are a lot of immobilization techniques used to attach enzymes on transducing element surface. These techniques includes entrapment, covalent binding using cross-linkers and physical adsorption.[75-77] Immobilization techniques exploits the different functional groups found on the side chains of these amino acids to bind it to the solid support through various linkages and interactions. The choice of immobilization technique depends on many factors such as the transducer used, nature of the enzyme, operating conditions, physicochemical properties and the stability of the enzyme under extreme environmental conditions. [53]

2.7.1 Covalent bonding

This technique involves the formation of covalent bond between the functional groups on the surface of the biomolecule and the supporting matrix. Enzymes contain functional groups such as amino, thiols, carboxylic, and phenolic groups which can be used for covelent bonding unto the supporting material. Covalent binding of the enzymes on a transducing material is more stable than other immobilization techniques. This technique is employed to achieve better density, uniformity and homogenous distribution of the enzyme on the supporting matrix to obtain an improved reproducibility and biosensor with higer acitivity.[78] This method overcomes the drawbacks of aggregation, leaching and poor stability observed in physical adsorption. Rahman covalently immobilized ChOx and HRP on poly (thionine)-modified GCE via the $–NH_2$ on the polymer and the NHS/EDC activated carboxylic group (COO^-) of ChOx and HRP forming a strong amide bond between the poly (thionine) and the enzymes.[79] A reusable and mediator free cholesterol biosensor was fabricated by Rahman by covalently immoblising ChOx on thioglycolic acid-self-assembled monolayer (TGA-SAM) via peptide conjugation. The amide bond between the enzyme ChOx and the TGA-SAM is formed from the carboxylic group ($-COO^-$) of the TGA and the amine group ($-NH_2$) of the enzyme.[80]

2.7.2 Adsorption

Adsorption on the supporting material can either be physical or electrostatic. It involves weak binding forces such as electrostatic interactions, ionic bonding, van der Waals interactions and hydrogen bonding.[72] This method is simple and

straightforward, and can be used under mild conditions. It is cost effective, retains high enzyme activity and involves relatively chemical-free enzyme binding.[81,82] Although, the method is simple, it has drawbacks such as enzyme leaching during operation due to washung, pH and temperature changes and also mechanical agitation. Adsorption can be done either by drop-coating or drip-coating.[83,84] In dip-coating, the supporting matrix is soaked into the solution of the enzyme and incubated to allow time for physical adsorption to occur. In drop-coating, the enzyme solution is dropped on the electrode surface, allowed to dry then washed off of the loosely held enzyme.

2.7.3 Entrapment

Entrapment involves the localization or entrapment of the enzyme within a supporting matrix such as fibers, lattice structure of a material or a polymer that allows the substrate and product to pass through except the enzyme.[85] In general, enzymes are mixed with monomer solution and then polymerised to gel-shape structure, where the enzyme is trapped in the gel. Materials such as nafion, chitosan, polyaniline, graphene and starch have been used as the trapping material.[75,86-88] Entrapment improve mechanical stability, minimize enzyme leaching and since the enzyme does not chemically interact with the polymer, enzyme denaturation is avoided.[89] One major drawback of this approach is decrease in reactivity of the enzyme or slow reaction kinetics.

2.8 NANOMATERIALS IN BIOSENSORS DEVELOPMENT

Nanomaterials are objects with at least one dimension in the nanometer range (1-100 nm). Based on the confinement of quasi-particle or particles in a particular direction, nanomaterials can be classified into 1) zero-dimensional (0D): for example quantum dots, nanoparticles, nanocapsules, fullerenes. 2) One-dimensional (1D): for example nanowire, nanotubes, nanorods. 3) Two-dimensional (2D): for example nanosheets, nanoplates, nanowalls, nanodisks.[90] These materials have found applications in various fields such as manufacturing, energy, water treatment, biomedicine, etc. due to their interesting properties (electrical, mechanical, chemical, optical, etc.). In biomedicine, nanostructured materials have been used

for the development of new biosensors and enhancing the performance of existing biosensors by increasing sensitivity, lowering the detection limit and also increasing the loading capacity of bioreceptor. They have found application in biosensors simply because biomolecules themselves are also nanometric material. They provide biomolecules such as enzymes and DNA with new "comfortable" environment, by optimizing the pH and of the surrounding. Nanomaterials such as noble metal nanoparticles[91], carbon nanostructures, magnetic nanoparticles and quantum dots have been extensively used for biomolecular diagnosis, drug delivery and disease treatment. Umar used magnetic α-Fe_2O_3 micro-pine shaped hierarchical nanostructures and co-immobilized them with ChOx to design a cholesterol biosensor with sensitivity of 78.56 μA μM^{-1} cm^{-2}, detection limit of 0.08 mM with a linearity of 0.1-8.0 mM.[26] Lata and co-workers exploited the conductivity of gold nanoparticles and carboxylated carbon nanotubes to develop an amperometric cholesterol biosensor which is reusable for more than 45 times.[69] It had a detection limit of 0.01 mM, uses low potential of 0.27 and was highly stable for 60 days.[69] Li fabricated ChOx/CS-GR/GCE cholesterol biosensor by covalently immobilising ChOx on chitosan-graphene (CS-GR) nanocomposite-modified GCE [92] They first immobilized Chitosan-graphene oxide (CS-GO) nanocomposite and observed that these nanocomposite blocks electron transfer, then they decided to deoxyginated the GO,obtaining pure graphene (GR) which provided excellent electron transfer than GO. When the enzyme was immobilized, an increase in Nyquist semicircle was observed and this was due to the resistance that the non-conducting enzyme causes. The presence of the nanocomposite did not only increase electron transfer, but also enhanced the amount of ChOx immobilized, showing that it provide a large surface area.[92] A new electrochemical biosensor was designed by CaO and co-workers to determine the level of cholesterol in food.[88] The biosensor consist of ChOx immobilized on platinum-palladium-chitosan-graphene hybrid nanocomposite (PtPd/CS/GS) modified glassy carbon electrode (GCE). The nanocomposite did not only enhance electron transfer, but also enhanced the amount of the enzyme immobilized, meaning that its provided large surface area.[88] The sensor exhibited great sensitivity with detection limit of 0.75 μM and a linear range of 2.2×10^{-6} – 5.2×10^{-4} M. A response time of less than 7 s and a Michaelis-Menten constant of 0.11 mM were reported.[88] Lot of nanomaterials have been

exploited in cholesterol development, but here, the focus is on the use of quantum dots (QDs).

2.9 QUANTUM DOTS (QDs)

Quantum dots are colloidal, luminescent inorganic nanocrystals semiconductors with particle size that is comparable or smaller than the exciton Bohr radius (1-10 nm).[93-95] These are zero-dimensional (0D) nanostructure, where both the charge carriers (e^- and h^+) are confined in all directions and it is this confinement that gives them excellent photophysical (optical) and photochemical (electronic) properties. It is these properties that makes them better and promising alternative to organic fluorophores in various application such as energy conversion,[94] catalysis,[93,96] material science, biological applications[94] (bio-imaging, diagnosis, biosensors, therapeutics, and drug delivery) and electronics. These nanostructured materials are mainly made up of elements from group II-VI (e.g. CdSe, ZnSe, CdTe), III-IV (e.g. InAs, GaAs) and group IV-VI (e.g. PbSe, PbTe) of the periodic table.[93] QDs can exist as only core QDs (e.g. CdTe), core/shell (e.g. CdTe/CdS), core mutlishell (e.g. CdTe/CdSe/ZnSe) and also as an alloy (e.g. ZnTeSe). QDS emits lights over a wide range of wavelengths, from visible to infrared light depending on their particle size, shape, chemical compositions and the passivating material.[97] The smaller the QDs size, the larger the band gap energy due to quantum confinement effect, and the shorter is the emission wavelength.[98] Quantum dots are also nanostructured materials with large surface area to volume ratio, therefore they can allow covalent immobilization of bioreceptor such as enzymes, antibodies, nucleic acids and peptides for biological applications. The image in Fig.2.3 shows the relationship between the QDs size and wavelength. The bigger the nanoparticle, the longer is the wavelength. Fig. 2.3 also shows an image of core/shell QDs.

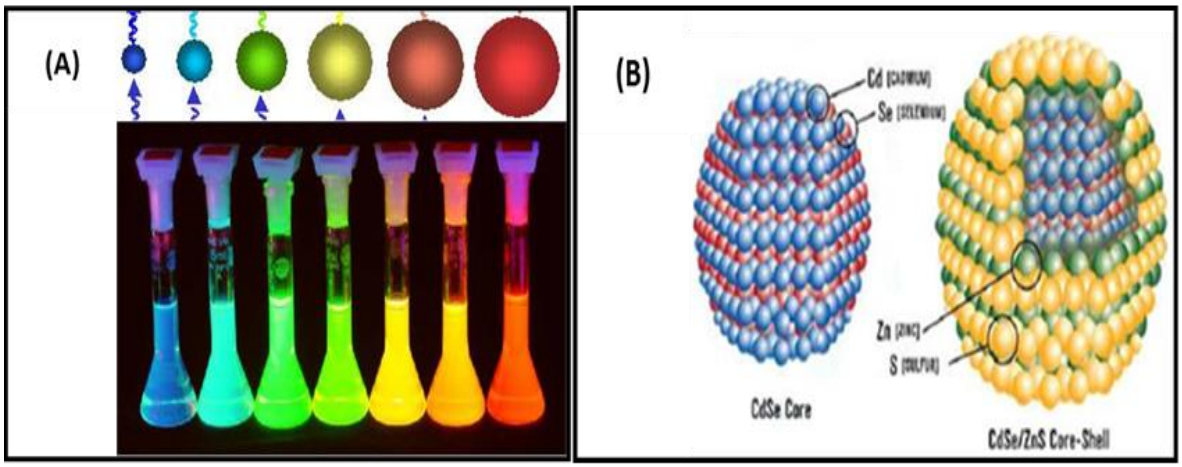

Figure 2. 3: Images of quantum dots. Quantum dots size is directly related to its wavelength, therefore is colour (A). Image of core and core/shell quantum dots (B).[99]

2.9.1 Limitations of quantum dots and surface modifications

Although quantum dots are good alternatives to organic dyes, they still have some limitations such as toxicity, low water solubility, biocompatibility, low stability and other surface defects which limits their applications in biological processes. Cadmium chalcogenide QDs have been extensively used *in vitro* and *in vivo* applications due to their versatile surface chemistry and excellent optical properties.[100,101] However, the heavy metal cadmium and selenium are very toxic to cells and living organisms hindering their applications in vivo processes.[100] In 2004, Derfus and co-workers[102] used a primary hepatocytes liver model to study the cytotoxicity of uncoated CdSe QDs. They found out that the QDs were very toxic and the toxicity was due to the release of free Cd^{2+} ions when the lattice of the QDs were deteriorating.[102] Liu, *et al*.[103] used prostate cancer PC3 cells, human breast cancer MCF7 and MBA-MD-231 cells to examine the cytotoxicity of CdTe and CdHgTe quantum dots *in vivo* and *in vitro* over 40 days. Both quantum dots were toxic to the selected cells. However, the toxicity of CdTe was both concentration and time dependent, whereas that of CdHgTe remained constant as time increase.[103] To reduce the toxicity of cadmium-based quantum dots, one can replace the toxic metal (Cd) with a non-toxic or less toxic metal element such as zinc (Zn) and indium (In) or passivate the toxic core with biocompatible, non-toxic and large bandgap inorganic material.[104-106] The quantum dots surface can be further functionalised

with hydrophilic groups such as mercaptopropionic acid (MPA), mercaptoacetic acid (MAA), peptides, polymers etc. to improve its water solubility and biocompatibility so that they may be applied in biosensors.[106-109] Passivating the QDs core with organic ligands is very difficult because the ligand cannot simultaneously passivate both the anionic and the cationic surface traps. Therefore it is better to grow inorganic semiconductor shells over the QDs and inhibit photo-oxidation.

2.9.2 Core/shell quantum dots.

One can eliminate the limitations of quantum dots listed above by growing nontoxic shells around the core QDs. Core/shell semiconductor quantum dots consist of an inner inorganic core (e.g. CdTe) that is responsible for the optical and electronic properties of the nanocrystal and a shell (e.g. CdSe) of another semiconducting material (usually one with higher band gap, E_g, than the core) responsible for protecting the active site of the core. Passivation of QDs-core with thick inorganic defect-free shell improves the optical properties and stability of the QDs by confining the charge carriers within the core/shell interface and isolating them from external environment.[110] This increases the quantum yield, prevent the nanocrystal from photo-oxidation and also reduces its toxicity. QDs can exist either as type I or type II heterostructure depending on the band gap energy of the shell and the core. In type I nanocrystal (e.g. CdSe/ZnSe), both the valence and conduction bands of the core are within the bandgap of the shell, confining both the charge carries (electrons and holes) within the core. However, in type II (e.g. CdTe/CdSe) both the valence and conduction bands of the core are either higher or lower than the ones of the shell, localising one charge carrier in the core while the other one is in the shell. Therefore, the band gap energy in type I quantum dots is smaller than the one in type II. In order to achieve low band gap energy in type II QDs, an extra shell of larger band gap (e.g. ZnSe) can be used to passivate the core/shell.[110] This will confine both the charge carriers within the CdTe/CdSe core/shell and subsequently increase indirect recombination of the excitons at the core and the inner shell interface.[110] Fig. 2.4 shows type I and type II core shell QDs.

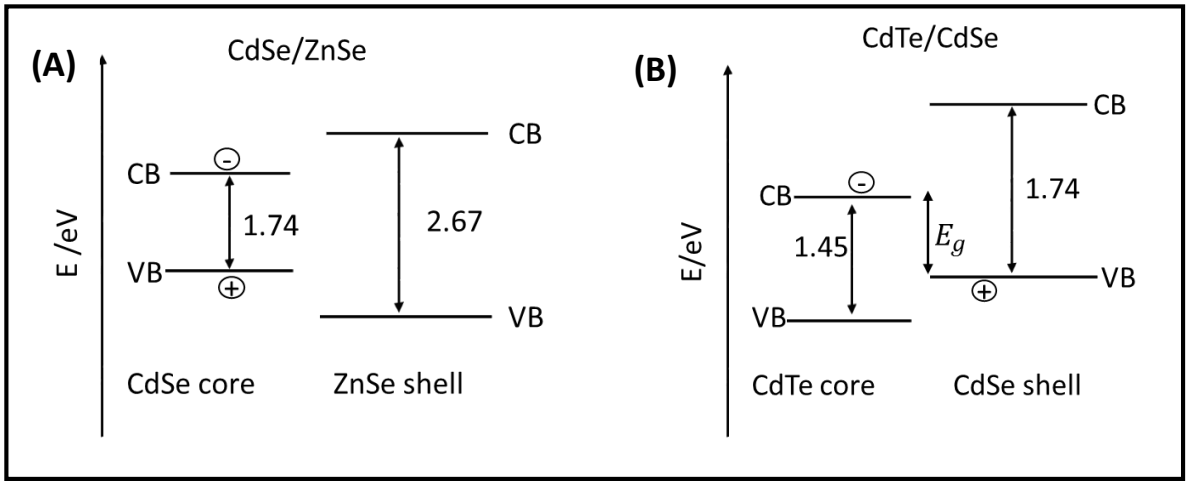

Figure 2. 4: Two types of core/shell nanostructures. Type I nanocrystal (A) and type II nanocrystal (B).

2.9.3 Synthesis of quantum dots

In the early years of QDs synthesis, QDs were mostly prepared using physical methods and the main goal was to produce high purity QDs. Over the years, new synthetic routes with controlled particle size and shape have emerged. Quantum dots have been synthesized using organometallic and aqueous synthetic methods. In organometallic colloidal synthesis (OCS), the solvents used are usually high boiling points organic solvent such as tri-n-octylphosphine oxide (TOPO), trioctylphosphine (TOP) or hexadecyal amine (HAD). This method was developed by Murray *et al.* in the early 1980s.[111] In a typical organometallic colloidal synthesis, high temperature (≈ 300 °C) are used in conjunction with organic solvents TOPO or TOP and metal/chalcogenide precursors. The coordinating solvents act as both the solvent and the ligand that cap the QDs. These ligands from the solvents attach their functional groups to the QDs surface living their alkyl chains dangling away from the QDs surface. As a result, the long chains alkyl monolayers around the QDs makes the QDs highly hydrophobic and only soluble in non-polar solvents such as chloroform, toluene and hexane. This type of QDs are prepared in inert atmosphere and requires quick hot injection of metal precursor. QDs produced from OCS are known to have high quantum yield (QY) but very poor sensing properties. OCS is a non-green synthetic method because it requires the use of hazardous chemicals ($Cd(Me)_2$, H_2Te) and high temperatures. Therefore, a “greener” method which uses

mild conditions and non-toxic metal precursors for the production of high quantum yield QDs is required. Cheap and less toxic metal precursor such as cadmium acetate (Cd $(Ac)_2$) and solvents such as oleic acid have been used to overcome the disadvantages of OCS and lower the toxicity of the nanocrystal.

In aqueous colloidal synthesis (ACS) of QDs, the TOPO or TOP capping ligand is substituted by a ligand which is water-soluble and biocompatible with biomolecules. Molecules such as amines and thiols have been used to make the QDs hydrophilic through ligand exchange. However, this ligand exchange tends to decrease the photoluminescence properties of the QDs. To overcome this problem, QDs are directly synthesized using aqueous method where water is used as the solvent and metal precursors such as Cd $(Ac)_2$ and $CdCl_2$ are used. The QDs are then capped by hydrophilic ligands such as mercaptopropionic acid (MPA), mercaptoacetic acid (MAA), thioglycolic acid (TGA) and L-cysteine (L-Cys). Fig. 2.5 shows organic and aqueous colloidal synthesis of QDs and Table 2.1 compares these two synthesis.

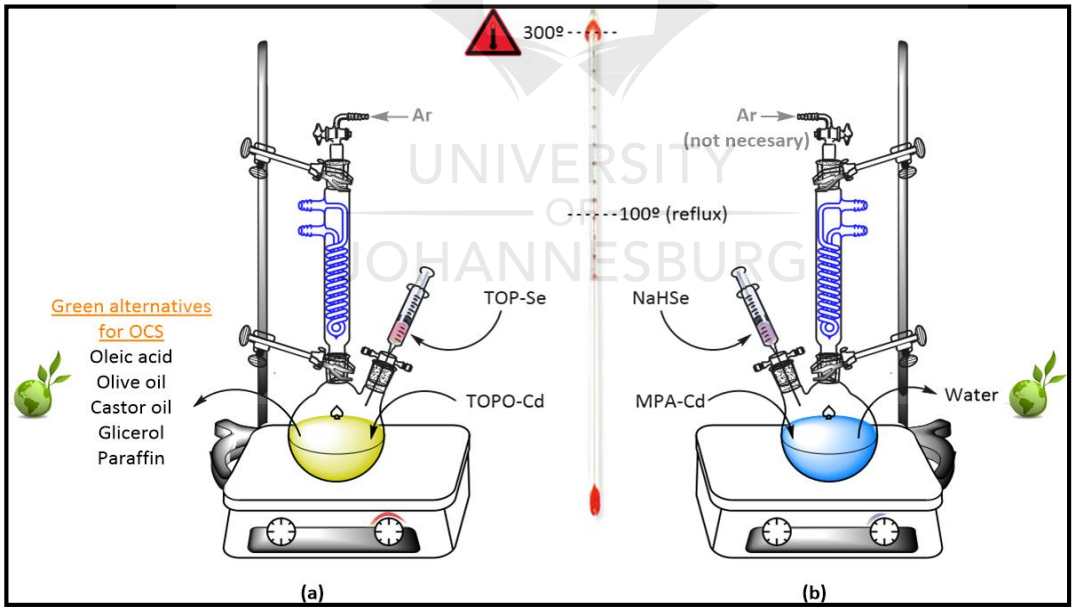

Figure 2. 5: Schematic representation of organometallic (a) and aqueous colloidal synthesis of quantum dots (b).[112]

Table 2. 1: Comparison between organometallic and aqueous synthesis of quantum dots.

Organometallic colloidal synthesis (OCS)	Aqueous colloidal synthesis (ACS)
Uses organic solvent	Uses water
Operate at high temperatures	Operate at low temperatures, even at room temperature
Produces toxic QDs	Water soluble
Produces high fluorescent QDs	Produce low fluorescent QDs
Expensive and non-green method	Cheap, easier and greener method.
	Biological and environmental applications

2.9.4 Applications of QDs in enzyme-based biosensors

Quantum dots have found applications in many fields including energy, medicine and electronics. They can interact with certain molecules in such a way that their fluorescence emission is affected, and this effect can be used as a sensing signal. QDs have also been used in detection based on Forster resonance energy transfer (FRET), where an acceptor such as QDs is excited by light absorption, and by FRET process transfer its energy to the emitter, which will reach its excited state and re-emit energy (fluoresce) when relaxing back to ground state. The effect of FRET process on the analyte can be used as the detection principle. Kim *et al.* designed a cholesterol biosensor based on the photoluminescence (PL) intensity of MPA-CdSe/ZnS quantum dots.[52] The detection was based on the quenching of PL intensities as cholesterol concentration increases. This is due to the collisional quenching by H_2O_2 produced from the enzymatic reaction between ChOx and cholesterol.[52] Dhyani *et al*. developed an electrochemical biosensor using polyaniline (PANI) and CdS. ChOx was covalently immobilized on the PANI-CdS

matrix for a successful detection of cholesterol.[113] The biosensor response was studied using CV and EIS which showed an increase in charge transfer behaviour of the nanocomposite. A linear range of 50 to 500 mg.dL^{-1}, a detection limit of 47.8 mg.dL^{-1} and a Mechaelis constant of 0.82 mM were obtained from the ChOx/PANI-CdS/ITO bioelectrode.[113] Stewart *et al.* developed an electrochemiluminescence (ECL) cholesterol biosensor based on near infrared (NIR) 2- (dimethylamino) ethanthiol (DAET) capped CdSeTe/ZnS (800 nm) incoperated into a chitosan film.[114] The biosensor displayed a linear range response of 0.25 to 5 mM and showed a strong ECL signal at -1.35 V vs. Ag/AgCl.[114] This sensor showed a good linear dependence on cholesterol concentrations over clinically relevant range, thus it has a potential of being used in clinical analysis. An oxygen-sensitive photobioelectrochemical glucose biosensor was designed by Tanne et al. using CdSe/ZnS nanocrystal.[115] The biosensor was used to monitor the consumption of oxygen during oxidation of glucose catalysed by glucose oxidase (GOx) enzyme.[115] When the biosensor was illuminated with light, a cathodic photocurrent peak was obtain and the signal is suppressed as more oxygen is consumed. This means that more glucose is oxidized. The biosensor had a short time analysis and a linear range of 100 µM to 5 mM.[115]

2.10 DENDRIMERS

Dendrimers are novel three dimensional (3D), hyper-branched, monodispersed, globular nanometric synthetic macromolecule with “container-like” properties obtained by re-iterative sequence of reactions.[116,117,118,119] One dendrimer is made up of three regions: a core, inner shell and outer shell. Outside the core, branches of other atoms called “dendrons” continue to grow through various chemical reactions resulting in a branched structure called “generation”. These novel hyperbrached macromolecules were first discovered by Fritz Vogtle in 1978 and later by Donald Tomaila and co-workers in the early 1980s. Dendrimers are classified according to their generations (number of the repeated branches around the core). For example, a dendrimer with four repeated braches around the core is called a generation four (G4) dendrimer. The higher the generation number, the higher the molecular weight and the more exposed are the functional groups where

biomolecule materials can attach. Dendrimers are generally synthesized using either convergent or divergent method.[119]

Dendrimers are not the first class of materials to be used to provide a “comfortable” environment for biomolecules. Molecules such as cyclodextrin[120,121], chitosan[120-122], and conducting polymers[66,79,123] have also been exploited, but their limitation arises when they cannot provide the sort of “nanoenvironment” present in proteins. Higher molecular weight linear polymer matrices cannot deeply penetrate into the active sites of biomolecules because these biomolecules are also surrounded by matrix of large molecular weight and also these polymers are mainly hydrophobic in nature and their sizes are more than 100 nm. Materials that have similar size to biomolecules and excellent conductivity are thus needed to reach out to the active site of the biomolecule. Dendrimers are the closest synthetic analogues of small enzymes in terms of their size, functional complexity and structural precision. Dendrimers are friendly to biomolecules such as enzymes because of their biocompatibility, nanoscopic size and large surface area-to-volume ratio, cationic nature and have multiple attachment sites[119,124].

Currently, dendrimers are becoming more popular as nanomaterial stabilising agent or biomolecule vehicle. This is due to the high loading capacity in their nanoscale cavities and hundreds of dendritic active-sites in the outer shell.[116,119,124] Most dendrimers are amphiphilic in nature, with the interior being hydrophobic and the exterior hydrophilic.[117] Thus, they enhance the solubility of the material capped by it.[116] unlike most conventional polymers, dendrimers can be functionalised on their surfaces (periphery) to improve their water solubility, control their toxicity, crystallinity and chirality and increase their chemical reactivity. They can also be customised to suit particular application. Most dendrimers have found application in drug delivery, gene delivery, sensors, solar cells and cancer treatment. Fig. 2.6 shows the schematic representation of G3 dendrimer.

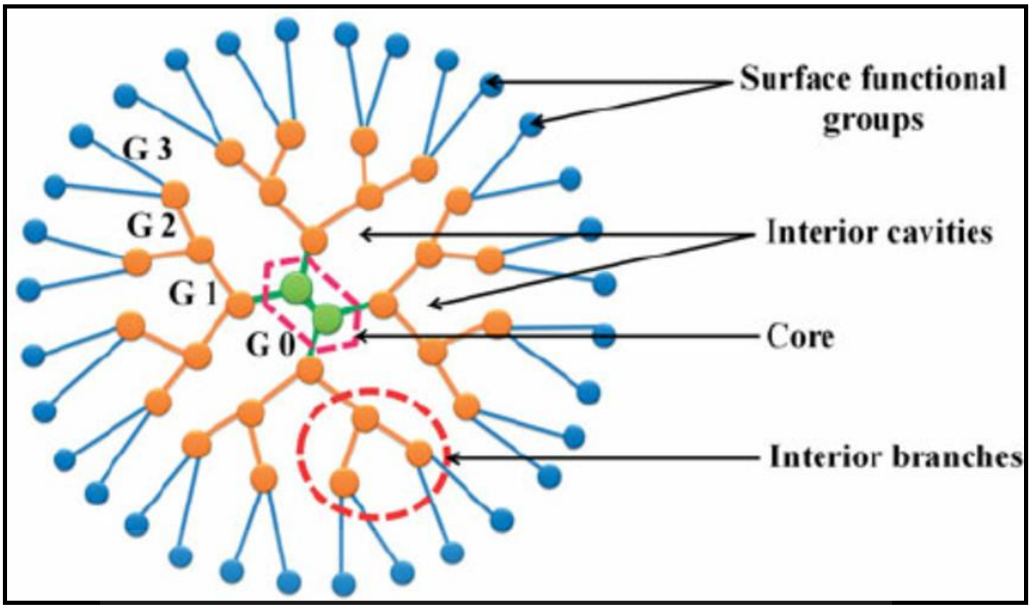

Figure 2. 6: Schematic representation of a typical dendrimer with three generations (G3).[125]

2.10.1 Poly (propylene imine) (PPI) dendrimer

Poly(propylene imine) dendrimers were first synthesized by de Brabander-van den Berg *et al.* where they were trying to improve the method proposed by Vogtle to produce dendrimertic structure.[126] They produced a large scale of pure PPI which could not be obtained using Vogtle method.[126] PPI dendrimers are sometimes called "DAB dendrimers" (Diaminobutane) or POPAM (Poly(Propylene Amine)).[127] PPI dendrimers are poly-alkyl amines with primary amines as the end groups and the interior is made up of numerous tertiary amine moieties. PPI is one of the notable and fascinating dendrimer that is compatible with bioreceptor elements such as enzymes and DNA and has been used in bio-sensing to improve the performance of biosensors. Due to the presence of easily accessible multiple amine terminals (-NH_2), PPI is ideal for construction of star-shaped polymer conjugations and can be applied in biosensor platform for fabrication of enzyme based biosensors. Their high surface area and solubility makes them ideal catalysts. The dendritic shell can provide a micro-environment that is favourable for catalytic reactions, therefore they exhibit characteristics that are associated with homogenous catalysis such as specificity, fast kinetics and solubility. Some information about each generation of

the PPI dendrimers known are listed in Table 2.3. Fig. 2.7 shows generation two (G2) PPI dendrimer.

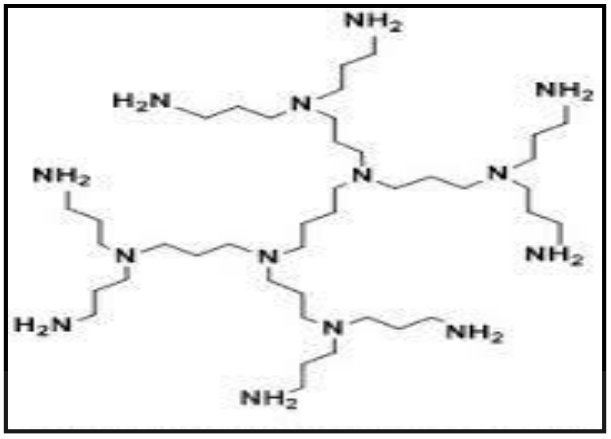

Figure 2. 7: Schematic representation of generation two (G2) dendrimer. The interior is made up of tertiary amines while the exterior is made of reactive primary amine end groups.

Table 2. 2: Information about different generations of poly (propylene imine) dendrimers.

Dendrimer generation(G)	Molecular weight (g/mol)	Molecular formula	Number of periphery NH_2	Interior tertiary amines	Diameter (nm)
1	316.5	$C_{16}H_{40}N_6$	4	2	1.22
2	773.3	$C_{40}H_{96}N_{14}$	8	6	1.76
3	1686.8	$C_{88}H_{238}N_{30}$	16	14	2.36
4	3513.9	$C_{104}H_{432}N_{62}$	32	30	3.12
5	7168.1	$C_{378}H_{880}N_{126}$	64	62	3.96

When using the dendrimer, the nanoparticle and biomolecules can either be non-covalently encapsulated on the dendrimer cavities or covalently attached to the dendritic surface of it. The study here demonstrate the use of G4 poly (propylene imine) dendrimer (G4-PPI) to control the orientation of the biomolecule on the

surface of the electrode and also to increase the surface area of the sensing platform. PPI is chosen because of its good water solubility, biocompatibility and high loading capacity for the nanoparticles.[124,128] The other problems with quantum dots nanocrystals is their uncontrolled arrangement at a nanoscale and this has an impact on the final properties of the nanoparticles, hence its application. Therefore, the dendrimer is used to help arrange the quantum dots at a nanoscale for application in electrochemical biosensors. The flexibility structure of the dendrimer allows incorporation of almost any kind of nanoparticle (e.g. QDs) in its template and this could lead to an improvement in the optical properties of the hybrid material.[128] It can also increase the life time of proposed biosensor by encapsulating a large amount of the enzyme and releasing it at a slower rate.

CHAPTER 3

EXPERIMENTAL METHODOLOGY

3.1 LIST AND SOURCES OF CHEMICALS AND MATERIALS

Cadmium acetate ($Cd(Ac)_2$), potassium tellurite (K_2O_3Te), zinc acetate ($Zn(Ac)_2$), 3-mercaptopropionic acid (MPA), sodium borohydride ($NaBH_4$), sodium hydroxide (NaOH), selenium powder (Se) and sodium sulphite (Na_2SO_3), redox probe ($K_3Fe(CN)_6$, $K_3Fe(CN)_6$)), KCl, (1-ethyl-3-(3-dimethylaminopropyl) carbodiimide hydrochloride (EDC), N-hydroxysuccinimide (NHS), phosphate buffer components (K_2HPO_4, KH_2PO_4), cholesterol oxidase from *Streptomyces species*, EC, cholesterol 1 × 1 mL chloroform 10 $mg.mL^{-1}$, alumina powders, and platinum wire (Pt) were all purchased from Sigma Aldrich, generation 2 (G2) (propylene imine) dendrimer from SyMO-Chem, screen printed carbon electrode (SPCE) from DropSens, and glassy carbon electrode (GCE) and Ag/AgCl (3 M Cl^-) electrode were from BASi. All chemicals were of analytical grade and used as purchased. Ultra-pure water from Millipore synergy water purification and deionized water were used throughout the synthesis and biosensor design.

3.2 RESEARCH DESIGN

This research project is based firstly on the synthesis and characterization of MPA-capped CdTe/CdSe/ZnSe quantum dots. Then sequential steps involving these nanoparticles (QDs) and poly (propylene imine) dendrimer are followed to develop an enzyme-based electrochemical biosensor. Electrochemical measurement were carried out after every modification/fabrication step to check if the expected results are obtained. The expected results were based on the theory obtained from literature. The following flow diagrams (Fig. 3.1) summarizes the research design of this project.

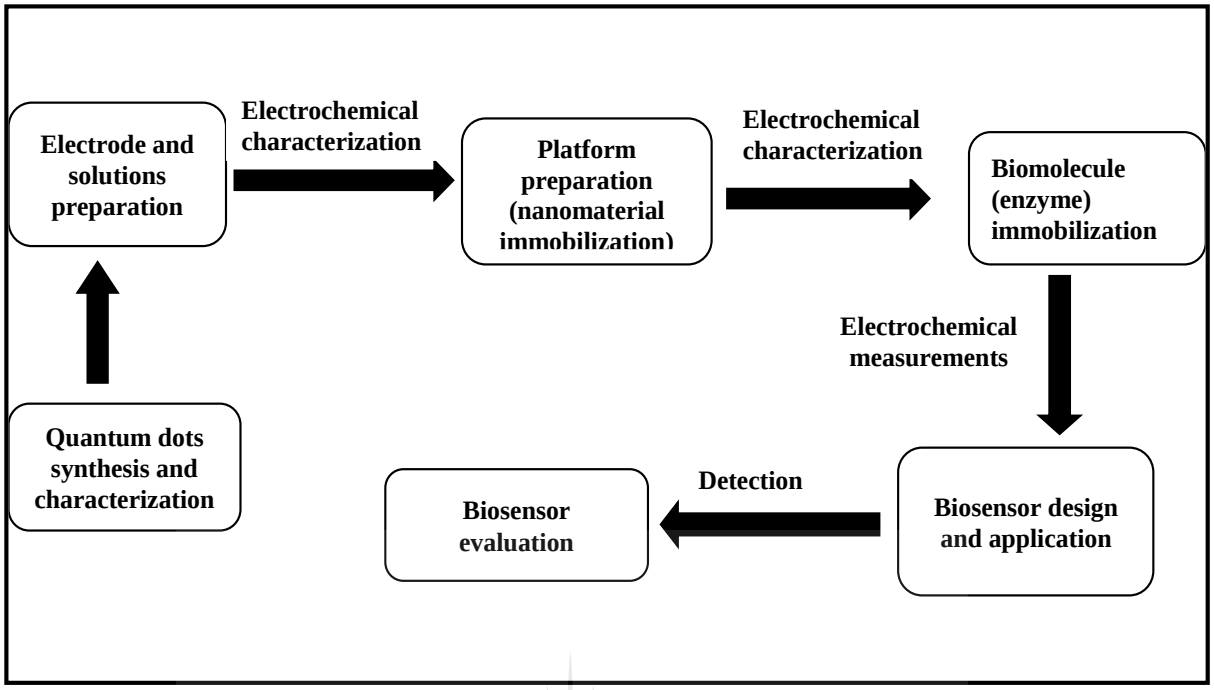

Figure 3. 1: Flow chart of research design.

The following steps were used in carrying out this project:

1. Quantum dots synthesis and characterization: This step involves the synthesis and characterization (using TEM, PL, UV-Vis, XRD, CV and EIS) of CdTe/CdSe/ZnSe quantum dots (QDs).

2. Electrode and solution preparation: This step involves the cleaning and electrochemical measurements of bare glassy carbon electrode (GCE) to confirm its cleanliness in the presence of PBS.

3. Modification and characterization of bare GCE: This step involves the modification of GCE with PPI dendrimer and CdTe/CdSe/ZnSe QDs. PPI dendrimer was electrodeposited on the electrode surface followed by drop-drying of QDs. After every modification, the electrode was characterized using CV, SWV and EIS.

4. Enzyme immobilization: Drop and dry method was used to immobilize the ChOx enzyme on the modified electrode.

5. Biosensor design and application: This step involves the sensing of the analyte (cholesterol) using electrochemical methods such as cyclic voltammetry (CV) and square wave voltammetry (swv).

6. Biosensor evaluation: This involves checking the stability of the biosensor, its sensitivity, detection limit and selectivity towards the analyte.

3.3 GENERAL EXPERIMENTAL

3.3.1 Electrode cleaning

Prior to electrochemical utilization, the working glassy carbon electrode (GCE) was cleaned consecutively with aqueous slurries of 1.0, 0.3 and 0.05 µm alumina powders, respectively on a micro-cloth pad and then rinsed thoroughly with doubly distilled water between each polishing step. Residual polishing material on the electrode was removed by washing successively with a solution of ethanol and distilled water (1:1) in an ultrasonic bath, air-dried and then used immediately for measurements. The cleanliness of the electrode surface was confirmed by running cyclic voltammetry (CV) measurements in PBS solution (pH 7.2) from -0.3 V to 1.0 V at a scan rate of 50 $mV.s^{-1}$, where no peak was obtained.

3.3.2 Preparation of 10 mM potassium ferri/ferrocyanide as ($[Fe(CN)_6]^{-3/-4}$) in 0.1 M KCl solution.

Ferrocyanide solution was prepared by dissolving 0.823 g $K_3[Fe(CN)_6]$, 1.056 g $K_4[Fe(CN)_6]$ and 1.864 g KCl in a 250 mL volumetric flask containing distilled water. Making an electrolyte with concentration ratio of (1:1:10) ferri/ferrocyanide: KCl. This solution was used as $[Fe(CN)_6]^{-3/-4}$ electrolyte.

3.3.3 Preparation of 10 mM phosphate buffer saline (PBS) solution.

Phosphate buffer saline solution (10 mM, pH 7.2) was prepared by dissolving 1.361 g KH_2PO_4, 1.742 g K_2HPO_4 and 22.365 g KCl (0.3 M) in 1000 mL volumetric flask

using double distilled water. 0.1 M HCl and 0.1 NaOH were prepared and used to adjust the pH of the solution to the desired pH.

3.3.4 Preparation of poly (propylene imine) dendrimer (PPI) solution

Poly (propylene imine) dendrimer (10 mM) was prepared by dissolving 0.773 g of PPI into 100 mL of PBS (pH 7.2) solution and stored in the refrigerator when not in use.

3.3.5 Preparation of cholesterol oxidase (ChOx) enzyme solutions

Cholesterol oxidase (20 $mg.mL^{-1}$) solution was prepared in PBS (pH 7.2) and stored at 4 °C when not used. From the 20 $mg.mL^{-1}$ solution, other concentrations of the enzymes were prepared (1, 2, 4, 6, 8, 12 $mg.mL^{-1}$) for optimization studies. The solution was prepared in 10 mM PBS (pH 7.2).

3.3.6 Preparation of cholesterol solution

Triton-X 100 (5 mL) and of isopropanol (5 mL) were mixed and heated at 50 °C and then 0.193 g of cholesterol was slowly added to the solution until fully dissolved. Then, 40 mL of 10 mM PBS (pH 7.2) was added with continuous stirring to produce 10 mM stock solution of cholesterol. Different concentrations of cholesterol were prepared by proper dilution of the stock solution using the ratio 1:1:8 triton-X 100: isopropanol: PBS.

3.3.7 Preparation of Rhodamine 6G dye solution

The stock solution of Rhodamine G6 dye (0.1 M) was prepared by dissolving 2.395 g in 50 mL of ethanol. For determination of quantum yield (QY) parameters, the concentration of the dye was varied by diluting with ethanol until its absorbance at 450 nm was around 0.07. This lower concentration was used for quantum yield determination to prevent the sample from self-quenching.

3.3.8 Electrochemical cell assembly

A three-electrode system was used to carry out all the electrochemical experiments (CV, SWV and EIS). Glassy carbon electrode (GCE) with diameter of (3.0 mm) was used as the working electrode (WE); a platinum wire (Pt) used as the auxiliary electrode and Ag/AgCl (3M Cl^-) as the reference electrode. All the solutions were degassed by bubbling argon gas through for 5 min before analysis. Fig 3.2 shows three electrode system used in this work.

Figure 3. 2: Electrochemical cell system showing the working, reference and counter electrode.

3.4 CHARACTERIZATION TECHNIQUES

3.4.1 Ultraviolet and visible light spectroscopy (UV-vis spectroscopy)

PerkinElmer Lambda 25 UV-vis spectrophotometer was used to carry out the absorption spectra of the as-synthesized QDs in the 200-900 nm wavelength range at room temperature with a resolution of 1 nm and scanning speed of 480 $nm.min^{-1}$. During analysis, QDs samples were placed in a quartz cuvette of 1 cm path length.

UV-vis was used to monitor the growth of CdTe core, CdTe/CdSe core/shell and CdTe/CdSe/ZnSe core/multishell quantum dots at different reaction time.

3.4.2 Photoluminescence spectroscopy (PL)

Shimadzu RF-6000 photoluminescence spectrophotometer was used to monitor the photoluminescence properties and the growth of the as-synthesized quantum dots from 200 – 900 nm wavelength. The samples were placed into a quartz cuvette and analysed at an excitation wavelength of 450 nm. Determination of quantum yield (QY) of the QDs was achieved by comparing the integrated emission peak areas (F) of the QDs in deionized water to that of Rhodamine 6G dye in ethanol. The QY of QDs was calculated using the following equation:

$$\boldsymbol{\Phi = \Phi_{Ref} \times \frac{F}{F_{ref}} \times \frac{A_{ref}}{A} \times \frac{\eta^2}{\eta^2_{ref}}} \qquad \text{eq.3.1}$$

Where Φ, A, F and η (1.33) represent the PLQY, absorbance, integrated emission peak area and refractive indices of the QDs solution, while Φ_{ref} (95 % ethanol) A_{ref}, F_{ref} and η_{ref} (1.36) stand for corresponding parameters of rhodamine G6.

3.4.3 X-ray diffraction spectroscopy (XRD)

Crystalline properties of the as-synthesized quantum dots were investigated using X-ray diffractometer (X'Pert Philips) equipped with monochromatic Cu Kα (0.1540 nm). The span of the scanning process was kept within 4 ° to 90 ° range of the 2θ position with a scan step of 1 °S^{-1}. In 1918, Paul Scherrer proposed an equation and assumed that the average grain size of a particle is related to the width (β) of the X-ray diffraction peak in the following relationship:

$$D = \frac{K\lambda}{\beta \cos \theta} \qquad \text{eq.3.2}$$

Where D is the average crystallite size, K is the Scherrer constant (typical value~ 0.9), λ is the wavelength of the X-ray, and β is the line broadening at half the maximum intensity (FWHM). This equation is only applicable for materials at a nanoscale; you cannot use it for particles more than ~ 0.1 to 0.02 µM. This equation was used to determine the average particle size of the QDs.

3.4.4 Fourier transform infrared spectroscopy (FTIR)

Perkin Elmer Spectrum Two, FTIR spectrometer equipped with universal attenuated total reflectance (ART) sampling accessory was used to confirm the capping of the QDs by mercaptopropionic acid (MPA). The FTIR measurement were carried out in the transmission mode within 4000-400 cm^{-1} range with a 4 cm^{-1} resolution and 100% transmittance, maintaining a total of 50 scans for each sample analysed. All the sample were liquids and were drop-dried on the sample holder before analysis.

3.4.5 Scanning electron microscopy (SEM)

TESCAN Vega TC instrument (VEGA 3 TESCAN software) SEM instrument coupled with energy dispersive X-ray (EDX) was used to study the surface of the quantum dots, the dendrimer and the cholesterol oxidase enzyme at a voltage of 8.0 kV. It was also used to confirm successful immobilization of PPI, QDs and ChOx on screen-printed carbon electrode (SPCE). The EDX was used to confirm the elemental composition in the as-synthesized quantum dots.

3.4.6 Transmission electron microscopy (TEM)

TEM works by transmitting electrons instead of light through the sample. A high-energy beam of electrons produced from tungsten filament is shone through the sample, and the interaction between these electrons and the sample's atoms create an image of the sample. TEM (JEOL 2100 HRTEM 200 kV, Japan) was used to study the quantum dots shape, size and size distribution, composition, growth of layers and the quality of the QDs.

3.4.7 Electrochemical characterization

All electrochemical measurements were carried out using Ivium Technologies Compact-stat potentiostat (Ivium Nertherlands) using three electrodes system as described in section 3.4.8. The electrochemical techniques used were cyclic voltammetry (CV), square wave voltammetry (SWV) and electrochemical impedance spectroscopy (EIS). CV works by scanning the applied potential from

initial potential to final potential (oxidation/forward reaction) and then back to initial potential (reduction/reverse reaction) at a certain scan rate while monitoring the current produced by the redox–active species in an electrochemical cell. In SWV, the current is measured while the potential between the working and reference electrode is swept linearly in time at a certain frequency and amplitude. EIS measures the charge transfer resistance between the working electrode and the electrochemically active solution. By varying the excitation frequency of the applied potential over a range of frequencies, one can calculate the complex impedance of the system as a function of frequency. EIS combines the analysis of both imaginary and real component of impedance, which are electrical reactance and electrical resistance.[16,129] A typical Nyquist and Bode plots related to impedance spectroscopy are shown in Fig. 3.3.

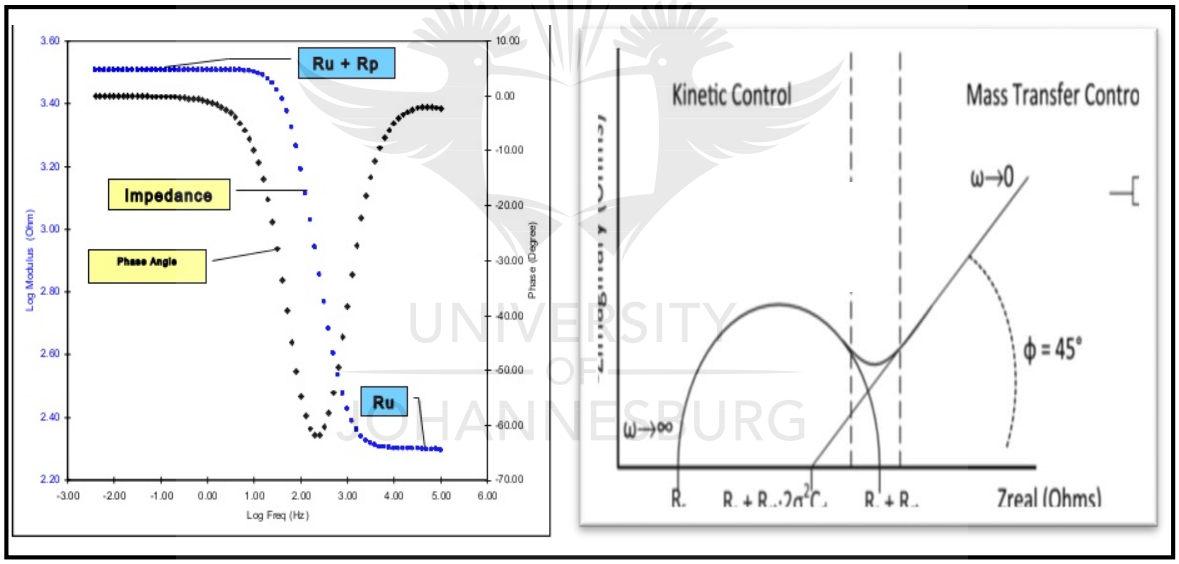

Figure 3. 3: Electrochemical Impedance spectroscopy- Nyquist and Bode plot.

CHAPTER 4

SYNTHESIS AND CHARACTERIZATION OF MPA-CAPPED CdTe/CdSe/ZnSe QDs

4.1 INTRODUCTION

This chapter focuses on characterization of MPA-capped CdTe/CdSe/ZnSe quantum dots. Several non-toxic and wide band-gap semiconducting materials such as ZnSe (3.68 eV)[24,130] and ZnS (3.8 eV)[131-133] have been employed over the years as shell materials for core quantum dots. In this work, ZnSe was employed to provide perfect passivation of CdTe core and to reduce the toxicity of the cadmium based QDs via inhibiting the release of Cd^{2+}.[134] However, the lattice mismatch between CdTe and ZnSe is large and can cause strains between the CdTe core and ZnSe shell.[134,135] The defects caused by ZnSe shell have negative influence on both the PL efficiency (PLQY) and the stability of the core/shell. Due to this lattice mismatch and defects, the CdTe core was first coated with CdSe shell because its band gap and lattice spacing lies at an intermediate level between those of the CdTe core and the ZnSe shell. This act decreases toxicity, improves the PLQY and the photostability of the quantum dot. This is the reason why CdTe/CdSe/ZnSe core mutlishell quantum dots were synthesized.

In the present work, CdTe/CdSe/ZnSe QDs were synthesized using reflux method and were characterized using optical and microscopic techniques before being used for the development of an efficient electrochemical cholesterol biosensor. During the synthesis, Cd-MPA complex solution was milky white and after pH optimization to pH 12.01 using NaOH, the solution turned colourless. After the addition of telluride (Te) precursor and $NaBH_4$, the complex solution turned yellow and became very intense as the reaction temperature approaches 90 °C indicating the formation of CdTe core QDs. As the reaction time was increased, the solution in the reaction mixture changed from intense yellow to orange colour and finally to deep red, indicating an increase in particle size of the core. CdTe/CdSe core/shell QDs were

formed by adding selenium precursor to the CdTe solution after an hour of refluxing. The formation of CdTe/CdSe was shown by a deep red colour in the reaction mixture immediately after adding sodium selenosulfate. After adding Zn-MPA complex into the CdTe/CdSe solution, the solution turned brown. Prelimenary work on the effect of temperature on the optical properties of the QDs was done. According to the preliminary results obtained from the method used, high luminescence CdTe QDs cannot be synthesized at temperatures less than 90 °C. Therefore, 90 °C was the minimum temperature used. However, upon addition of other precursors, the temperature was increased to 98 °C to assist in increasing reaction rate and the depletion of the precursors to form the desired quantum dots. High temperatures accelerate chemical reaction producing agglomerating nanoparticles. At high reaction temperatures, ligands are more likely to desorb from the surface of the QDs allowing monomers to add to nanocrystal surface resulting in QDs with larger particle size.[136] At 98 °C, the growth of the nanoparticles was relatively slow minimizing the effect of Ostwald ripening. Most of the characterization techniques used were able to confirm that indeed CdTe/CdSe/ZnSe core multishell QDs were synthesized.

4.2 SYNTHESIS OF CdTe/CdSe/ZnSe QUANTUM DOTS

CdTe/CdSe/ZnSe core multishell QDs were synthesized using the reflux method reported by Ncapayi, *et al*.[24] In a typical experiment, 0.051 g (0.2 mmol) cadmium acetate dihydrate was dissolved in 50 mL of deionized water in a beaker containing a magnetic stirring bar. Then 17 µL (0.2 mmol) of 3-mercaptopropanoic acid (MPA) was added under continuous stirring. The pH of the Cd-MPA complex solution was adjusted from pH 3.67 to 12.01 using 1 M NaOH. The solution was then transferred into 100 mL three-necked round bottom flask on a heating mantle and continuously stirred at a speed of 400 rpm. After 5 min of stirring, potassium tellurite solution prepared by dissolving 0.010 g (0.04 mmol) K_2O_3Te in 50 mL deionized water was added to the Cd-MPA complex solution. The mixture was allowed to react for further 5 min under continuous stirring, followed by addition of solid 0.08 g (2.0 mmol) $NaBH_4$. This was also allowed to react for 5 min, followed by refluxing at 98 °C. The

molar ratio of Cd:Te:MPA:$NaBH_4$ was fixed at 1:0.2:1:10. Aliquots were taken at different time intervals to monitor the growth of CdTe core.

After an hour refluxing the above MPA-CdTe solution, 0.5 mL (1.8 mmol) sodium selenosulfate (Na_2SeSO_3) solution was swiftly injected into it using a graduated pipette. The solution was further refluxed for an hour while taking aliquots at different time interval to monitor the formation of the CdTe/CdSe core/shell. The molar ratio of Cd:Te:Se was 1:0.2:9.

In another flask, zinc (Zn) precursor solution was prepared by dissolving 0.044 g (0.2 mmol) zinc acetate in 50 mL of deionized water followed by addition of 17 µL (0.2 mmol) mercaptopropionic acid (3-MPA) and pH optimization to pH 12.02 using 1M NaOH. After an hour of refluxing the above core/shell solution, Zn-MPA complex solution was swiftly added under continuous stirring. The molar ratio of Cd:Te:Se:Zn was 1:0.2:9:1. The prepared CdTe/CdSe/ZnSe core/shell/shell was further stirred and refluxed for 7 h at 98 °C. Aliquots were taken at different time intervals to monitor the growth of CdTe/CdSe/ZnSe core/multi shell nanoparticles. Fig. 4.1 depict the schematic representation involving synthesis of the QDs. After QDs synthesis, each sample from CdTe, CdTe/CdSe to CdTe/CdSe/ZnSe were diluted with water because they were too concentrated. For quantum yield determination, the each QDs sample was diluted with water until their absorbance were approximately 0.07 at 450 nm.

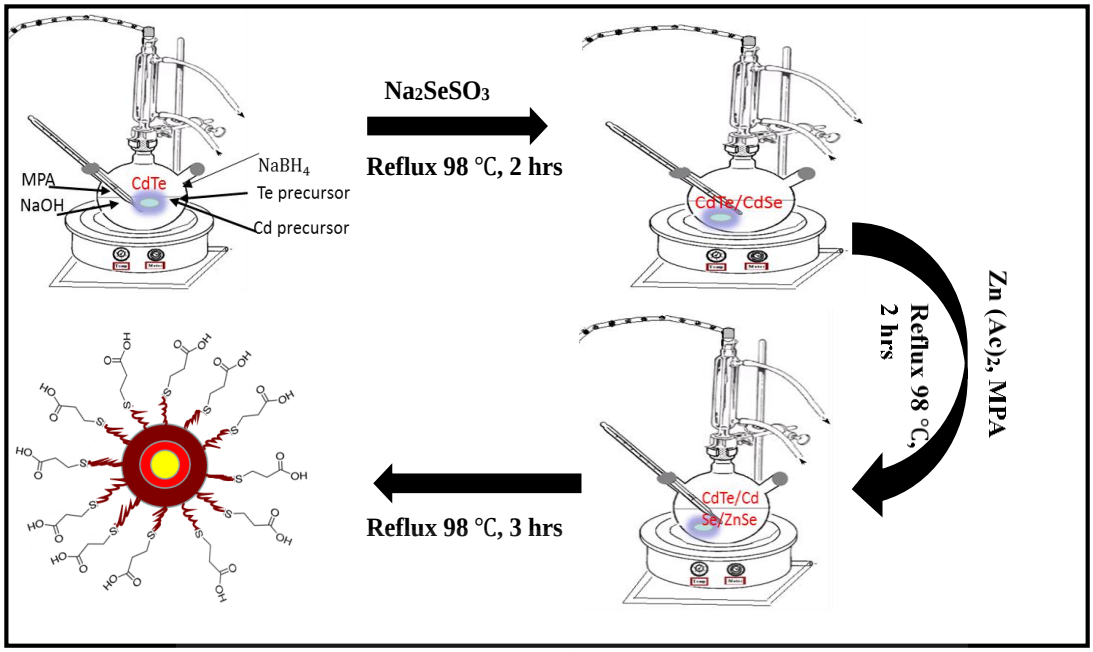

Figure 4. 1: Schematic representation for the synthesis of CdTe/CdSe/ZnSe quantum dots.

4.3 CHARACTERIZATION OF MPA-CAPPED CdTe/CdSe/ZnSe QDs

4.3.1 Ultraviolet-visible (UV-vis) and photoluminescence (PL) spectroscopy

The results of the absorption and emission spectra of CdTe/CdSe/ZnSe core/shell/shell QDs at different growth stages and reaction time is shown in Fig. 4.2A-B. Fig. 4.2C-D shows digital images of the as-synthesized CdTe/CdSe/ZnSe QDs at different growth stages and reaction time under UV-lamp irradiations of 254 nm and 350 nm. For CdTe core and CdTe/CdSe core/shell, there is a systematic and dramatic red shift with an increase in absorbance and intensities as the reaction time increased. (Fig. 4.2A-B). This indicate the growth of the QDs.[137] The absorption spectra (Fig. 4.2A) of the QDs show three stages of growth indicating the formation of three layers, which are CdTe core (502 to 610 nm, 0 min – 1 h), CdTe/CdSe core/shell (602 to 626 nm, 0 min – 2 h) and CdTe/CdSe/ZnSe core multishell (630 to 647 nm, 0 min – 7 h). The significant red-shifts of about 24 nm and 17 nm, 1 h after adding selenium and zinc precursors into the CdTe core and CdTe/CdSe core/shell solutions, respectively, confirm the formation of CdSe shell around the CdTe core (CdTe/CdSe) and ZnSe shell around the CdTe/CdSe core/shell

(CdTe/CdSe/ZnSe). This red-shift shows that there is an increased leakage of excitons into the shells and formation of the core/shell and core/multishell QDs rather than formation of alloyed QDs.[137-139] The emission spectra (Fig. 4.2B) of the QDs also show three stages of growth as reaction time increased and after addition of both Se and Zn precursor respectively with band edge luminescence at excitation wavelength of 450 nm. The narrowing of emission peaks and high intensities indicate that the particles have focused size distribution.[137] This can be attributed to proper passivation of the quantum dots by the shells via reduction of the electronic defects at the surface of the QDs.[140,141] The absorbance and PL intensities of the as-synthesized QDs increased from 15 min to 2 h of synthesis indicating that the CdTe core is being formed and that the core is also properly passivated by the CdSe shell. However, immediately after addition of Zn precursor (forming CdTe/CdSe/ZnSe QDs), the absorbance and PL intensities decreased. This can be attributed to increase in particle size, high concentration of the unreacted Zn precursor and formation of excess layers of ZnSe shell.[24,139,142] However, after 5 h of synthesis, the intensity of CdTe/CdSe/ZnSe core/shell/shell increased again. This can be associated with proper passivation of the QDs and depletion of excess precursor concentration as reaction time is increased.[137] The smaller shift in wavelength imply that the QDs size stabilizes with increasing growth time. When the solutions of the QDs were placed under the UV-lamp light of 254 nm excitation, low intensities of yellow to red fluorescence were observed for CdTe core and high intensities of brown fluorescence were observed for CdTe/CdSe and CdTe/CdSe/ZnSe. At excitation of 350 nm, a yellow (CdTe) to deep red (CdTe/CdSe/ZnSe) emissions with higher intensities were observed (Fig. 4.2C-D). This shows that the QDs are red-shifting growing towards near infrared (NIR) as reaction time is increased.

The diameter (D) of the quantum dots is directly related to the excitonic peak wavelength (λ) in the absorption spectrum, and was calculated using the following equation (eq 4.1):[131,143,144]

$$D\ (nm) = (9.8127 \times 10^{-7})\lambda^3 - (1.7417 \times 10^{-3})\lambda^2 + (1.0064)\ \lambda - (194.84) \qquad \text{eq.4. 1}$$

Where D (nm) is the QDs diameter and λ (nm) is the wavelength of the first excitonic absorption peak of the corresponding sample (QDs). From the calculations, the diameter of the CdTe core, CdTe/CdSe core/shell, and CdTe/CdSe/ZnSe core/shell/shell were found to be 3.75 nm, 3.94 nm, and 4.28 respectively, according to the excitation peak wavelength (nm) in the UV-vis spectra.

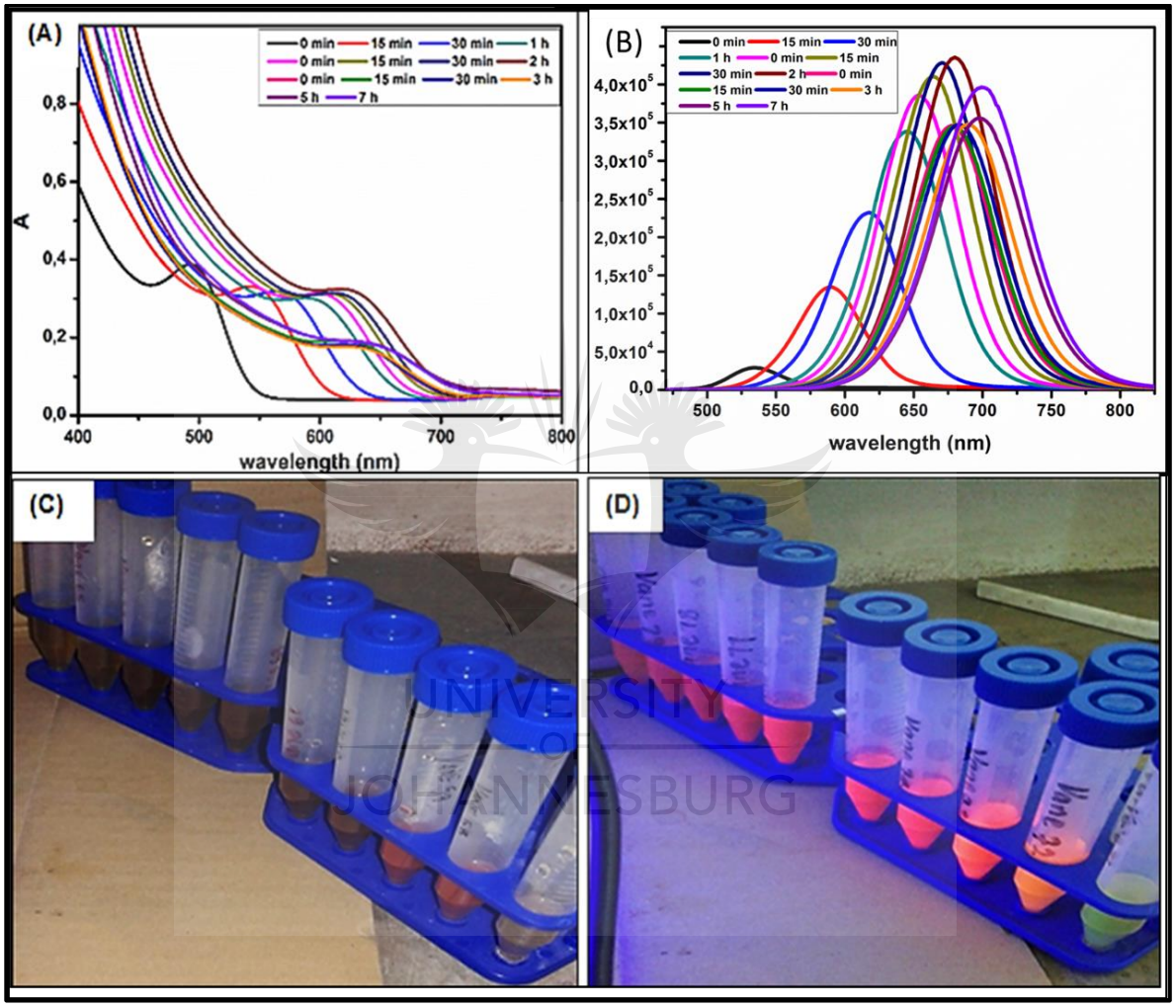

Figure 4. 2: UV-vis (A) and PL (B) spectra of MPA-capped CdTe/CdSe/ZnSe core-multishell quantum dots at different growth stages and reaction time. Digital images of the as-synthesized CdTe/CdSe/ZnSe (at different reaction time) under UV-lamp at excitation of 250 nm (C) and 350 nm (D).

4.3.1.1 Quantum yield (QY)

Fluorescence quantum yield (Φ_F) is described as the ratio of photons absorbed to photons emitted through fluorescence.

$$(\Phi_F) = \frac{\text{Photons absorbed}}{\text{Photons emitted}} \qquad \text{eq.4. 2}$$

Table 4.1 shows different absorbance obtained and the quantum yield (QY) for each QDs sample. The average QY of CdTe, CdTe/CdSe and CdTe/CdSe/ZnSe QDs are 33.8%, 69.2 % and 57%, respectively. Table 4.1 shows that the PL efficiencies of the CdTe core QDs are increasing with reaction time, showing that the CdTe core is forming as reaction time increased. After adding Se precursor to form CdSe shell, the QYs increased and this can be attributed to proper passivation of the surface trap state by the shell. However, after 30 min of forming CdTe/CdSe, the QY decreased. When more CdSe shells are formed, more surface defects will exist and this is due to limited cadmium atoms than selenium atoms. Selenium can form dangling bonds because of its valency of 6 while cadmium cannot.[145,146] Immediately after addition of Zn precursor, the QY increased and this is due to Zn atoms filling the holes created by missing cadmium atoms at the surface before forming the ZnSe shell.[134,147] When the concentration of Zn precursor is higher than that of selenium, better passivation of the surface will occur, thus increasing QY. However if there is a large excess of Zn precursor in the reaction mixture, the QY will decrease due to formation of thicker ZnSe shells and this is why the QY of the as-synthesized CdTe/CdSe/ZnSe QDs decreases as reaction time increases.

Table 4. 1: Photoluminescence properties of CdTe, CdTe/CdSe and CdTe/CdSe/ZnSe QDs at pH 12.01.

Sample name	Reaction time	PL (nm)	Intensity	UV (nm)	Absorbance (A)	PLQY (%)
Rhodamine 6G dye	-	-	-	-	-	97
CdTe 1	0 min	534	47 369	502	0.3687	10,5

CdTe 2	15 min	589	147 406	560	0.2973	23,9
CdTe 3	30 min	620	232 088	582	0.2919	42,3
CdTe 4	1 h	646	242 143	610	0.2212	58,5
CdTe/CdSe 1	0 min	655	385 866	602	0.3123	67,2
CdTe/CdSe 2	15 min	663	410 024	613	0.3093	72,0
CdTe/CdSe 3	30 min	671	428 248	619	0.3107	69,9
CdTe/CdSe 4	2 h	680	435 509	626	0.3208	67,7
CdTe/CdSe/ZnSe 1	0 min	677	345 991	630	0.1875	69,7
CdTe/CdSe/ZnSe 2	15 min	680	345 367	633	0.1855	66,3
CdTe/CdSe/ZnSe 3	30 min	683	347 523	632	0.1776	73.0
CdTe/CdSe/ZnSe 4	3 h	689	347 996	640	0.1718	69,4
CdTe/CdSe/ZnSe 5	5 h	697	317 496	644	0.1838	67,4
CdTe/CdSe/ZnSe 6	7 h	699	395 566	647	0.1796	52,3

4.3.2 Powdered X-ray diffraction spectroscopy (XRD)

The crystallinity and the core/shell/shell structure of the as-synthesized quantum dots were confirmed by XRD shown in Fig. 4.3**.** The XRD patterns of CdTe, CdTe/CdSe and CdTe/CdSe/ZnSe QDs consist of three diffraction peaks corresponding to (111), (220) and (311) cubic zinc blended structures.[148] For CdTe core, the diffraction peaks were located at 25.25°, 41.88° and 49.23° whereas for CdTe/CdSe and CdTe/CdSe/ZnSe the diffraction peaks were located at 25.73°, 42.38°, 50.38° and at 26.04°, 43.97° and 51.09°, respectively. After growing the CdSe and ZnSe shells on to the CdTe core, the diffraction peaks shifted to higher angles while the peak width broaden, indicating the growth of the nanoparticles as the CdSe and ZnSe shells are grown around the core. The shifting of the diffraction peaks to higher angles also confirms the formation of core/shell and core/shell/shell structure rather than an alloyed structure.[132,149] The average crystallite size of CdTe, CdTe/CdSe and CdTe/CdSe/ZnSe calculated using Scherrer's equation (eq. 3.2) are 3.82 nm 4.06 nm, and 4.32 nm which is in agreement with the trend of the particle size calculated from the absorption spectra. The stronger and narrower (111) peak in Fig. 4.3 indicates that the nanocrystals were elongated along the *c*-

axis.[150] Furthermore, the broad nature of the XRD peaks is attributed to the nano-crystalline nature of the as-synthesized QDs, which is also consistent with the result from the optical spectroscopy.

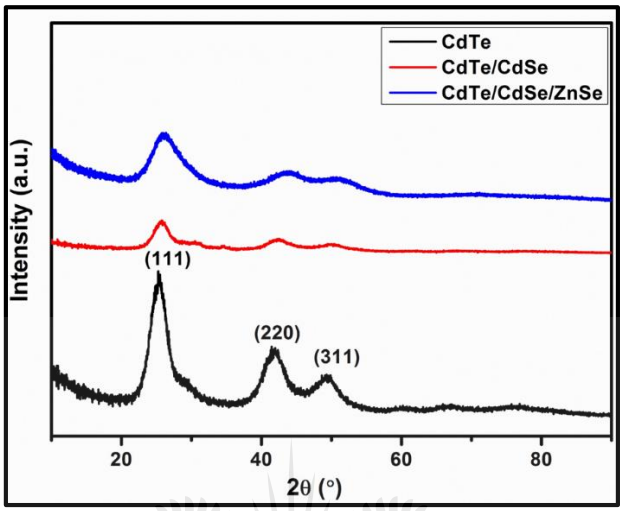

Figure 4. 3: XRD spectra of MPA-capped CdTe, CdTe/CdSe and CdTe/CdSe/ZnSe QDs.

4.3.3 Fourier transform infrared spectroscopy (FTIR)

The FTIR spectra of MPA and the as-synthesized MPA-capped CdTe/CdSe/ZnSe QDs over the range 500 to 4000 cm^{-1} are shown in Fig.4.4. The stretching bands in MPA between 2570 and 2670 cm^{-1} shows the presence of sulfhydryl (-SH) group which immediately disappeared in MPA-CdTe/CdSe/ZnSe. The MPA ligand also shows a sharp and strong band around 1700 cm^{-1} which is due to the C=O stretching of the carbonyl group in the acid. The vibrations at 2940 cm^{-1} and 3250 cm^{-1} are due to the stretching bonds of C-H and –OH groups present in MPA. For MPA-capped CdTe/CdSe/ZnSe QDs, the peaks at 3417 cm^{-1}, 1560 cm^{-1} and 1400 cm^{-1} are attributed to the O-H stretching vibration, C=O asymmetric stretching vibration of carboxylic acid and S-CH_2 wagging vibration of MPA molecular, respectively.[151] The large difference between the vibrational frequency of the carbonyl group (C=O) of MPA and MPA-QDs was due to the formation of asymmetric and symmetric C=O during the capping of the QDs. The absence of S-H stretching bond between 2570 cm^{-1} and 2670 cm^{-1} proves that MPA was covalently bonded to the CdTe/CdSe/ZnSe QDs through the thiol groups possibly via complexation with Cd

ions of the core and Zn ions of the ZnSe shell.[152-154] The vibration at 1200 cm^{-1} and 1100 cm^{-1} are due to the –C-O bond in MPA and MPA-capped CdTe/CdSe/ZnSe QDs, respectively.[137] The presence of –OH group shows that, the quantum dots are water soluble and biocompatible.

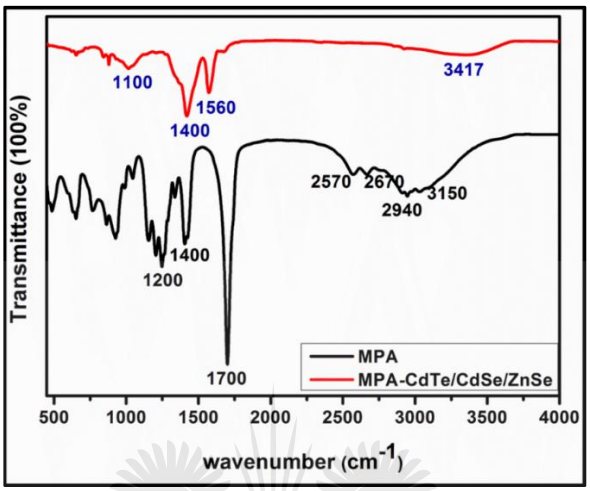

Figure 4. 4: FTIR spectra of MPA and MPA capped CdTe/CdSe/ZnSe QDs**.**

4.3.4 Microscopic characterization of CdTe/CdSe/ZnSe QDs

The TEM image and corresponding selected area electron diffraction (SAED) patterns of the as-synthesized CdTe/CdSe/ZnSe QDs are shown in Fig. 4.5A-B. According to Fig. 4.5A, the nanoparticles exhibit monodispersed spherically-shaped morphology with average particle size of 4.08 nm for CdTe/CdSe/ZnSe QDs. This is in the same range with the estimated crystallite size of the nanostructure obtained from the XRD analysis and UV-Vis spectroscopy. The slight difference between the TEM size and the XRD size can be explained based on the fact that, TEM measures core particle diameter while XRD measures crystallite diameter. The SAED pattern in Fig. 4.5B shows diffused rings pattern corresponding to (111), (220) and (311) reflections of a cubic crystal structure of Zn-blended CdTe/CdSe/ZnSe. This further confirmed the cubic zinc blended structures obtained from the XRD analysis. The SEM micrograph in Fig. 4.5C also confirms the spherical morphology of the as-synthesized CdTe/CdSe/ZnSe QDs. The elemental composition of the as-synthesized CdTe/CdSe/ZnSe QDs obtained using EDX (Fig. 4.5D) confirms the presence of Cd, Te, Se, and Zn present in CdTe/CdSe/ZnSe QDs. The higher

percentage of oxygen in the EDX spectrum of the QDs can be due to the oxygen group present in the capping agent, MPA . The one's from the carboxylic group of the MPA. The atmospheric oxygen might also have contributed to the oxygen percentage in the nanoparticle.

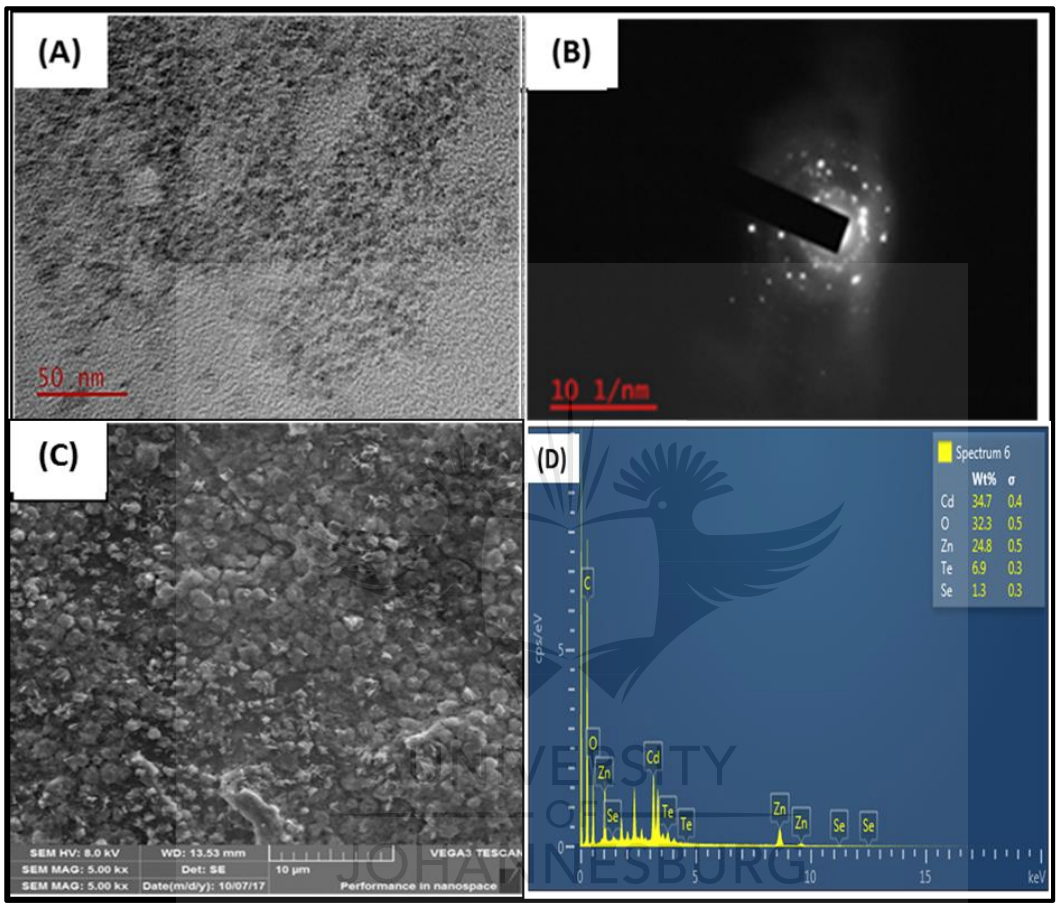

Figure 4. 5: TEM images (A), SAED patterns (B), SEM image (C) and EDX of CdTe/CdSe/ZnSe quantum dots (D).

4.4 SUB-CONCLUSION

Highly fluorescent water-soluble MPA capped CdTe/CdSe/ZnSe core/multishell quantum dots were successfully synthesized in aqueous phase and characterized using various analytical techniques. UV-vis, PL and XRD confirmed the growth of the as-synthesized QDs while FTIR confirmed the capping of CdTe/CdSe/ZnSe by MPA. The QDs were also highly fluorescent under UV-lamp of 350 nm and red shifting. The TEM and SEM shows that the QDs were spherical and mono-dispersed.

CHAPTER 5

DEVELOPMENT OF GCE/PPI/QDs/ChOx BASED ELECTROCHEMICAL CHOLESTEROL BIOSENSOR

5.1 INTRODUCTION

The results discussed in this chapter proceed from the experimental procedures outlined in chapter 3. A novel PPI/QDs nanoplatform, used as a suitable immobilization layer for ChOx in the development of cholesterol biosensor was prepared and electrochemically characterized using CV and EIS. The nanoplatform was designed by first electrodepositing PPI dendrimer on a glassy carbon electrode via cyclic voltammetry using 10 cycle scan at 50 $mV.s^{-1}$. The dendrimer electrode was further modified by drop-coating NHS/EDC activated quantum dots and the two were covalently bonded. The PPI/QDs nanoplatform was interrogated in phosphate buffer and ferrocyanide electrolytes before the immobilization of the enzyme. Finally a biosensor comprising of GCE/PPI/QDs/ChOx was developed and used for the determination of cholesterol. From the results obtained, the surface coverage, the active surface area of the electrode, the detection limit and the sensitivity were calculated.

5.2 DEVELOPMENT OF GCE/PPI/QDS/ChOx BASED BIOSENSOR

A bare glassy carbon electrode (GCE) was polished (section 3.3.1) and dried at room temperature before modification. On the other hand, screen printed carbon electrode (SPCE) was cleaned by scanning 0.5 M H_2SO_4 solution using cyclic voltammetry before use.[155] The GCE and SPCE were modified by electrodepositing PPI from a 10 mM PPI solution on the electrode surface using 10 cycles at 50 $mV.s^{-1}$ from -0.5 V to 1.2 V. The electrodes were left to dry at room temperature overnight and then stored at 4 °C before use. SEM analysis was carried out on the modified SPCE. The PPI modified electrode was modified with quantum dot as follows: A 1

mL volume of the MPA-QDs was first mixed with 20 mg.mL^{-1} of NHS/EDC solution for 5 h with gentle stirring at room temperature. Then 50 µL of the solution was drop-coated on the surface of the PPI modified GCE (GCE/PPI) and allowed to dry at room temperature before use. The resulting electrode was cleaned with a solution of PBS (pH 7.2) to remove the unbound QDs on the electrode. CV and EIS measurements were also carried out on the GCE/PPI/QDs. Finally, the GCE/PPI/QDs/ChOx bio-nanoelectrode was developed by immobilising 50 µL of ChOx (2 mg.mL^{-1}) onto the GCE/PPI/QDs electrode and allowed to dry for 3 h at 4 °C. The GCE/PPI/QDs/ChOx electrode was also characterized using CV and EIS. This electrode (i.e. the biosensor) was used for the detection of cholesterol. All electrochemical measurements were carried out using three electrodes system made of GCE (working electrode), Ag/AgCl (reference electrode) and Pt wire (counter electrode) in probes such as PBS and [Fe (CN)$_6$]$^{3-/4-}$ (in 0.1 M KCl). The scheme that highlights the experimental protocol for the biosensor is depicted in Fig. 5.1.

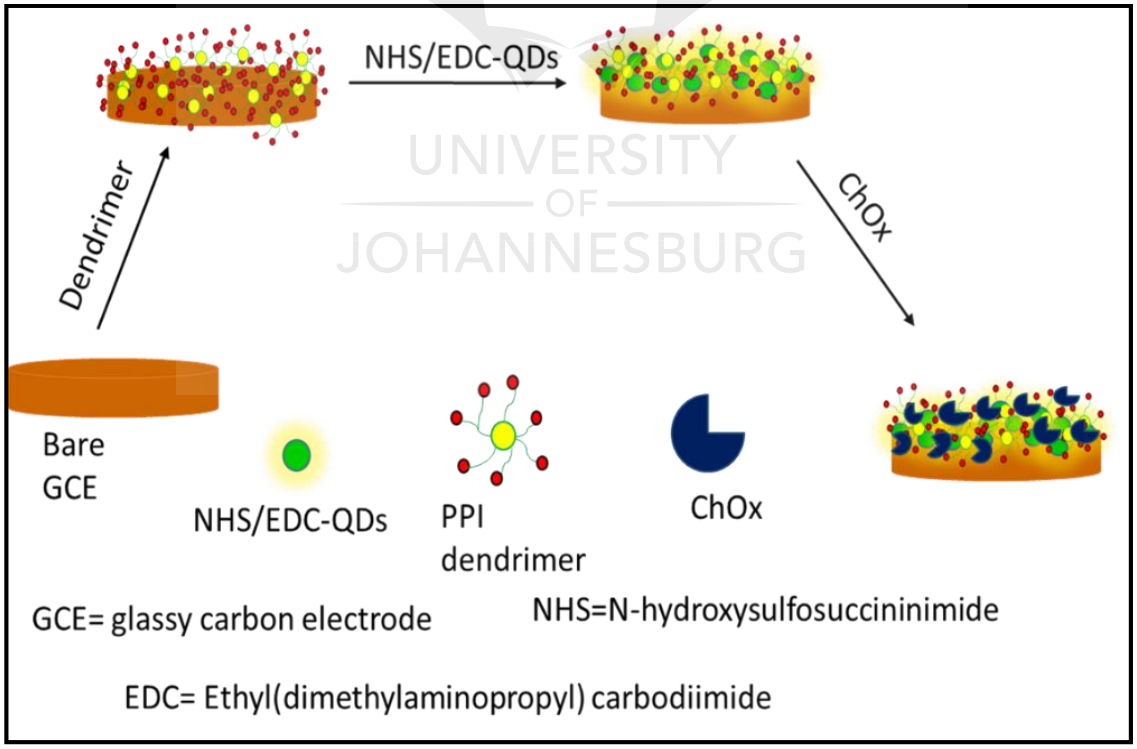

Figure 5. 1: Overview of how the cholesterol biosensor is fabricated.

5.3 CHARACTERIZATION OF THE MODIFIED ELECTRODES

5.3.1 Electrodeposition and preparation of the PPI/QDs modified electrodes

The PPI modified electrode was prepared by electrodeposition using CV technique (Fig. 5.2). The current decreased with increase in scan cycles depicting electrodeposition.[124] The mechanism of electrodeposition of PPI is based on the formation of an amine cation radical which creates a C-N linkage between the primary amine and the carbon on the SPCE electrode. During the anodic scan, the primary amine of PPI dendrimers were electro-oxidised onto the SPCE surface to form a C-N bond between the SPCE-PPI.[124,156] The MPA-capped quantum dots were activated using NHS/EDC and they interacted with the cationic PPI dendrimer matrix via electrostatic interaction and hydrogen bonding with $–NH_2$ groups.

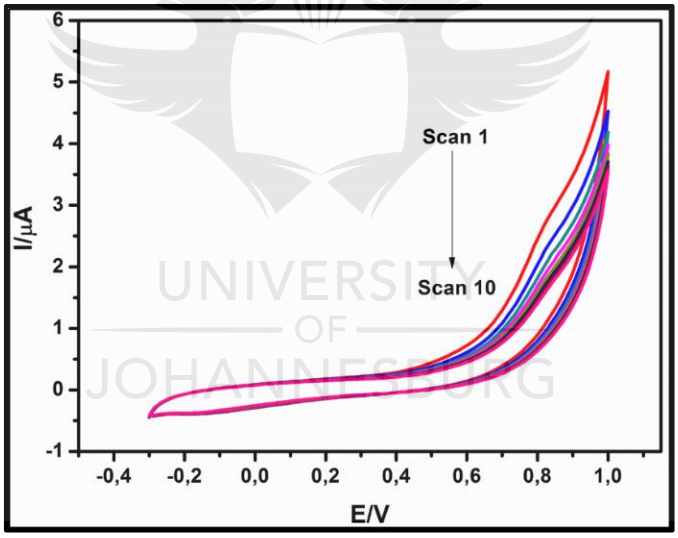

Figure 5. 2: Cyclic voltammograms of electrodeposited PPI on GCE using 10 cycles at 50 $mV.s^{-1}$ from - 0.5 to 1.2 V.

5.3.2 Scanning electron microscopy (SEM) characterization of the modified SPCE

The morphology of modifiers (dendrimer and QDs) play a significant role in the immobilization of enzymes which reflects on the performance of the enzyme electrode. Fig. 5.3 presents the SEM images of the modified SPCE electrodes.

According to Fig. 5.3A, the MPA-CdTe/CdSe/ZnSe QDs are uniformly distributed on the electrode surface with almost no sign of aggregation. This is also discussed in section 4.3.4. A nano-globular morphology of dendrimer can be seen in Fig. 5.3B confirming that the PPI dendrimer was successfully electrodeposited on the SPCE. In the same vein, the SEM image of GCE/PPI/QDs (Fig. 5.3C) exhibits a uniformly distributed spherical nanostructure with few aggregations on top of the nano-globular PPI. Finally, Fig. 5.3D shows the SEM image of GCE/PPI/QDs/ChOx where the change in morphology (in comparison with Fig. 5.3C) can be taken as an indication of the immobilized enzyme.

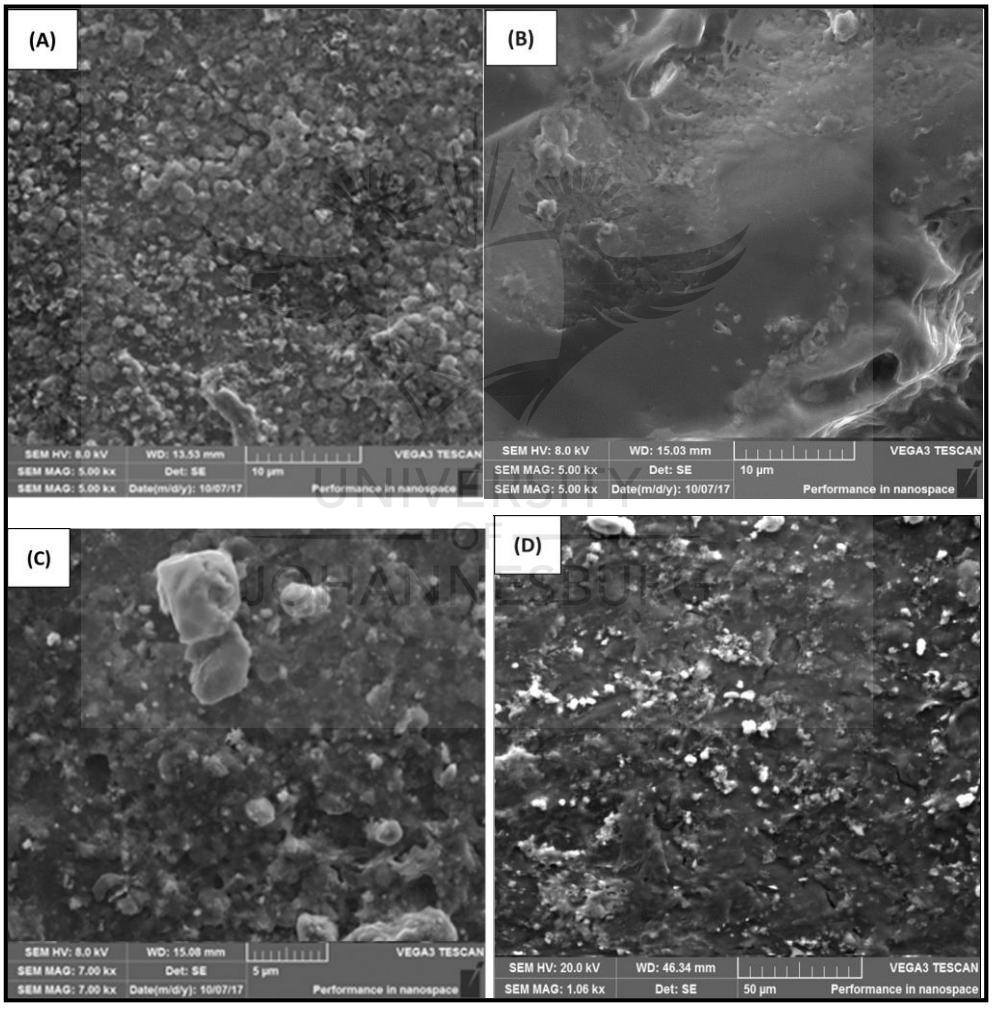

Figure 5. 3: SEM image of SPCE/QDs (A), SPCE/PPI (B), SPCE/PPI/QDs (C) and SPCE/PPI/QDs/ChOx (D).

5.3.3 Electrochemical characterization

All electrochemical measurements were carried out in 10 mM PBS (pH 7.2) and in 10 mM ferro/ferricyanide ($[Fe(CN)_6]^{3-/4-}$) as supporting electrolytes at 25 °C. Fig. 5.4 shows cyclic voltammograms of different electrodes in 10 mM PBS (pH 7.2) at 50 $mV.s^{-1}$. For bare GCE (Fig. 5.4 (i)), no redox peaks were observed because there was no electroactive specie in the electrochemical cell. The presence of CdTe/CdSe/ZnSe QDs on the electrode resulted in a small irreversible cathodic peak which may be attributed to an electrochemical reaction on the electrode as a result of the presence of the QDs (Fig. 5.4 (ii)). For the dendrimer modified electrode (Fig. 5.4 (iii)), i.e. the GCE/PPI, a redox pair emerges at 0.295 V and 0.213 V (versus Ag/AgCl (0.1 M)). This redox couples can be attributed to the presence of the PPI dendrimer on the electrode surface. Similar electrochemical signatures have been reported by Arotiba *et al.*[124,156,157] after the electrodeposition of PPI on carbon electrodes. The presence of QDs on the GCE/PPI/QDs (Fig. 5.4 (iv)) amplified the current observed in the redox couple attributed to PPI earlier (Fig, 5.4 (iii)). This amplification is a favourable property that may enhance the performance of the biosensor. It is interesting to note that after modification of the GCE/PPI/QDs with the enzyme, the redox peak due to the dendrimer and QDs was not quenched (Fig 5.4 insert). This shows that the PPI/QDs platform is able to act as molecular wire that permits redox signal and thus a suitable platform for the immobilization of the ChOx. Fig. 5.4 inset resulted from scan rate study of the GCE/PPI/QDs/ChOx. It can be observed that there was no apparent shifting of the potential of the anodic or cathodic peak currents. This phenomenon can be used to infer the stability of the enzyme on the GCE/PPI/QDs platform. Again, this shows the suitability of the platform as immobilization layer in biosensor development.

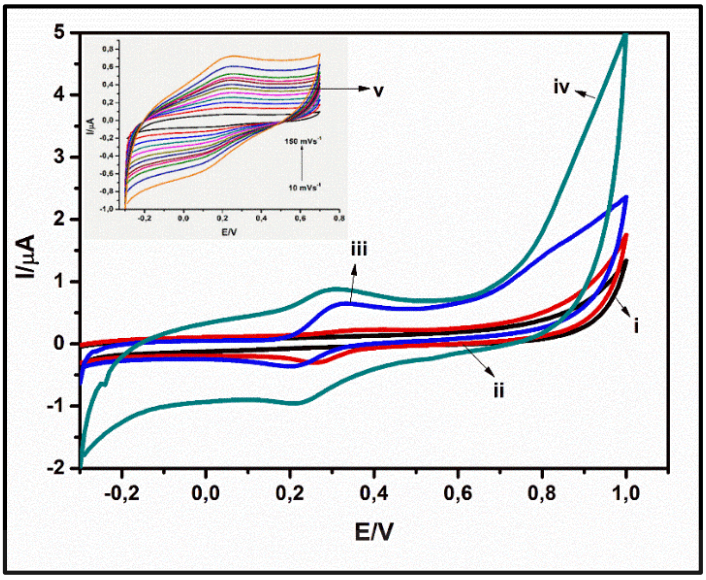

Figure 5. 4: Cyclic voltammograms of GCE (i), GCE/QDs (ii), GCE/PPI (iii), GCE/PPI/QDs (iv), in 10 mM PBS (pH 7.2) at 50 mV.s^{-1}. Insert: PPI/QDs/ChOx (v) in 10 mM PBS (pH 7.2) at different scan rates (10-150 mV.s^{-1}).

Fig. 5.5 shows electrochemical behaviour of all the modified electrodes (including bare GCE) being studied in the potential range 0.3 to 1.0 V at a scan rate of 50 mV.s^{-1} in 10 mM [Fe $(CN)_6$]$^{3-/4-}$/0.1 M KCl. It also shows a simple scan rate study for GCE/PPI/QDs/ChOx and a plot of anodic peak and cathodic peak currents vs square root of scan rate. Cyclic voltammograms of bare GCE (Fig. 5.5A (i)) exhibits the well-known voltammograms of ferrocyanide redox probe with a sharp oxidation peak at 0.39 V with peak current value of 126.7 µA and a reduction peak at 0.17 V and I_{pc} value of -146.9 µA. However, after modifying the bare GCE with CdTe/CdSe/ZnSe QDs (Fig. 5.5A (ii)), the oxidation and reduction peaks shifted to lower potential 0.30 V and 0.096 respectively, with insignificant changes in the I_p values. The slight shift in potential suggests possible changes in reaction mechanism of the ferrocynide ([Fe $(CN)_6$]$^{3-/4-}$) as a result of the QDs on the surface of the electrode. It demonstrate electrocatalytic properties of QDs. When the bare GCE was modified with PPI (Fig. 5.5A (iii)), the redox peaks shifted to lower potentials with an increase in the values of I_p, this is because PPI is cationic in nature and its nanometric dimensions provide large surface area. PPI was able to attract the negatively charged [Fe$(CN)_6$]$^{3-/4-}$ to its surface, therefore enhancing interfacial electron transfer between the electrode surface and the [Fe$(CN)_6$]$^{3-/4-}$ solution. This

also shows that PPI is electrocatalytic towards the reaction occurring in the solution. From Fig. 5.5A (iv), it is very clear that the combination of these two nanomaterials (GCE/PPI/QDs) provides more active surface area on the electrode than either PPI or QDs alone, thus more electrons produces from the electrolytes (PBS and $[Fe(CN)_6]^{3-/4}$) are being transferred to the electrode surface and enhancing the current of the system. The reversible electrochemistry of $[Fe(CN)_6]^{3-/4}$ was remarkably increased after modification using both PPI and QDs as compared to using PPI or QDs alone. The combination of PPI-QDs nanocomposite further enhanced the redox peaks by improving the electrode conductivity and electroactive surface area. However, upon the addition/immobilization of ChOx on GCE/PPI/QDs, the oxidation and reduction peak currents decreased, suggesting the formation of the insulating layer (enzyme) on the electrode surface leading to decrease in electron transfer efficiency (Fig. 5.5A (v)).[158] The ChOx enzyme was linked to the electrode surface using the NHS/EDC protocol, where the carboxylic groups on the QDs were activated using NHS/EDC. CV was also used to study the interfacial kinetics of the bio-nanoelectrode (GCE/PPI/QDs/ChOx) by varying scan rates from 10 to 150 $mV.s^{-1}$. As the scan rate increases, the anodic and cathodic peaks of the bioelectrode also increases, but in opposite direction suggesting that the redox process is quasi-reversible (Fig 5.5B). Fig. 5.5C shows the plot of I_p vs. square root of scan rate for GCE/PPI/QDs/ChOx bioelectrode in $[Fe(CN)_6]^{3-/4-}$. The current varies linearly with an increase in the scan rate suggesting that the kinetics of $[Fe(CN)_6]^{3-/4-}$ is diffusion controlled on the PPI/QDs/ChOx modified electrode, with correlation coefficients of 0.9956 and 0.9906 for anodic peaks and cathodic peaks, respectively. The presence of QDs and PPI wired the enzyme onto the electrode surface thereby enhancing the electron transfer. This is one of the importance of using nanomaterials in biomolecular immobilization. These conductive nanomaterials penetrate into the core redox moiety of the enzyme and facilitate the electron transfer between the electrode surface and the biomolecule redox site. The effective surface area (A_e) of the modified electrode was calculated using Randle-Sevcik equation (eq. 5.1 and eq. 5.2):

$$I_p = (2.69 \times 10^5) \times n^{3/2} \times A_e \times D^{1/2} \times C_0 \times v^{1/2} \qquad \text{eq. 5. 1}$$

Where I_p is the current, n is number of electrons involved in redox reaction, A_e is the effective surface area of the electrode (cm^2), C_0 is concentration of the redox species in solution ($mol.cm^{-3}$) and D is the diffusion coefficient of the molecules in solution ($6.67\times10^{-6}\ cm^2.s^{-1}$) and *v* is the scan rate ($V.s^{-1}$),

$$A_e = \left(\frac{\mathbf{Slope}}{(\mathbf{2.69\times10^5})}\right)n^{3/2} \times C_0 \times D^{1/2} \qquad \text{eq. 5.2}$$

Where slope is obtained from the linear regression of I_p versus $v^{1/2}$. The effective surface area (A_e) of bare GCE and GCE/PPI/QDs/ChOx electrode was calculated as 0.0024 cm^2 and 0.096 cm^2 respectively, using eq. 5.3. This results shows that the presence of quantum dots and PPI on the electrode increase the active surface area of bare GCE, thereby, improved electron transfer process between the redox probe and the electrode surface, even though the enzyme tried reduce the transfer.

The surface coverage of the adsorbed redox ChOx can be calculated by integrating the charge Q under the voltammetric peak using the formula in eq. 5.3:

$$\mathbf{\Gamma} = \frac{\mathbf{Q}}{\mathbf{nFA}} \qquad \text{eq. 5.3}$$

Where A is the surface area of the bare GCE (28.27 mm^2), n is the number of electrons transferred in the redox process ($1e^-$) and F is the Faraday constant (96548.33 $Cmol^{-1}$). Q (0.0239 C) was calculated by integrating one complete cycle of GCE/PPI/QDs/ChOx cyclic voltammogram and obtaining the absolute area of the peaks. The calculated surface coverage (Γ) of GCE/PPI/QDs/ChOx was 8.7565 $\times\ 10^{-7}\ cm^2$.

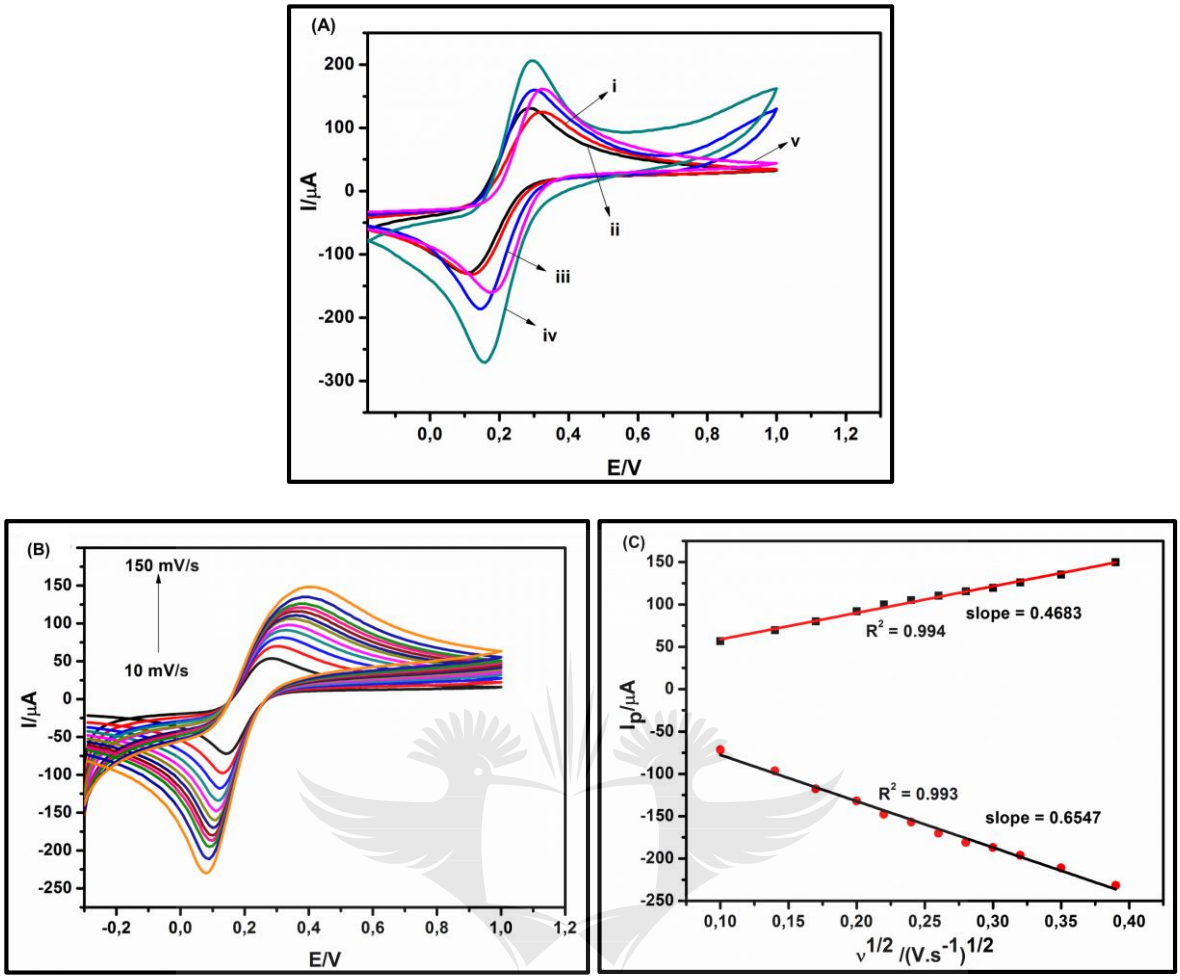

Figure 5. 5: Cyclic voltammograms of GCE (i), GCE/QDs (ii), GCE/PPI (iii), GCE/PPI/QDs (iv), and GCE/PPI/QDs/ChOx (v) in 10 mM $[Fe(CN)_6]^{3-/4-}$/0.1 M KCl at 50 $mV.s^{-1}$ (A). Cyclic voltammograms of GCE/PPI/QDs/ChOx in 10 mM $[Fe(CN)_6]^{3-/4-}$ at scan rate of 10-150 $mV.s^{-1}$ (B). Randle-Sevcik plot of GCE/PPI/QDs/ChOx (C).

The Nyquist plots of GCE and its modified forms are presented in Fig. 5.6. EIS measurements were carried out at a potential of 0.2 V and a frequency of 100 kHz to 100 mHz using 10 mM $[Fe(CN)_6]^{3-/4}$] redox couple (1:1) with 0.1 M KCl as the supporting electrolyte. The value of the electron-transfer resistance (R_{ct}) of the modified electrode was estimated by the semicircle diameter. Compared to bare GCE (Fig. 5.6 (i)), the diameter of the semicircle increased after modifying the GCE with MPA-capped CdTe/CdSe/ZnSe QDs (Fig. 5.6 (ii)) and this could be due to the electrostatic repulsion between the negatively charged $[Fe(CN)_6]^{3-/4-}$ redox couple and the negative charge on the MPA-capped QDs. This also confirms that the QDs

were successfully attached on the electrode surface. PPI (Fig. 5.6 (iii)) is cationic in nature and has nanometric dimension, therefore its surface area is also large. PPI was able to attract the negatively charged $[Fe(CN)_6]^{3-/4-}$ to its surface and also facilitated electron transfer. GCE/PPI/QDs nanocomposite (Fig. 5.6 (iv) provided a better platform than either one of them because the results shows that the redox kinetics of $[Fe(CN)_6]^{3-/4-}$ were faster, thus this platform can be suitable for biosensors development. This agrees with the enhance redox signal from CV in Fig. 5.5A (iv). When the GCE/PPI/QDs electrode was modified with 50 µL of ChOx (Fig. 5.6 (v)), an increase in electron transfer resistance was observed and this can be due to the poor conducting nature of the enzyme and also a possible electrostatic repulsion of the $[Fe(CN)_6]^{3-/4-}$ owing to the negatively charged enzyme. This increase in resistance shows that the enzyme was successfully immobilized on the platform.

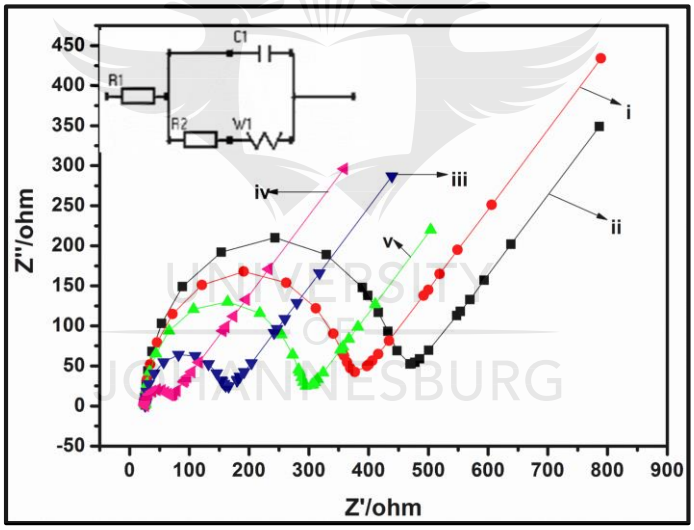

Figure 5. 6: EIS of GCE (i), GCE/QDs (ii), GCE/PPI (iii), GCE/PPI/QDs (iv), and GCE/PPI/QDs/ChOx (v) in 10 mM $[Fe(CN)_6]^{3-/4-}$/0.1 M KCl.

5.4 OPTIMIZATION STUDIES OF GCE/PPI/QDs/ChOx

5.4.1 Effect of pH, temperature and cholesterol oxidase

Enzymes are pH and temperature sensitive and might lose their bioactivity at certain pH. Therefore, the effect of pH and temperature on the developed biosensor was studied in 10 mM cholesterol solution in the pH range 2.0-10.0 and temperature of

10-50 °C. The effect of the immobilized ChOx enzyme concentration was also investigated. Fig. 5.7 illustrates the effect of pH, temperature and ChOx concentration on the current response of the fabricated biosensor based on GCE/PPI/QDs/ChOx electrode. The optimum pH, temperature and ChOx concentration of the biosensor was 7.2, 37-40 °C and 8 mg.mL^{-1}, respectively.

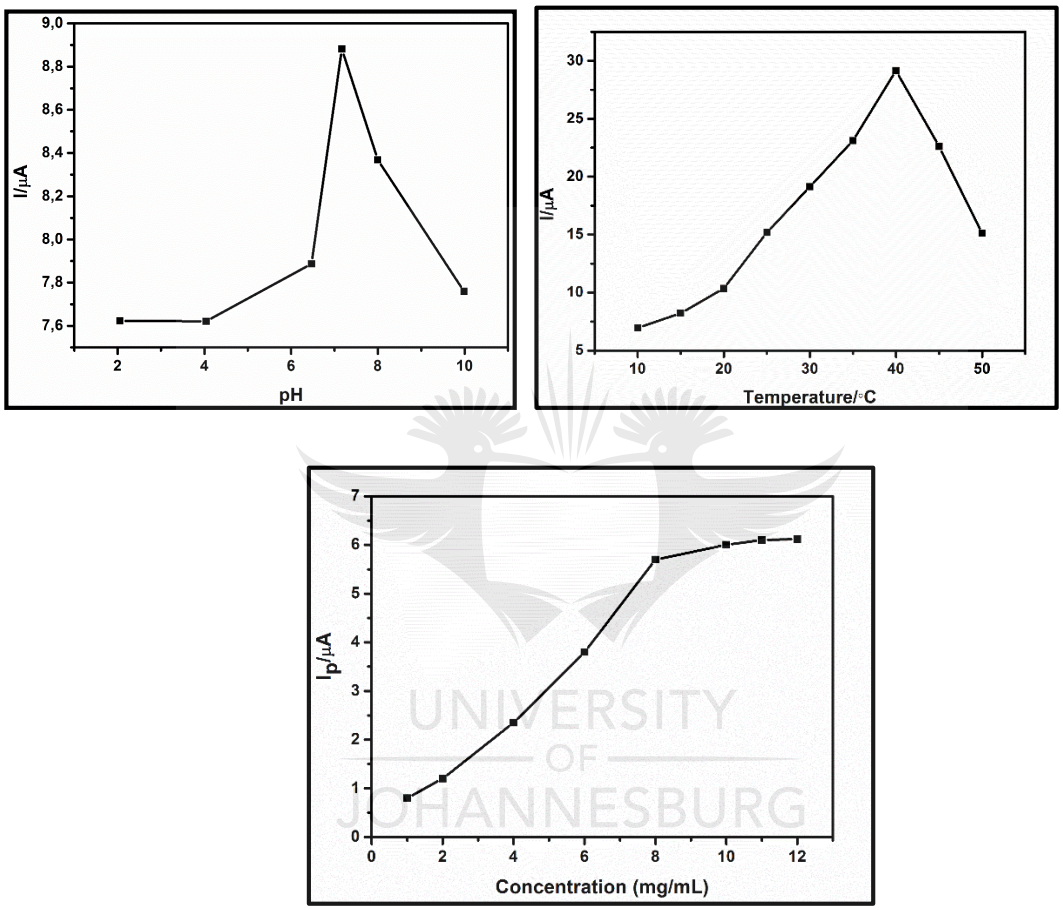

Figure 5. 7: Effect of pH (pH 2.0-10), temperature (10-50 °C), and amount of enzyme (1-12 mg. mL^{-1}) on current response of the fabricated GCE/PPI/QDs/ChOx cholesterol biosensor in 10 mM cholesterol solution.

5.5 APPLICATION OF GCE/PPI/QDs/ChOx BASED ELECTROCHEMICAL BIOSENSOR

5.5.1 Detection of cholesterol

The detection of cholesterol was carried out with square wave voltammetry (SVW) and cyclic voltammetry (CV). For SVW analysis, an amplitude of 25 mV, frequency

of 25 Hz, scan rate of 50 $mV.s^{-1}$ and working potential of -0.3 – +1.0 V were used. CV was used to study effect of different modifiers on the electrocatalytic reaction between the biosensor and cholesterol solution. The biosensor was also investigated in the presence of PBS and 10 mM cholesterol solution using CV (Fig. 5.8 A). There was an insignificant response when the bioelectrode was immersed in PBS solution. However, upon the addition of 10 mM cholesterol solution, there was an increased response with two large redox peaks, indication the electrocatalytic process of the biosensor (ChOx) towards the cholesterol molecule. In Fig.5.8B, the GCE modified with QDs (Fig. 5.8 (i)) and PPI (Fig.5.8 (ii)) did not show any significant redox current because there was no electrocatalytic reaction with the cholesterol. However, when ChOx was immobilized on the electrodes (Fig. 5.8 (iii, iv)), some redox peaks were observed. Obviously, these peaks are from the enzymatic catalytic oxidation of cholesterol in the solution and reduction of hydrogen peroxide (H_2O_2) produced as one of the products. The GCE/PPI/ChOx electrode shows a higher redox peak than that of GCE/QDs/ChOx. This suggests the biocompatible nature of dendrimer and a better immobilization ability than QDs. This is expected for the following reasons: 1. Electrostatic attraction between the positively charged PPI and the negatively charged enzyme. 2. The presence of amino groups on the PPI which could interact with the acidic group of the enzyme and 3. The nano-voids and opposite charge would have facilitated enzyme entrapment, host-guest chemistry or supramolecular chemistry.[159] Fig. 5.8 (v), showed the highest redox current. This must have resulted from a synergic combination of PPI and QDs which enhanced the ChOx catalytic reduction of the cholesterol. Furthermore, the presence of QDs must have enhanced the enzyme wiring thereby facilitating the exchange or flow of electron from the redox centre of ChOx to the analyte (Cholesterol).

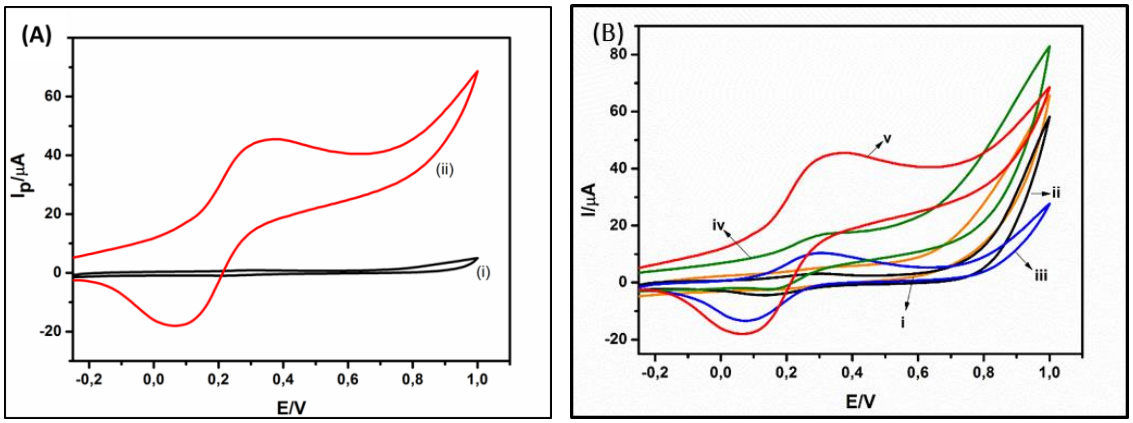

Figure 5. 8: Cyclic voltammograms of GCE/PPI/QDs/ChOx in PBS (i) and 10 mM cholesterol (ii) (A) and of GCE/QDs (i), GCE/PPI (ii), GCE/PPI/ChOx (iii) GCE/QDs/ChOx (iv) and GCE/PPI/QDs/ChOx (v) in 10 mM cholesterol solution at 50 $mV.s^{-1}$ (B).

Fig. 5.9 shows the relationship between the current response and cholesterol concentrations during the bio-recognition process. It is observed that the current increased in a direct proportion to the cholesterol concentration (Fig. 5.9A-B). When cholesterol is oxidised in the presence of the enzyme cholesterol oxidase and oxygen, it produces cholestenone and hydrogen peroxide (H_2O_2).[58] The produced H_2O_2 is further reduced at the electrode surface producing electrons which increase the current of the solution being detected by the electrode. The other by products are oxygen and hydrogen ions. According to stoichiometric ratios in eq. 5.4-5.5, one can conclude that the concentration of the analyte (cholesterol) is directly proportional to the hydrogen peroxide produced and also to the current produced.[160] Fig.5.10 shows the schematic presentation of the cholesterol sensing mechanism of PPI/QDs/ChOx-based electrode.

$$\text{Cholesterol} + O_2 \xrightarrow{\text{ChOx}} \text{cholestenone} + H_2O_2 \qquad \text{eq 5. 1}$$

$$H_2O_2 \rightarrow 2H^+ + O_2 + 2e^- \qquad \text{eq 5. 2}$$

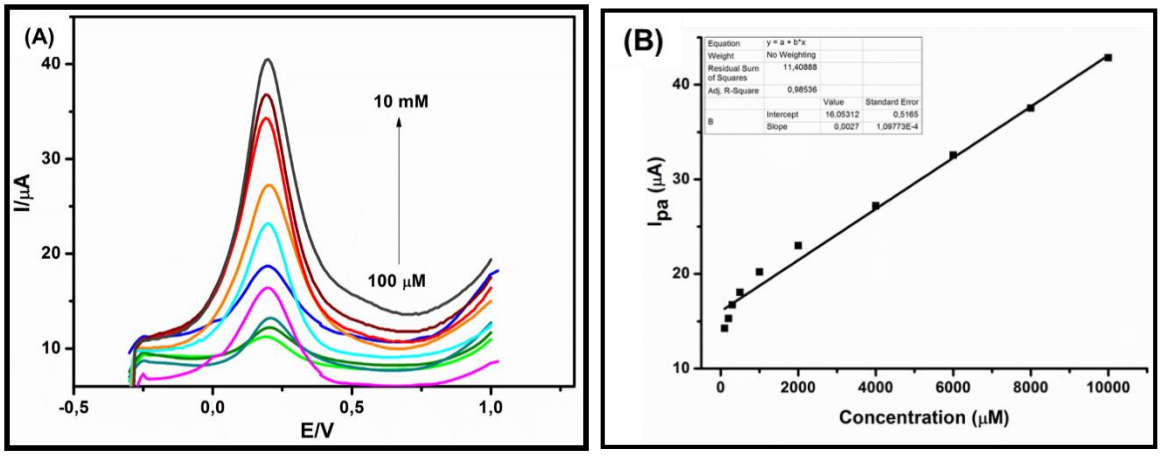

Figure 5. 9: SWV plot of the proposed biosensor under different concentrations (100 µM -10 mM) of cholesterol at pH 7.2 and at room temperature (A). Corresponding calibration plot of the proposed biosensor (B).

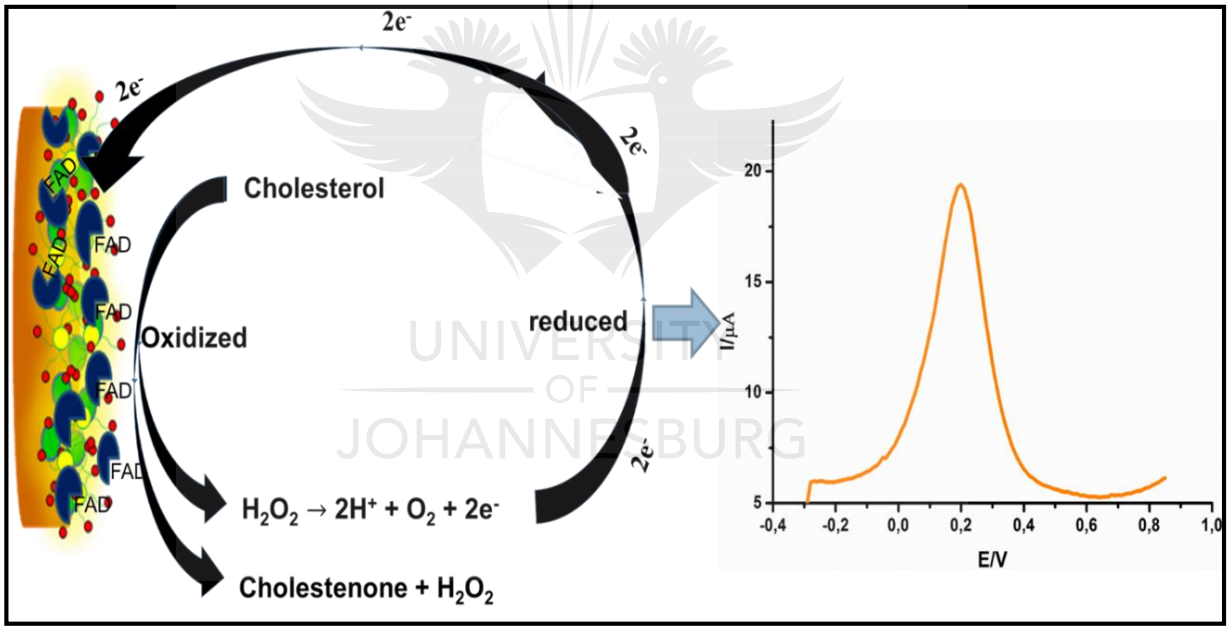

Figure 5. 10: Schematic representation of electrochemical detection of cholesterol based on GCE/PPI/QDs/ChOx.

The optimum conditions used for this type of biosensor involved the use of 10 mM PBS (pH 7.2) solution with ChOx enzyme concentration of 2 $mg.mL^{-1}$, detection potential of +0.3 V and scan rate of 50 $mV.s^{-1}$. Under the selected conditions, a calibration curve was obtained in the linear range of 100 µM and 10 mM, with a correlation coefficient of 0.9854. The limit of detection (LOD) and limit of quantification (LOQ) were found to be 0.35 µM and 0.95 µM respectively. The

biosensor also had a sensitivity of 283.3 μA μM^{-1} cm^{-2}. The equations (eq. 5.6, 5.7 and 5.8) below were used to calculate the parameters above. Table 5.1 compares the analytical performances of different cholesterol biosensors in literature.

$$\text{Limit of detection (LOD)} = \frac{\mathbf{3 \times standard\ deviation\ (SD)}}{\mathbf{slope}} \quad \text{eq 5. 3}$$

$$\text{Limit of quantification (LOQ)} = \frac{\mathbf{10 \times standard\ deviation\ (SD)}}{\mathbf{slope}} \quad \text{eq 5. 4}$$

$$\text{Sensitivity} = \frac{\mathbf{slope}}{\mathbf{effective\ surface\ area}} \quad \text{eq 5. 5}$$

Table 5. 1: Comparison of analytical performance of some cholesterol biosensors constructed based on different modified electrode materials.

Electrode material	Linear range	Detection limit	Sensitivity	Ref.
Nafion/ChOx/α-Fe_2O_3/Ag	0.1 – 8.0 mM	0.018 mM	78.56 μA μM^{-1} cm^{-2}	26
(ChOx/AuNPs/IL/HTNSs/ITO)	8.33×10^{-9} - 4.17×10^{-7} M	6.30×10^{-9} M	-	161
(TGPHs/TGHs/AuNPs/ChOx)	5.0×10^{-8} – 5.9×10^{-4} M	0.017 μM	-	45
ChOx/PANI/PVP/Graphene	50 μM -10 mM	1.0 μM	34.77 μA μM^{-1} cm^{-2}	162
ChOx/Chit./ZnO@ZnS/GCE	0.4 – 4.0 mM	0.02 mM	52.67 mA.M^{-1} cm^{-2}	7
Nafion/ChOx/ZnO/Au	1.0 – 500 nM	0.37 nM	23.7 μA mM^{-1} cm^{-2}	163
ChOx-PB-modified SPE	0.05 – 0.30 mM	3.7 μM	26.0 mA.M^{-1} cm^{-2}	164
AuNP/Carbon IDE	0.005 – 10.0 mM	1.28 μM	993.91 μA $\mu M^{-1}cm^{-2}$	3
GCE/PTH/ChOx/HRP	25 – 125 μM	6.3 μM	0.18 μA μM^{-1} cm^{-2}	79
PPI/QDs/ChOx	100 μM – 10 mM	0.35 μM	283.3 μA μM^{-1} cm^{-2}	This work

5.5.2 Selectivity and stability of cholesterol biosensor

The selectivity of the biosensor was evaluated in the presence of interferents such as glucose (Glu), ascorbic acid (AA) and uric acid (UA) which co-exist with cholesterol in the serum. The effect of interferences was determined by adding the interference species (e.g Glu) in the reaction mixture containing cholesterol (Fig. 5.11). The response of these inteferents at the prepared electrode were 6.16%, 7.31% and 8.71% for UA, AA and Glu, respectively. For cholesterol, the current produced was *ca*. 78% higher than the interferents. Thus, the biosensor (GCE/PPI/OQDs/ChOx) shows good selectivity and therefore has the potential to be used in real samples.

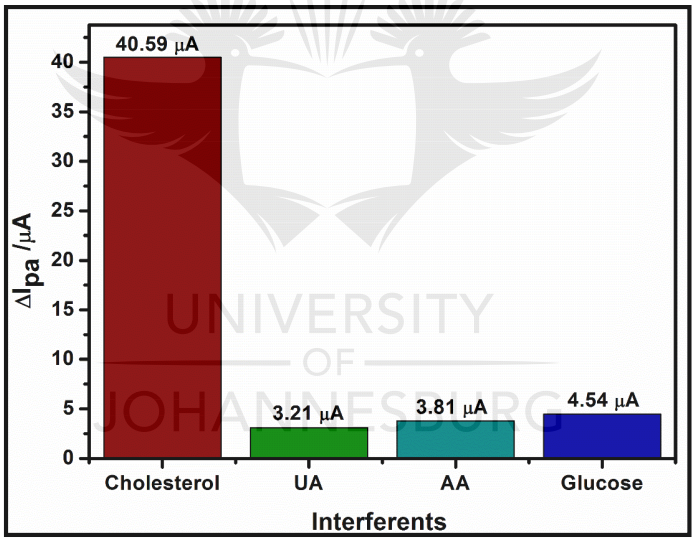

Figure 5. 11: Selectivity of the biosensor (GCE/PPI/OQDs/ChOx) in the presence of 10 mM cholesterol and interferents - 10 mM uric acid (UA), 5 mM ascorbic acid (AA) and 5 mM glucose in PBS (pH 7.2) solution.

For stability studies, the biosensor was stored in the refrigerator at 4 °C when not in use and cleaned using 10 mM PBS (pH 7.2) before utilisation. The stability of the working electrode was investigated for over four weeks in 5 mM cholesterol at 25 °C. After a month of storage at 4 °C, the biosensor retained 98% of its original response in the same sample, indicating that the biosensor had good stability when stored correctly (Fig. 5.12).

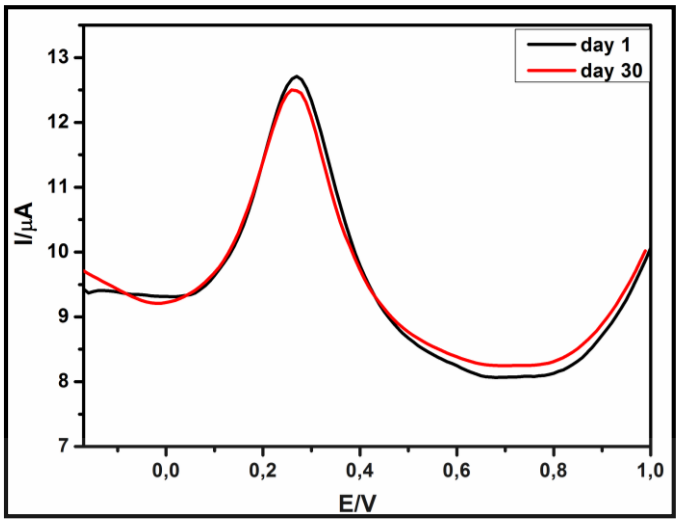

Figure 5. 12: Stability studies of the biosensor at day 1 and day 30 in 5 mM cholesterol solution (pH 7.2).

5.6 SUB-CONCLUSION

This chapter exploited the applicability of QDs and PPI in developing a suitable nanoplatform for immobilization of ChOx. The nanoplatform exhibited reversible electrochemistry, excellent catalytic properties towards $[Fe(CN)_6]^{3-/4-}$ probe and good electron transportation. This cholesterol biosensor had good sensitivity and selectivity, detection limit of 0.35 μM and a dynamic linearity of 100 μM – 10 mM for cholesterol. SEM Images also confirmed the successful immobilization of PPI, QDs and ChOx on the electrode.

CHAPTER 6

CONCLUSION AND RECOMMENDATIONS

6.1 CONCLUSION

The aim of this work was to explore the applicability of PPI dendrimers and the as-synthesized quantum dots (QDs) nanocomposite in developing a suitable nanoplatform and modifiers for the development of an enzyme-based electrochemical cholesterol biosensor. Firstly, the MPA capped QDs were successfully synthesized in aqueous phase and characterized using UV-visible, PL, FTIR, XRD, TEM, SEM and EDX. During synthesis, the CdTe solution was yellow and became very intense as reaction time increased, indicating the formation of CdTe core. The CdTe/CdSe solution was orange and turned red as reaction time increased, while the CdTe/CdSe/ZnSe solution was deep red, changing to brown as reaction time increased. Both the absorption and emission spectra of the as-synthesized QDs showed systematic and dramatic red-shift as reaction time increased. This depicts the growth of the QDs. The increase in intensity of the as-synthesized QDs after adding selenium precursor and an hour after adding Zn precursor indicated proper passivation of the QDs by the CdSe shell and ZnSe shell. The successful capping of the QDs by MPA was confirmed by FTIR spectroscopy. The structural and morphological characterizations shows that the as-synthesized QDs were small, spherical monodispersed and highly crystalline with average particle size of 4.08 nm CdTe/CdSe/ZnSe QDs. Electrochemical cholesterol biosensor was developed by immobilising the PPI dendrimer, QDs and ChOx enzyme on a glassy carbon electrode (GCE). After each immobilization, the electrochemical property of the modified GCE was exploited using CV, SWV and EIS in PBS and ferricyanide solution. The applicability of the designed biosensor was evaluated on cholesterol solutions and interferents such as glucose, uric acid and ascorbic acid. It was able to detect cholesterol even at lower concentrations, but for the interferents, the detection was negligible. A detection limit of 0.35 µM and sensitivity of 283.3 µA μM^{-1} cm^{-2} was obtained in a linear range of 100 µM – 10 mM.

Enzymatic electrochemical biosensors have been extensively exploited for the detection of glucose, cholesterol, pesticides etc…) due to their high selectivity, sensitivity, ease of use, reusability and fast response time. Polypropylene imine (PPI) dendrimer nanomaterial and its nanocomposite possess suitable electrochemical properties that makes them applicable in developing an electrochemical biosensors. In this study, glassy carbon electrode (GCE) was modified with PPI dendrimer and quantum dots and was used to develop a novel electrochemical cholesterol biosensor by effectively entrapping ChOx enzyme into the PPI/QDs composite matrix. The nanocomposite was able to provide a suitable environment for the enzyme and also provided good orientation for efficient electronic communication between the active site of ChOx and the electrode surface. Based on the synergistic effect between the PPI and the QDs, the composite enhanced the electrocatalytic activity of ChOx toward cholesterol molecule and improved electron communication, thus producing a cholesterol biosensor with enhanced analytical performances. The designed biosensor had analytical performances such as good selectivity and sensitivity, long term stability, wide detection range with low detection limit and good reproducibility. This novel platform can be applicable in developing high performance cholesterol biosensor for clinicians.

6.2 FUTURE WORK AND RECOMMENDATIONS

This work may be considered successful, but there are some recommendations made for future work and they include:

- Characterization of the as-synthesized QDs and PPI dendrimer with X-ray photoelectron spectroscopy (XPS) and field emission scanning electron microscopy (FE-SEM) so as to understand the surface chemistry that took place in the both materials.

- Even though this QDs have showed less or no toxicity for cells in some studies, it still contains the toxic heavy metal cadmium. So we recommend the use of non-toxic metals such as silver (Ag) and copper (Cu) for the synthesis of the core and core/shell QDs.

- The electrodeposition variables can be manipulated or optimized to vary the size of the nanomaterial on the platform.
- Temperature studies must also be carried out on the designed biosensor.
- Though QDs was immobilized after electrodeposition of PPI dendrimer, co-electrodeposition of the two materials is recommended.

REFERENCES

(1) Chamorro-Garcia, A.; Merkoçi, A. Nanobiosensors in diagnostics. *Nanobiomedicine* **2016**, *3*, 1-26.

(2) Pabbi, M.; Mittal, S. K. An electrochemical algal biosensor based on silica coated ZnO quantum dots for selective determination of acephate. *Analytical Methods* **2017**, *9*, 1672-1680.

(3) Sharma, D.; Lee, J.; Seo, J.; Shin, H. Development of a Sensitive Electrochemical Enzymatic Reaction-Based Cholesterol Biosensor Using Nano-Sized Carbon Interdigitated Electrodes Decorated with Gold Nanoparticles. *Sensors* **2017**, *17*, 2128-2137.

(4) Qureshi, R. N.; Kaal, E.; Janssen, H.-G.; Schoenmakers, P. J.; Kok, W. T. Determination of cholesterol and triglycerides in serum lipoproteins using flow field-flow fractionation coupled to gas chromatography–mass spectrometry. *Analytica Chimica Acta* **2011**, *706*, 361-366.

(5) Yildiz, H. B.; Talaz, O.; Kamaci, M.; Caliskan, A.; Caliskan, S. Novel Photoelectrochemical Biosensors for Cholesterol Biosensing by Photonic “Wiring” of Cholesterol Oxidase. *Journal of Macromolecular Science, Part A* **2013**, *50*, 1182-1193.

(6) Sharma, D.; Lee, J.; Seo, J.; Shin, H. Development of a Sensitive Electrochemical Enzymatic Reaction-Based Cholesterol Biosensor Using Nano-Sized Carbon Interdigitated Electrodes Decorated with Gold Nanoparticles. *Sensors* **2017**, *17*, 2128-2144.

(7) Giri, A. K.; Charan, C.; Saha, A.; Shahi, V. K.; Panda, A. B. An amperometric cholesterol biosensor with excellent sensitivity and limit of detection based on an enzyme-immobilized microtubular ZnO@ ZnS heterostructure. *Journal of Materials Chemistry A* **2014**, *2*, 16997-17004.

(8) Nakaminami, T.; Kuwabata, S.; Yoneyama, H. Electrochemical oxidation of cholesterol catalyzed by cholesterol oxidase with use of an artificial electron mediator. *Analytical Chemistry* **1997**, *69*, 2367-2372.

(9) Bunney, J.; Williamson, S.; Atkin, D.; Jeanneret, M.; Cozzolino, D.; Chapman, J. The Use of Electrochemical Biosensors in Food Analysis. *Current Research in Nutrition and Food Science Journal* **2017**, *5*, 183-195.

(10) Thakur, M.; Ragavan, K. Biosensors in food processing. *Journal of Food Science and Technology* **2013**, *50*, 625-641.

(11) Leonardo, S.; Toldrà, A.; Campàs, M. Trends and prospects on electrochemical biosensors for the detection of marine toxins. *Comprehensive Analytical Chemistry* **2017**, *78*, 303-341.

(12) Biosensors Market worth 27.06 Billion USD by 2022. https:/www.marketsandmarkets.com/PressReleases/biosensors.asp (accessed 05 April 2017).

(13) Chaniotakis, N. A. Enzyme stabilization strategies based on electrolytes and polyelectrolytes for biosensor applications. *Analytical and Bioanalytical Chemistry* **2004**, *378*, 89-95.

(14) Kim, K.-E.; Kim, T. G.; Sung, Y.-M. Fluorescent cholesterol sensing using enzyme-modified CdSe/ZnS quantum dots. *Journal of Nanoparticle Research* **2012**, *14*, 1-9.

(15) Ó'Fágáin, C. Enzyme stabilization—recent experimental progress. *Enzyme and Microbial Technology* **2003**, *33*, 137-149.

(16) Grieshaber, D.; MacKenzie, R.; Voeroes, J.; Reimhult, E. Electrochemical biosensors-sensor principles and architectures. *Sensors* **2008**, *8*, 1400-1458.

(17) Saxena, U.; Das, A. B. Nanomaterials towards fabrication of cholesterol biosensors: key roles and design approaches. *Biosensors and Bioelectronics* **2016**, *75*, 196-205.

(18) Saxena, U.; Chakraborty, M.; Goswami, P. Covalent immobilization of cholesterol oxidase on self-assembled gold nanoparticles for highly sensitive amperometric detection of cholesterol in real samples. *Biosensors and Bioelectronics* **2011**, *26*, 3037-3043.

(19) Sotiropoulou, S.; Vamvakaki, V.; Chaniotakis, N. A. Stabilization of enzymes in nanoporous materials for biosensor applications. *Biosensors and Bioelectronics* **2005**, *20*, 1674-1679.

(20) Kim, J.; Grate, J. W.; Wang, P. Nanostructures for enzyme stabilization. *Chemical Engineering Science* **2006**, *61*, 1017-1026.

(21) Yu, T.; Wang, W.; Chen, J.; Zeng, Y.; Li, Y.; Yang, G.; Li, Y. Dendrimer-encapsulated Pt nanoparticles: an artificial enzyme for hydrogen production. *The Journal of Physical Chemistry C* **2012**, *116*, 10516-10521.

(22) Liu, X.; Zeng, Y.; Zhang, X.; Yu, T.; Chen, J.; Li, Y. Dendrimers-merging biomimics and photoenergy conversion. *Science China Chemistry* **2015**, *58*, 390-399.

(23) Ravotto, L.; Mazzaro, R.; Natali, M.; Ortolani, L.; Morandi, V.; Ceroni, P.; Bergamini, G. Photoactive dendrimer for water photoreduction: a scaffold to combine sensitizers and catalysts. *The Journal of Physical Chemistry Letters* **2014**, *5*, 798-803.

(24) Ncapayi, V.; Parani, S.; Songca, S. P.; Kodama, T.; Oluwafemi, O. S. Simple green synthesis of amino acid functionalised CdTe/CdSe/ZnSe core-multi shell with improved cell viability for cellular imaging. *Materials Letters* **2017**, *189*, 168-171.

(25) Rahman, M. M.; Asiri, A. M. One-step electrochemical detection of cholesterol in the presence of suitable $K_3Fe(CN)_6$/phosphate buffer mediator by an electrochemical approach. *Talanta* **2015**, *140*, 96-101.

(26) Umar, A.; Ahmad, R.; Hwang, S.; Kim, S.; Al-Hajry, A.; Hahn, Y. Development of highly sensitive and selective cholesterol biosensor based on cholesterol Oxidase Co-immobilized with α-Fe_2O_3 micro-pine shaped hierarchical structures. *Electrochimica Acta* **2014**, *135*, 396-403.

(27) Expert Panel on Detection, E. Executive summary of the Third Report of the National Cholesterol Education Program (NCEP) expert panel on detection, evaluation, and treatment of high blood cholesterol in adults (Adult Treatment Panel III). *Jama* **2001**, *285*, 2486.

(28) Panel, N. C. E. P. N. E. Third report of the National Cholesterol Education Program (NCEP) expert panel on detection, evaluation, and treatment of high blood cholesterol in adults (Adult Treatment Panel III) final report. *Circulation* **2002**, *106*, 3143.

(29) Norman, R.; Bradshaw, D.; Schneider, M.; Joubert, J.; Groenewald, P.; Lewin, S.; Steyn, K.; Vos, T.; Laubscher, R.; Nannan, N. A comparative risk assessment for South Africa in 2000: towards promoting health and preventing disease. *South African Medical Journal* **2007**, *97*, 637-641.

(30) Steyn, K.; Goldberg, Y.; Kotze, M.; Steyn, M.; Swanepoel, A.; Fourie, J.; Coetzee, G.; Van der Westhuyzen, D. Estimation of the prevalence of familial hypercholesterolaemia in a rural Afrikaner community by direct screening for three

Afrikaner founder low density lipoprotein receptor gene mutations. *Human Genetics* **1996**, *98*, 479-484.

(31) Kotze, M.; Langenhoven, E.; Warnich, L.; Plessis, L. d.; Retief, A. The molecular basis and diagnosis of familial hypercholesterolaemia in South African Afrikaners. *Annals of Human Genetics* **1991**, *55*, 115-121.

(32) Understanding what your cholesterol level mean. https://www.cholesterolmenu.com/cholesterol-levels-chart/ (accessed 15 May 2017).

(33) John, J.; Reghuwanshi, A.; Aravind, U. K.; Aravindakumar, C. Development and validation of a high-performance thin layer chromatography method for the determination of cholesterol concentration. *Journal of Food and Drug Analysis* **2015**, *23*, 219-224.

(34) Hojo, K.; Hakamata, H.; Ito, A.; Kotani, A.; Furukawa, C.; Hosokawa, Y.-Y.; Kusu, F. Determination of total cholesterol in serum by high-performance liquid chromatography with electrochemical detection. *Journal of Chromatography A* **2007**, *1166*, 135-141.

(35) Kim, H.-J.; Park, J.-M.; Lee, J.-H.; Kim, J.-M. Detection for non-milk fat in dairy product by gas chromatography. *Korean Journal for Food Science of Animal Resources* **2016**, *36*, 206-215.

(36) Lian, K.; Zhang, P.; Wang, W.; Dai, T.; Li, L. Determination of Total Cholesterol in Serum by Gas Chromatography-Mass Spectrometry. *Asian Journal of Chemistry* **2014**, *26*, 2646-2648.

(37) Wei, X. E.; Korth, J.; Brown, S. H.; Mitchell, T. W.; Truscott, R. J.; Blanksby, S. J.; Willcox, M. D.; Zhao, Z. Rapid Quantification of Free Cholesterol in Tears Using Direct Insertion/Electron Ionization–Mass SpectrometryQuantification of Free Cholesterol in Tears via DI/EI-MS. *Investigative Ophthalmology & Visual Science* **2013**, *54*, 8027-8035.

(38) Šabović, I.; De Toni, L.; Tescari, S.; De Filippis, V.; Menegazzo, M. Detection of Cholesterol and its Oxidized Derivatives in Human Sperm Membranes through a Fast and Reliable LC-MS Method. *Journal of Clinical and Laboratory Medicine* **2017**, *2*.

(39) Zhang, X.; Wei, M.; Lv, B.; Liu, Y.; Liu, X.; Wei, W. Sensitive colorimetric detection of glucose and cholesterol by using Au@ Ag core–shell nanoparticles. *RSC Advances* **2016**, *6*, 35001-35007.

(40) Kejík, Z.; Havlík, M.; Bříza, T.; Kaplánek, R.; Dolenský, B.; Králová, J.; Martásek, P.; Král, V. Methinium colorimetric sensors for the determination of cholesterol sulfate in an aqueous medium. *Sensors and Actuators B: Chemical* **2017**, *245*, 1032-1038.

(41) Ghannam, M.; Abdelhalim, M.; Moussa, S.; Al-Mohy, Y.; Al-Ayed, M. Ultraviolet-visible and fluorescence spectroscopy techniques are important diagnostic tools during the progression of atherosclerosis: Diet zinc supplementation retarded or delayed atherosclerosis. *Atherosclerosis* **2015**, *241*, 121-122.

(42) Xu, S.; Wang, Y.; Zhou, D.; Kuang, M.; Fang, D.; Yang, W.; Wei, S.; Ma, L. A novel chemiluminescence sensor for sensitive detection of cholesterol based on the peroxidase-like activity of copper nanoclusters. *Scientific Reports* **2016**, *6*, 1234–1242.

(43) Sun, L.; Li, S.; Ding, W.; Yao, Y.; Yang, X. Fluorescence detection of cholesterol using a nitrogen-doping graphene quantum dots/chromium picolinate complex-based sensor. *Journal of Materials Chemistry B* **2017**, *5*, 90006-99014.

(44) Mansano, F. V.; Kazaoka, R. M.; Ronsein, G. E.; Prado, F. M.; Genaro-Mattos, T. C.; Uemi, M.; Mascio, P. D.; Miyamoto, S. Highly sensitive fluorescent method for the detection of cholesterol aldehydes formed by ozone and singlet molecular oxygen. *Analytical Chemistry* **2010**, *82*, 6775-6781.

(45) Cao, S.; Zhang, L.; Chai, Y.; Yuan, R. An integrated sensing system for detection of cholesterol based on TiO_2–graphene–Pt–Pd hybridnanocomposites. *Biosensors and Bioelectronics* **2013**, *42*, 532-538.

(46) Cammann, K. Bio-sensors based on ion-selective electrodes. *Fresenius' Zeitschrift für Analytische Chemie* **1977**, *287*, 1-9.

(47) Mehrotra, P. Biosensors and their applications–A review. *Journal of Oral Biology and Craniofacial Research* **2016**, *6*, 153-159.

(48) Thevenot, D. R.; Toth, K.; Durst, R. A.; Wilson, G. S. Electrochemical biosensors: recommended definitions and classification. *Pure and Applied Chemistry* **1999**, *71*, 2333-2348.

(49) Holzinger, M.; Le Goff, A.; Cosnier, S. Nanomaterials for biosensing applications: a review. *Frontiers in Chemistry* **2014**, *2*, 63.

(50) Murugaiyan, S. B.; Ramasamy, R.; Gopal, N.; Kuzhandaivelu, V. Biosensors in clinical chemistry: An overview. *Advanced Biomedical Research* **2014**, *3*, 67-75.

(51) Clark, L. C.; Lyons, C. Electrode systems for continuous monitoring in cardiovascular surgery. *Annals of the New York Academy of Sciences* **1962**, *102*, 29-45.

(52) Kim, K.-E.; Kim, T. G.; Sung, Y.-M. Fluorescent cholesterol sensing using enzyme-modified CdSe/ZnS quantum dots. *Journal of Nanoparticle Research* **2012**, *14*, 1179.

(53) Zhu, C.; Yang, G.; Li, H.; Du, D.; Lin, Y. Electrochemical sensors and biosensors based on nanomaterials and nanostructures. *Analytical Chemistry* **2014**, *87*, 230-249.

(54) Syahir, A.; Usui, K.; Tomizaki, K.-y.; Kajikawa, K.; Mihara, H. Label and label-free detection techniques for protein microarrays. *Microarrays* **2015**, *4*, 228-244.

(55) Luo, X.; Davis, J. J. Electrical biosensors and the label free detection of protein disease biomarkers. *Chemical Society Reviews* **2013**, *42*, 5944-5962.

(56) de la Escosura-Muñiz, A.; Merkoçi, A. Nanochannels preparation and application in biosensing. *ACS Nano* **2012**, *6*, 7556.

(57) Štěpánková, Š.; Vorčáková, K. Cholinesterase-based biosensors. *Journal of Enzyme Inhibition and Medicinal Chemistry* **2016**, 1-14.

(58) Volontè, F.; Pollegioni, L.; Molla, G.; Frattini, L.; Marinelli, F.; Piubelli, L. Production of recombinant cholesterol oxidase containing covalently bound FAD in Escherichia coli. *BMC Biotechnology* **2010**, *10*, 33.

(59) Vrielink, A.; Ghisla, S. Cholesterol oxidase: biochemistry and structural features. *The FEBS Journal* **2009**, *276*, 6826-6843.

(60) Coulombe, R.; Yue, K. Q.; Ghisla, S.; Vrielink, A. Oxygen access to the active site of cholesterol oxidase through a narrow channel is gated by an Arg-Glu pair. *Journal of Biological Chemistry* **2001**, *276*, 30435-30441.

(61) D'Orazio, P. Biosensors in clinical chemistry. *Clinica Chimica Acta* **2003**, *334*, 41-69.

(62) Chaubey, A.; Malhotra, B. Mediated biosensors. *Biosensors and Bioelectronics* **2002**, *17*, 441-456.

(63) Ibupoto, Z. H.; Elhag, S.; Nur, O.; Willander, M. Fabrication of sensitive potentiometric cholesterol biosensor based on Co_3O_4 interconnected nanowires. *Electroanalysis* **2014**, *26*, 1928-1934.

(64) Nikoleli, G.-P.; Ibupoto, Z.; Nikolelis, D.; Likodimos, V.; Psaroudakis, N.; Tzamtzis, N.; Willander, M.; Hianik, T. Potentiometric cholesterol biosensing application of graphene electrode with stabilized polymeric lipid membrane. *Open Chemistry* **2013**, *11*, 1554-1561.

(65) Thévenot, D. R.; Toth, K.; Durst, R. A.; Wilson, G. S. Electrochemical biosensors: recommended definitions and classification. *Biosensors and Bioelectronics* **2001**, *16*, 121-131.

(66) Singh, K.; Chauhan, R.; Solanki, P. R.; Basu, T. Development of Impedimetric Biosensor for Total Cholesterol Estimation Based on Polypyrrole and Platinum Nanoparticle Multi Layer Nanocomposite. *International Journal of Organic Chemistry* **2013**, *3*, 262-274.

(67) Luppa, P. B.; Sokoll, L. J.; Chan, D. W. Immunosensors—principles and applications to clinical chemistry. *Clinica Chimica Acta* **2001**, *314*, 1-26.

(68) Wang, J. Electrochemical biosensors: towards point-of-care cancer diagnostics. *Biosensors and Bioelectronics* **2006**, *21*, 1887-1892.

(69) Lata, K.; Dhull, V.; Hooda, V. Fabrication and Optimization of ChE/ChO/HRP-AuNPs/c-MWCNTs Based Silver Electrode for Determining Total Cholesterol in Serum. *Biochemistry Research International* **2016**, *2016*, 780-791.

(70) Nantaphol, S.; Chailapakul, O.; Siangproh, W. A novel paper-based device coupled with a silver nanoparticle-modified boron-doped diamond electrode for cholesterol detection. *Analytica Chimica Acta* **2015**, *891*, 136-143.

(71) Dhand, C.; Singh, S.; Arya, S. K.; Datta, M.; Malhotra, B. Cholesterol biosensor based on electrophoretically deposited conducting polymer film derived from nano-structured polyaniline colloidal suspension. *Analytica Chimica Acta* **2007**, *602*, 244-251.

(72) Mohamad, N. R.; Marzuki, N. H. C.; Buang, N. A.; Huyop, F.; Wahab, R. A. An overview of technologies for immobilization of enzymes and surface analysis techniques for immobilized enzymes. *Biotechnology & Biotechnological Equipment* **2015**, *29*, 205-220.

(73) Asuri, P.; Karajanagi, S. S.; Sellitto, E.; Kim, D. Y.; Kane, R. S.; Dordick, J. S. Water-soluble carbon nanotube-enzyme conjugates as functional biocatalytic formulations. *Biotechnology and Bioengineering* **2006**, *95*, 804-811.

(74) Xie, T.; Wang, A.; Huang, L.; Li, H.; Chen, Z.; Wang, Q.; Yin, X. Recent advance in the support and technology used in enzyme immobilization. *African Journal of Biotechnology* **2009**, *8*, 4724-4733,.

(75) Rocchitta, G.; Spanu, A.; Babudieri, S.; Latte, G.; Madeddu, G.; Galleri, G.; Nuvoli, S.; Bagella, P.; Demartis, M. I.; Fiore, V. Enzyme biosensors for biomedical applications: Strategies for safeguarding analytical performances in biological fluids. *Sensors* **2016**, *16*, 780-801.

(76) Arya, S. K.; Datta, M.; Malhotra, B. D. Recent advances in cholesterol biosensor. *Biosensors and Bioelectronics* **2008**, *23*, 1083-1100.

(77) Andreescu, S.; Marty, J.-L. Twenty years research in cholinesterase biosensors: from basic research to practical applications. *Biomolecular Engineering* **2006**, *23*, 1-15.

(78) Ovsejevi, K.; Manta, C.; Batista-Viera, F. Reversible covalent immobilization of enzymes via disulfide bonds. *Immobilization of Enzymes and Cells: Third Edition* **2013**, 89-116.

(79) Rahman, M. M.; Li, X.-b.; Kim, J.; Lim, B. O.; Ahammad, A. S.; Lee, J.-J. A cholesterol biosensor based on a bi-enzyme immobilized on conducting poly (thionine) film. *Sensors and Actuators B: Chemical* **2014**, *202*, 536-542.

(80) Rahman, M. M. Reusable and mediator-free cholesterol biosensor based on cholesterol oxidase immobilized onto TGA-SAM modified smart bio-chips. *PLoS One* **2014**, *9*, 100327.

(81) Huang, L.; Cheng, Z.-M. Immobilization of lipase on chemically modified bimodal ceramic foams for olive oil hydrolysis. *Chemical Engineering Journal* **2008**, *144*, 103-109.

(82) Chronopoulou, L.; Kamel, G.; Sparago, C.; Bordi, F.; Lupi, S.; Diociaiuti, M.; Palocci, C. Structure–activity relationships of Candida rugosa lipase immobilized on polylactic acid nanoparticles. *Soft Matter* **2011**, *7*, 2653-2662.

(83) Joshi, K. A.; Tang, J.; Haddon, R.; Wang, J.; Chen, W.; Mulchandani, A. A disposable biosensor for organophosphorus nerve agents based on carbon nanotubes modified thick film strip electrode. *Electroanalysis* **2005**, *17*, 54-58.

(84) Joshi, K. A.; Prouza, M.; Kum, M.; Wang, J.; Tang, J.; Haddon, R.; Chen, W.; Mulchandani, A. V-type nerve agent detection using a carbon nanotube-based amperometric enzyme electrode. *Analytical Chemistry* **2006**, *78*, 331-336.

(85) Subramanian, A.; Kennel, S. J.; Oden, P. I.; Jacobson, K. B.; Woodward, J.; Doktycz, M. J. Comparison of techniques for enzyme immobilization on silicon supports. *Enzyme and Microbial Technology* **1999**, *24*, 26-34.

(86) Ambrózy, A.; Hlavatá, L.; Labuda, J. Protective membranes at electrochemical biosensors. *Acta Chimica Slovaca* **2013**, *6*, 35-41.

(87) Gholivand, M. B.; Khodadadian, M. Amperometric cholesterol biosensor based on the direct electrochemistry of cholesterol oxidase and catalase on a graphene/ionic liquid-modified glassy carbon electrode. *Biosensors and Bioelectronics* **2014**, *53*, 472-478.

(88) Cao, S.; Zhang, L.; Chai, Y.; Yuan, R. Electrochemistry of cholesterol biosensor based on a novel Pt–Pd bimetallic nanoparticle decorated graphene catalyst. *Talanta* **2013**, *109*, 167-172.

(89) Shen, Q.; Yang, R.; Hua, X.; Ye, F.; Zhang, W.; Zhao, W. Gelatin-templated biomimetic calcification for β-galactosidase immobilization. *Process biochemistry* **2011**, *46*, 1565-1571.

(90) Tiwari, J. N.; Tiwari, R. N.; Kim, K. S. Zero-dimensional, one-dimensional, two-dimensional and three-dimensional nanostructured materials for advanced electrochemical energy devices. *Progress in Materials Science* **2012**, *57*, 724-803.

(91) Doria, G.; Conde, J.; Veigas, B.; Giestas, L.; Almeida, C.; Assunção, M.; Rosa, J.; Baptista, P. V. Noble metal nanoparticles for biosensing applications. *Sensors* **2012**, *12*, 1657-1687.

(92) Li, Z.; Xie, C.; Wang, J.; Meng, A.; Zhang, F. Direct electrochemistry of cholesterol oxidase immobilized on chitosan–graphene and cholesterol sensing. *Sensors and Actuators B: Chemical* **2015**, *208*, 505-511.

(93) Huang, H.; Zhu, J.-J. The electrochemical applications of quantum dots. *Analyst* **2013**, *138*, 5855-5865.

(94) Esteve-Turrillas, F. A.; Abad-Fuentes, A. Applications of quantum dots as probes in immunosensing of small-sized analytes. *Biosensors and Bioelectronics* **2013**, *41*, 12-29.

(95) Klostranec, J. M.; Chan, W. C. Quantum dots in biological and biomedical research: recent progress and present challenges. *Advanced Materials* **2006**, *18*, 1953-1964.

(96) Butwong, N.; Zhou, L.; Moore, E.; Srijaranai, S.; Luong, J. H.; Glennon, J. D. A highly sensitive hydrogen peroxide biosensor based on hemoglobin immobilized on cadmium sulfide quantum dots/chitosan composite modified glassy carbon electrode. *Electroanalysis* **2014**, *26*, 2465-2473.

(97) Shao, L.; Gao, Y.; Yan, F. Semiconductor quantum dots for biomedicial applications. *Sensors* **2011**, *11*, 11736-11751.

(98) de Mello Donega, C. Synthesis and properties of colloidal heteronanocrystals. *Chemical Society Reviews* **2011**, *40*, 1512-1546.

(99) Quantum dots fluorescence http://www.infobarrel.com/Quantum_Dot_Fluorescence (accessed 20 June 2017).

(100) Bhanoth, S.; Kshirsagar, A. S.; Khanna, P. K.; Tyagi, A.; Verma, A. K. Biotoxicity of CdS/CdSe Core-Shell Nano-Structures. *Advances in Nanoparticles* **2016**, *5*, 1.

(101) Zhao, M.-X.; Zeng, E.-Z. Application of functional quantum dot nanoparticles as fluorescence probes in cell labeling and tumor diagnostic imaging. *Nanoscale Research Letters* **2015**, *10*, 1-9.

(102) Derfus, A. M.; Chan, W. C.; Bhatia, S. N. Probing the cytotoxicity of semiconductor quantum dots. *Nano Letters* **2004**, *4*, 11-18.

(103) Liu, L.; Zhang, J.; Su, X.; Mason, R. P. In vitro and in vivo assessment of CdTe and CdHgTe toxicity and clearance. *Journal of Biomedical Nanotechnology* **2008**, *4*, 524-528.

(104) Girma, W. M.; Fahmi, M. Z.; Permadi, A.; Abate, M. A.; Chang, J.-Y. Synthetic strategies and biomedical applications of I–III–VI ternary quantum dots. *Journal of Materials Chemistry B* **2017**, *5*, 6193-6216.

(105) Brichkin, S. B.; Razumov, V. F. Colloidal quantum dots: synthesis, properties and applications. *Russian Chemical Reviews* **2016**, *85*, 1297-1309.

(106) Shambetova, N.; Chen, Y.; Xu, H.; Li, L.; Solandt, J.; Zhou, Y.; Wang, J.; Su, H.; Brismar, H.; Fu, Y. Acid dissociation of 3-Mercaptopropionic acid coated CdSe–CdS/Cd0. 5Zn0. 5S/ZnS core–multishell quantum dot and strong ionic interaction with Ca^{2+} ion. *The Journal of Physical Chemistry C* **2016**, *120*, 3519-3529.

(107) Zhang, Y.; Clapp, A. Overview of stabilizing ligands for biocompatible quantum dot nanocrystals. *Sensors* **2011**, *11*, 11036-11055.

(108) Kirchner, C.; Liedl, T.; Kudera, S.; Pellegrino, T.; Muñoz Javier, A.; Gaub, H. E.; Stölzle, S.; Fertig, N.; Parak, W. J. Cytotoxicity of colloidal CdSe and CdSe/ZnS nanoparticles. *Nano Letters* **2005**, *5*, 331-338.

(109) Sperling, R. A.; Parak, W. Surface modification, functionalization and bioconjugation of colloidal inorganic nanoparticles. *Philosophical Transactions of the Royal Society of London A: Mathematical, Physical and Engineering Sciences* **2010**, *368*, 1333-1383.

(110) Zhang, W.; Chen, G.; Wang, J.; Ye, B.-C.; Zhong, X. Design and synthesis of highly luminescent near-infrared-emitting water-soluble CdTe/CdSe/ZnS core/shell/shell quantum dots. *Inorganic Chemistry* **2009**, *48*, 9723-9731.

(111) Murray, C.; Norris, D. J.; Bawendi, M. G. Synthesis and characterization of nearly monodisperse CdE (E. *Journal of the American Chemical Society* **1993**, *115*, 8706-8715.

(112) Bonilla, C. A. M.; Kouznetsov, V. V.: "Green" Quantum Dots: Basics, Green Synthesis, and Nanotechnological Applications. In *Green Nanotechnology-Overview and Further Prospects*; InTech, **2016**.

(113) Dhyani, H.; Dhand, C.; Malhotra, B.; Sen, P. Polyaniline-CdS quantum dots composite for mediator free biosensing. *Journal of Biosensors and Bioelectronics* **2011**, *3*, 1-9.

(114) Stewart, A. J.; O'Reilly, E. J.; Moriarty, R. D.; Bertoncello, P.; Keyes, T. E.; Forster, R. J.; Dennany, L. A cholesterol biosensor based on the NIR electrogenerated-chemiluminescence (ECL) of water-soluble CdSeTe/ZnS quantum dots. *Electrochimica Acta* **2015**, *157*, 8-14.

(115) Tanne, J.; Schafer, D.; Khalid, W.; Parak, W.; Lisdat, F. Light-controlled bioelectrochemical sensor based on CdSe/ZnS quantum dots. *Analytical Chemistry* **2011**, *83*, 7778-7785.

(116) Malinga, S.; Arotiba, O.; Krause, R.; Mapolie, S.; Mamba, B. Synthesis and characterisation of generation 2 and 3 poly (propylene imine) dendrimer capped NiFe nanoalloy. *Materials Letters* **2012**, *68*, 324-326.

(117) Gupta, U.; Agashe, H. B.; Jain, N. K. Polypropylene imine dendrimer mediated solubility enhancement: effect of pH and functional groups of hydrophobes. *Journal of Pharmacy and Pharmaceutical Science* **2007**, *10*, 358-367.

(118) Tomalia, D. A.; Baker, H.; Dewald, J.; Hall, M.; Kallos, G.; Martin, S.; Roeck, J.; Ryder, J.; Smith, P. A new class of polymers: starburst-dendritic macromolecules. *Polymer Journal* **1985**, *17*, 117-132.

(119) Nigam, S.; Chandra, S.; Bahadur, D. Dendrimers based Electrochemical Biosensors. *Biomedical Research Journal* **2015**, *2*, 21-36.

(120) Dong, W.; Wang, K.; Chen, Y.; Li, W.; Ye, Y.; Jin, S. Construction and Characterization of a Chitosan-Immobilized-Enzyme and β-Cyclodextrin-Included-Ferrocene-Based Electrochemical Biosensor for H2O2 Detection. *Materials* **2017**, *10*, 868.

(121) Wang, D.; Jia, M.; Wang, L.; Song, S.; Feng, J.; Zhang, X. Chitosan and β-Cyclodextrin-epichlorohydrin Polymer Composite Film as a Plant Healthcare Material for Carbendazim-Controlled Release to Protect Rape against Sclerotinia sclerotiorum (Lib.) de Bary. *Materials* **2017**, *10*, 343.

(122) Dhyani, H.; Ali, M. A.; Pal, S. P.; Srivastava, S.; Solanki, P. R.; Malhotra, B. D.; Sen, P. Mediator-free biosensor using chitosan capped CdS quantum dots for detection of total cholesterol. *RSC Advances* **2015**, *5*, 45928-45934.

(123) Le Goff, A.; Holzinger, M.; Cosnier, S. Enzymatic biosensors based on SWCNT-conducting polymer electrodes. *Analyst* **2011**, *136*, 1279-1287.

(124) Arotiba, O.; Owino, J.; Songa, E.; Hendricks, N.; Waryo, T.; Jahed, N.; Baker, P.; Iwuoha, E. An electrochemical DNA biosensor developed on a nanocomposite platform of gold and poly (propyleneimine) dendrimer. *Sensors* **2008**, *8*, 6791-6809.

(125) Singh, J.; Jain, K.; Mehra, N. K.; Jain, N. Dendrimers in anticancer drug delivery: mechanism of interaction of drug and dendrimers. *Artificial cells, Nanomedicine, and Biotechnology* **2016**, *44*, 1626-1634.

(126) de Brabander-van den Berg, E.; Meijer, E. Poly (propylene imine) dendrimers: large-scale synthesis by hetereogeneously catalyzed hydrogenations. *Angewandte Chemie International Edition in English* **1993**, *32*, 1308-1311.

(127) Boas, U.; Christensen, J. B.; Heegaard, P. M. Dendrimers: design, synthesis and chemical properties. *Journal of Materials Chemistry* **2006**, *16*, 3785-3798.

(128) Astachov, V.; Garzoni, M.; Danani, A.; Choy, K.-L.; Pavan, G.; Fahmi, A. In situ functionalization of self-assembled dendrimer nanofibers with cadmium sulfide quantum dots through simple ionic-substitution. *New Journal of Chemistry* **2016**.

(129) Katz, E.; Willner, I. Probing biomolecular interactions at conductive and semiconductive surfaces by impedance spectroscopy: routes to impedimetric immunosensors, DNA-sensors, and enzyme biosensors. *Electroanalysis* **2003**, *15*, 913-947.

(130) Taniguchi, S.; Green, M.; Rizvi, S. B.; Seifalian, A. The one-pot synthesis of core/shell/shell CdTe/CdSe/ZnSe quantum dots in aqueous media for in vivo deep tissue imaging. *Journal of Materials Chemistry* **2011**, *21*, 2877-2882.

(131) Yuan, Z.; Yang, P. Effect of shells on photoluminescence of aqueous CdTe quantum dots. *Materials Research Bulletin* **2013**, *48*, 2640-2647.

(132) Gui, R.; An, X. Layer-by-layer aqueous synthesis, characterization and fluorescence properties of type-II CdTe/CdS core/shell quantum dots with near-infrared emission. *RSC Advances* **2013**, *3*, 20959-20969.

(133) Ratnesh, R.; Mehata, M. S. Synthesis and optical properties of core-multi-shell CdSe/CdS/ZnS quantum dots: Surface modifications. *Optical Materials* **2017**, *64*, 250-256.

(134) Xu, B.; Cai, B.; Liu, M.; Fan, H. Ultraviolet radiation synthesis of water dispersed CdTe/CdS/ZnS core–shell–shell quantum dots with high fluorescence strength and biocompatibility. *Nanotechnology* **2013**, *24*, 205601-205613.

(135) Trindade , T.; O'Brien, P.; Pickett, N. L. Nanocrystalline semiconductors: synthesis, properties, and perspectives. *Chemistry of Materials* **2001**, *13*, 3843–3858.

(136) Murray, C.; Sun, S.; Gaschler, W.; Doyle, H.; Betley, T.; Kagan, C. Colloidal synthesis of nanocrystals and nanocrystal supperlattice. *IBM Journal of Research and Development* **2001**, *45*, 47-56.

(137) Mohan, S.; Oluwafemi, O. S.; Songca, S. P.; Osibote, O. A.; George, S. C.; Kalarikkal, N.; Thomas, S. Facile synthesis of transparent and fluorescent epoxy-CdSe-CdS-ZnS core-multi shell polymer nanocomposite. *New Journal of Chemistry* **2014**, *38*, 155-162.

(138) Hai, L.; Nghia, N.; Nga, P.; Chinh, V.; Trang, N.; Hanh, V. Preparation and spectroscopic investigation of colloidal CdSe/CdS/ZnS core/multishell nanostructure. *Journal of Experimental Nanoscience* **2009**, *4*, 277-283.

(139) Talapin, D. V.; Mekis, I.; Götzinger, S.; Kornowski, A.; Benson, O.; Weller, H. CdSe/CdS/ZnS and CdSe/ZnSe/ZnS Core− Shell− Shell Nanocrystals. *The Journal of Physical Chemistry B* **2004**, *108*, 18826-18831.

(140) Wang, Y.; Liang, X.; Ma, X.; Hu, Y.; Hu, X.; Li, X.; Fan, J. Simple and greener synthesis of highly photoluminescence Mn^{2+}-doped ZnS quantum dots and its surface passivation mechanism. *Applied Surface Science* **2014**, *316*, 54-61.

(141) Jothi, N. N.; Joshi, A. G.; Vijay, R. J.; Muthuvinayagam, A.; Sagayaraj, P. Investigation on one-pot hydrothermal synthesis, structural and optical properties of ZnS quantum dots. *Materials Chemistry and Physics* **2013**, *138*, 186-191.

(142) Dabbousi, B. O.; Rodriguez-Viejo, J.; Mikulec, F. V.; Heine, J. R.; Mattoussi, H.; Ober, R.; Jensen, K. F.; Bawendi, M. G. (CdSe) ZnS core-shell quantum dots: synthesis and characterization of a size series of highly luminescent nanocrystallites. *The Journal of Physical Chemistry B* **1997**, *101*, 9463-9475.

(143) Yu, W. W.; Qu, L.; Guo, W.; Peng, X. Experimental determination of the extinction coefficient of CdTe, CdSe, and CdS nanocrystals. *Chemistry of Materials* **2003**, *15*, 2854-2860.

(144) He, Y.; Lu, H. T.; Sai, L. M.; Su, Y. Y.; Hu, M.; Fan, C. H.; Huang, W.; Wang, L. H. Microwave Synthesis of Water-Dispersed CdTe/CdS/ZnS Core-Shell-Shell Quantum Dots with Excellent Photostability and Biocompatibility. *Advanced Materials* **2008**, *20*, 3416-3421.

(145) Hines, M. A.; Guyot-Sionnest, P. Synthesis and characterization of strongly luminescing ZnS-capped CdSe nanocrystals. *The Journal of Physical Chemistry* **1996**, *100*, 468-471.

(146) Peng, X.; Schlamp, M. C.; Kadavanich, A. V.; Alivisatos, A. P. Epitaxial growth of highly luminescent CdSe/CdS core/shell nanocrystals with photostability and electronic accessibility. *Journal of the American Chemical Society* **1997**, *119*, 7019-7029.

(147) Grabolle, M.; Ziegler, J.; Merkulov, A.; Nann, T.; Resch-Genger, v. U. Stability and fluorescence quantum yield of CdSe–ZnS quantum dots—influence of the

thickness of the ZnS shell. *Annals of New York Academy of Science* **2008**, *1130*, 235-241.

(148) Smith, A. M.; Mohs, A. M.; Nie, S. Tuning the optical and electronic properties of colloidal nanocrystals by lattice strain. *Nature Nanotechnology* **2009**, *4*, 56-63.

(149) Yan, C.; Tang, F.; Li, L.; Li, H.; Huang, X.; Chen, D.; Meng, X.; Ren, J. Synthesis of aqueous CdTe/CdS/ZnS core/shell/shell quantum dots by a chemical aerosol flow method. *Nanoscale Research Letters* **2010**, *5*, 189.

(150) Son, J. S.; Park, K.; Kwon, S. G.; Yang, J.; Choi, M. K.; Kim, J.; Yu, J. H.; Joo, J.; Hyeon, T. Dimension-Controlled Synthesis of CdS Nanocrystals: From 0D Quantum Dots to 2D Nanoplates. *Small* **2012**, *8*, 2394-2402.

(151) Ke, J.; Li, X.; Shi, Y.; Zhao, Q.; Jiang, X. A facile and highly sensitive probe for Hg (II) based on metal-induced aggregation of ZnSe/ZnS quantum dots. *Nanoscale* **2012**, *4*, 4996-5001.

(152) Vo, N.; Ngo, H.; Vu, D.; Duong, A.; Lam, Q. Conjugation of E. coli O157: H7 antibody to CdSe/ZnS quantum dots. *Journal of Nanomaterials* **2015**, *2015*, 8.

(153) Li, Y.; Xu, J.; Xu, Y.; Huang, L.; Wang, J.; Cheng, X. Synthesis and characterization of fluorescent chitosan–ZnSe/ZnS nanoparticles for potential drug carriers. *RSC Advances* **2015**, *5*, 38810-38817.

(154) Koneswaran, M.; Narayanaswamy, R. Mercaptoacetic acid capped CdS quantum dots as fluorescence single shot probe for mercury (II). *Sensors and Actuators B: Chemical* **2009**, *139*, 91-96.

(155) Huang, Y.; Cui, L.; Xue, Y.; Zhang, S.; Zhu, N.; Liang, J.; Li, G. Ultrasensitive cholesterol biosensor based on enzymatic silver deposition on gold nanoparticles modified screen-printed carbon electrode. *Materials Science and Engineering: C* **2017**, *77*, 1-8.

(156) Shukla, S. K.; Mishra, A. K.; Mamba, B. B.; Arotiba, O. A. Zirconia-poly (propylene imine) dendrimer nanocomposite based electrochemical urea biosensor. *Enzyme and Microbial Technology* **2014**, *66*, 48-55.

(157) Arotiba, O. A.; Baker, P. G.; Mamba, B. B.; Iwuoha, E. I. The application of electrodeposited poly (propylene imine) dendrimer as an immobilisation layer in a simple electrochemical DNA biosensor. *International Journal of Electrochemistry Science* **2011**, *6*, 673-683.

(158) Sharma, A.; Sumana, G.; Sapra, S.; Malhotra, B. D. Quantum dots self assembly based interface for blood cancer detection. *Langmuir* **2013**, *29*, 8753-8762.

(159) Soda, N.; Arotiba, O. A polyamidoamine dendrimer-streptavidin supramolecular architecture for biosensor development. *Bioelectrochemistry* **2017**, *118*, 14-18.

(160) Ruecha, N.; Siangproh, W.; Chailapakul, O. A fast and highly sensitive detection of cholesterol using polymer microfluidic devices and amperometric system. *Talanta* **2011**, *84*, 1323-1328.

(161) Tang, S.; Zhao, Q.; Tu, Y. A sensitive electrochemiluminescent cholesterol biosensor based on Au/hollowed-TiO 2 nano-composite pre-functionalized electrode. *Sensors and Actuators B: Chemical* **2016**, *237*, 416-422.

(162) Ruecha, N.; Rangkupan, R.; Rodthongkum, N.; Chailapakul, O. Novel paper-based cholesterol biosensor using graphene/polyvinylpyrrolidone/polyaniline nanocomposite. *Biosensors and Bioelectronics* **2014**, *52*, 13-19.

(163) Umar, A.; Rahman, M.; Vaseem, M.; Hahn, Y.-B. Ultra-sensitive cholesterol biosensor based on low-temperature grown ZnO nanoparticles. *Electrochemistry Communications* **2009**, *11*, 118-121.

(164) Sekretaryova, A. N.; Beni, V.; Eriksson, M.; Karyakin, A. A.; Turner, A. P.; Vagin, M. Y. Cholesterol self-powered biosensor. *Analytical Chemistry* **2014**, *86*, 9540-9547.